INFLUENCE OF SULFATE-REDUCING BACTERIA AND SPARTINA ALTERNIFLORA ON MERCURY METHYLATION IN SIMULATED SALT MARSH SYSTEMS

A Thesis
Presented to
The Academic Faculty

by

Theresa T. Fu

In Partial Fulfillment
of the Requirements for the Degree
Master of Science
In the School of Civil and Environmental Engineering

Georgia Institute of Technology
August 2005

INFLUENCE OF SULFATE-REDUCING BACTERIA AND SPARTINA ALTERNIFLORA ON MERCURY METHYLATION IN SIMULATED SALT MARSH SYSTEMS

Approved by:

Dr. F. Michael Saunders, Advisor
School of Civil and Environmental Engineering
Georgia Institute of Technology

Dr. Marc E. Frischer
Skidaway Institute of Oceanography
University of Georgia

Dr. Richard A. Jahnke
Skidaway Institute of Oceanography
University of Georgia

Date Approved: July 15, 2005

This thesis is dedicated to my parents who have supported me through my education with their guidance, love, and encouragement. Thanks mom and dad.

ACKNOWLEDGEMENTS

I would like to acknowledge and thank all the people who have helped me to not only complete this thesis but to grow as a student, peer, and scientist. Most of all, I would like to thank God for guiding me through some difficult times in my life.

First of all, I would like to thank my advisor, Dr. F. Michael Saunders for giving me the chance to work on this project and for his support throughout my graduate career. I am so grateful for the times he and Jackie Tront came to Skidaway to help me sample in the BERM in the hot Savannah sun. Thank you for taking the time to help me when I really needed it.

I also have to thank Dr. Marc Frischer and Dr. Richard Jahnke for serving on my thesis committee and for their guidance through my experience at the Skidaway Institute of Oceanography (SkIO). They are extremely brilliant scientists in their fields and I have great respect for them. I would also like to thank Dr. Jeff King for his encouragement, generosity, and inspiration.

When I first came to SkIO in the summer of 1998, I discovered the true meaning of "southern hospitality". I would like to thank everyone at Skidaway for making it such a great place to work. I want to especially thank Dr. Herb Windom, Dr. Keith Maruya, Dr. Richard Lee, Jean Danforth, Lori Cowden, Debbie Wells, Debbie Jahnke, Bobby Sauer, and Michele Healy for their help in all aspects of this project.

Georgia Tech was the foundation for my education and I would like to thank all the faculty and staff for their efforts in making my time at Georgia Tech fun and valuable. My thanks also go out to Andrea Be and Sara Thomas at the Daniel Lab for being my liason between Skidaway and Georgia Tech. Last but not least, I am grateful to the EPA Hazardous Substance Research Center South/Southwest, Georgia Tech, and Skidaway Institute of Oceanography for providing the stipend for this project.

TABLE OF CONTENTS

DEDICATION		iii
ACKNOWLEDGEMENTS		iv
LIST OF TABLES		ix
LIST OF FIGURES		x
LIST OF SYMBOLS, ABBREVIATIONS, AND NOMENCLATURE		xiii
SUMMARY		xvi
CHAPTER 1	INTRODUCTION	1
	Problem Statements	3
	Objectives	4
CHAPTER II:	LITERATURE REVIEW	5
	Mercury in the Environment	5
	Properties and Uses of Mercury	5
	Sources of Mercury in the Environment	6
	Mercury Cycling and Attenuation in the Environment	7
	Mercury in Biota	9
	Mercury Attenuation in the Environment	11
	Current Mercury Contamination Research	12
	New Technologies in Mercury Research	14
	Salt Marsh Ecosystems	17
	Aerobic Oxidation in Salt Marsh Sediments	18
	Anaerobic Processes in Salt Marsh Sediment	20
	Mercury Methylation in the Environment	22
	Factors affecting Methylmercury Production	22
	Characteristics of Sulfate-Reducing Bacteria	27
	Speciation and Phylogeny of Sulfate-Reducing Bacteria (SRB)	28
	Identification of SRB using 16S rRNA Oligonucleotide Probes	29
	Mercury Methylation and Demethylation by Sulfate-Reducing Bacteria	33

	Influence of *Spartina alterniflora* on Microbial Community Structure and Biogeochemistry in Salt Marsh Sediments	37
	Sulfate Reduction Coupled to Mercury Methylation	38
CHAPTER III:	MATERIALS AND METHODS	44
	Site Description	44
	Bioremediation and Environmental Research Mesocosms	46
	Sample Collection	50
	Porewater extracted from Cores	51
	Porewater extracted from Sippers	52
	Physical Characteristics of the BERM Mesocosms	53
	Sediment Density and Porosity	53
	Underdrain Effluent Volume	54
	Temperature	55
	Salinity	55
	Above-ground *Spartina* Biomass Analysis	55
	Mesocosm Restoration and Maintenance	56
	Porewater Geochemistry Experimental Methods	57
	pH Analysis	57
	Porewater Sulfate Analysis	57
	Dissolved Sulfide Analysis	58
	Sulfate Reduction Rate Measurement	59
	Extraction of Porewater for Total Mercury	62
	Effect of Sample Volume on Mercury Analysis	64
	Extraction of Porewater for Methylmercury	66
	Enumeration of Sulfate Reducing Bacteria (SRB)	69
	Sulfate-Reducing Bacteria Pure Cultures	69
	Preservation of Sediment Samples	69
	Whole Cell Extraction	70
	Enumeration of Bacteria using DAPI	71
	Quantification of SRB 16S rRNA Using Oligonucelotide Probes	73
	Blotting Membranes for Hybridization	73
	Radioactive Labeling and Probing with 16S rRNA Probes	73
CHAPER IV:	DATA RESULTS	76
	Sampling Schedule	76
	Physical Characteristics of the BERM	76
	Sediment Density and Porosity	76
	Underdrain Effluent Volume	82
	Temperature	83

	Salinity	84
	Spartina Height Measurements	87
	Porewater Geochemistry	89
	Porewater Sulfate	89
	Porewater Sulfide	96
	Sulfate-Reduction Rates	100
	Sulfide Oxidation Rates	105
	Total Mercury in the Porewater	111
	Methylmercury in the Porewater	114
	Microbial Community Structure	117
	Relative Distribution of Sulfate-Reducing Bacteria in the Sediment	117
CHAPTER V:	APPLICATION OF RESULTS TO PREDICT MERCURY METHYLATION RATES	124
	Calculations of SRR for Individual Phylogenetic Groups	124
	Calculations of MMR Based on Observed SRR and Pure Culture f*	133
CHAPTER VI:	CONCLUSIONS AND RECOMMENDATIONS FOR FUTURE STUDIES	138
	Geochemical Stratification	138
	Seasonal Variability in Process Rate Measurements	141
	Total Mercury, Methyl Mercury, and Estimated MMR	144
	Distribution of Sulfate-Reducing Bacteria	146
	Implications for Mercury Methylation and Demethylation	148
	Relationship between Sulfate Reduction Rates and Mercury Methylation Rates	148
	Environmental Engineering Applications and Recommendations	151
APPENDIX A –	Map of Skidaway Island and the Location of Skidaway Institute of Oceanography	154
APPENDIX B –	Media for Sulfate-Reducing Bacteria Cultures	155
APPENDIX C –	Artificial Seawater	156
APPENDIX D –	Components Needed for the Identification of 16S rRNA	157
REFERENCES		158

LIST OF TABLES

Table 2.1	SRB-specific probes used in microbial community characterization	34
Table 4.1	BERM sampling schedule	77
Table 4.2	Physical characteristics of BERM sediment in July 2000	78
Table 4.3	Physical characteristics of BERM sediment in February 2001	79
Table 4.4	Physical characteristics of BERM sediment in May 2001	80
Table 4.5	Summary of sediment characteristics	81
Table 4.6	Underdrainage effluent volumes	83
Table 5.1	f* values determined by King *et al*. (1999, 2000, 2001)	133

LIST OF FIGURES

Figure 2.1	Mercury transformation in the environment	24
Figure 2.2	Phylogenetic groups of sulfate-reducing bacteria	30
Figure 2.3	Mercury methylation pathways	35
Figure 2.4	Mercury demethylation pathways	35
Figure 2.5	SRR in sediment cores from tidal marshes at SkIO	41
Figure 2.6	MMR in sediment cores from tidal marshes at SkIO	42
Figure 2.7	Values of f* for SRB phylogenetic groups	43
Figure 3.1	Schematic of BERM mesocosms	45
Figure 3.2	Schematic of BERM piping and electronic control system	47
Figure 3.3	Schematic of tidal cycle in BERM mesocosms	47
Figure 3.4	Results from mercury volume experiment	65
Figure 4.1	Depth profiles of temperature readings in BERM	85
Figure 4.2	Seasonal variations in air and BERM sediment temperature readings	86
Figure 4.3	Salinity in BERM surface water	87
Figure 4.4	*Spartina alterniflora* height measurements	88
Figure 4.5	Sulfate profile in Grove's Creek sediment	91
Figure 4.6	Comparison of sulfate profiles between Grove's Creek and BERM pristine vegetated sediment	92

Figure 4.7	Porewater sulfate profiles for vegetated and unvegetated mesocosms from July 2000 sampling	93
Figure 4.8	Porewater sulfate profiles for vegetated and unvegetated mesocosms from February 2001 sampling	94
Figure 4.9	Porewater sulfate profiles for vegetated and unvegetated mesocosms from May 2001 sampling	95
Figure 4.10	Porewater sulfide profiles for vegetated and unvegetated mesocosms from July 2000 sampling	97
Figure 4.11	Porewater sulfide profiles for vegetated and unvegetated mesocosms from February 2001 sampling	98
Figure 4.12	Porewater sulfide profiles for vegetated and unvegetated mesocosms from May 2001 sampling	99
Figure 4.13	SRR-depth profiles for July 2000 sampling	101
Figure 4.14	SRR-depth profiles for February 2001 sampling	102
Figure 4.15	SRR-depth profiles for May 2001 sampling	103
Figure 4.16	Seasonal variation of SRR in BERM mesocosms	104
Figure 4.17	Estimated SOR in all three mesocosms	112
Figure 4.18	Comparison of SRR and SOR over a seasonal cycle	113
Figure 4.19	Total porewater mercury in BERM sediment	115
Figure 4.20	Methylmercury in BERM sediment	116
Figure 4.21	Relative distribution of SRB in pristine sediment	118
Figure 4.22	Relative distribution of SRB in contaminated vegetated sediment	119
Figure 4.23	Relative distribution of SRB in contaminated unvegetated sediment	120

Figure 4.24	Distribution of SRB community in pristine sediment	121
Figure 4.25	Distribution of SRB community in contaminated vegetated sediment	122
Figure 4.26	Distribution of SRB community in contaminated unvegetated sediment	123
Figure 5.1	Calculated Z_i for each phylogenetic group averaged for each sampling event	126
Figure 5.2	Calculated Z_i for each phylogenetic group averaged for each mesocosm	127
Figure 5.3	Calculated SRR_i for each phylogenetic group averaged for each sampling event	131
Figure 5.4	Calculated SRR_i for each individual phylogenetic groups averaged over three sampling events for each mesocosm	132
Figure 5.5	Calculated MMR_i for each phylogenetic group averaged for each sampling event	134
Figure 5.6	Calculated MMR_i for each phylogenetic group averaged for each mesocosm	135
Figure 6.1	Relationship between SRR and porewater MeHg	149

LIST OF SYMBOLS, ABBREVIATIONS, AND NOMENCLATURE

µg	microgram (s)
µL	microliter (s)
µm	micrometer (s)
AVS	acid-volatile sulfide
BERM	Bioremediation and Environmental Research Mesocosm
CH_4	methane
CH_3Hg^+	methylmercury
$(CH_3)_2Hg$	dimethylmercury
cm	centimeter
CO_2	carbon dioxide
°C	temperature in Celsius
CRS	chromium-reducible sulfur
d	day (s)
dH_2O	deionized water
DBACTER	*Desulfobacter*
DSB	*Desulfobulbus*
DSBM	*Desulfobacterium*
DSC	*Desulfococcus*
DSV	*Desulfovibrio*
EPA	United States Environmental Protection Agency

Hg	mercury
Hg°	elemental mercury (Hg(0))
Hg^{2+}	inorganic mercury (Hg(II))
$HgCl_2$	mercuric chloride
H_2S	hydrogen sulfide
hr	hour (s)
km	kilometer (s)
m	meter (s)
min	minute (s)
mL	milliliter (s)
MMR	mercury methylation rate
nmol	nanomole (s)
N_2	nitrogen gas
pH	$-\log[H^+]$ with $[H^+]$ = mol/L
ppm	parts per million (mg/kg)
ppt	parts per thousand (salinity)
rRNA	ribosomal ribonucleic acid
sec	second (s)
S^{2-}	sulfide
SO_4^{2-}	sulfate
$[SO_4^{2-}]$	sulfate concentration (mol/L)

SRB	sulfate reducing bacteria
SRR	sulfate reduction rate (nmol/g_{dry}-hr)
SkIO	Skidaway Institute of Oceanography

SUMMARY

The interactions of sulfate-reducing bacteria and *Spartina alterniflora* marsh grass have been investigated using a simulated salt marsh system and these interactions have been quantified using geochemical and molecular approaches. Plant activities have a direct influence on the activity and composition of bacterial populations that methylate mercury and therefore control mercury transformation in the environment. Biogeochemical data show that sulfate and sulfide profiles change seasonally due to plant growth and senescence. Sulfate-reducing bacteria transform sulfate to sulfide (sulfate reduction) and consume over 50 % of organic matter in salt marsh sediment (Gibson, 1990; Jorgensen, 1977; Jorgensen, 1982). In addition, sulfate-reducing bacteria have been identified as the principal methylators of mercury (Andersson, *et al*., 1990; Compeau and Bartha, 1985; Compeau and Bartha, 1984; Blum and Bartha, 1980; Gilmour and Capone). Dissolved oxygen present in both porewater and plant root exudates transform sulfide back to sulfate (sulfide oxidation). Sulfate is not limiting in the vegetated sediment, even at the lower depths. Therefore, although sulfate reduction rates were high when plant activity was high, oxidative processes were also significant in the 0-2 cm depths of the sediment. In addition, demethylation of methylmercury to ionic Hg(II) in the porewater can occur through oxidative processes (Oremland *et al.*, 1991). Therefore, the significance of sulfide oxidation may have strong implications for methylmercury demethylation in marsh systems.

The net total mercury and methyl mercury species was not significantly affected by the presence or absence of *Spartina alterniflora*. Interestingly, total mercury is higher in the pristine sediment than in the contaminated sediment. No trends in total mercury and methyl mercury concentrations were observed during plant growth and senescence. In general, methylmercury makes up less than 1 % of total Hg in the sediment. This is puzzling since sulfate reduction rates were much higher than those observed in other salt marsh systems. Therefore, demethylation could be more significant in the vegetated sediment than the unvegetated sediment.

Mercury methylation rates were predicted using calculated sulfate reduction rates and the function f*. The f* values were defined in pure culture for each SRB phylogenetic group by King *et al*. (1999, 2000, 2001). The results showed that different groups of SRB methylate mercury at different rates. *Desulfobacterium* and *Desulfococcus* dominated the SRB groups with average mercury methylation rates of 7.5E-3 and 1.5E-3 nmol/cm^3/d, respectively.

CHAPTER I
INTRODUCTION

Mercury has been a well-known pollutant for decades. As early as the 1950s, it was established that emissions of mercury to the environment could have serious effects on human health. One well-documented case of severe methylmercury poisoning occurred in Minamata Bay, Japan in 1956, in which an industrial spill of mercury killed more than 900 people and seriously damaged the central nervous systems of more than 2,000 people (Hosokawa, 1995). Human uptake of methylmercury was attributed to ingestion of fish and shellfish that bioaccumulated high doses of methylmercury. Methylmercury is highly toxic and prone to biomagnification in muscle and fat tissues because of its lipid solubility. Methylmercury generally accounts for 1-10% of total mercury found in sediments (Stern *et al.*, 1996). However, 95% of total mercury in living organisms is methylmercury (Bloom, 1992). Several sites have been heavily impacted by mercury contamination, including Lavaca Bay, Texas, the Florida Everglades, and the LCP chemical Superfund site in Brunswick, GA (formerly a chlor-alkali plant). This project utilized contaminated salt marsh sediment from the Brunswick site in a state-of-the-art mesocosm facility to investigate plant-microbial interactions that control mercury methylation.

For nearly three decades, much research has gone into effects of mercury toxicity and effects on human health. However, little is known about mercury

transformation, fate, and transport in complex environmental systems. The biological and geochemical mechanisms of these reactions are also poorly understood. Fortunately, advances in analytical techniques have improved capabilities of measuring low-level mercury in the environment, producing more accurate quantifications.

Evidence in the literature has cited sulfate-reducing bacteria as principal methylators of mercury and established a correlation between sulfate reduction and mercury methylation in salt marsh sediments (Andersson *et al*., 1990; Compeau and Bartha, 1985; Compeau and Bartha, 1984; Blum and Bartha, 1980; Gilmour and Capone, 1987; King *et al*., 1999). In addition, King *et al*. (1999) developed a model to predict mercury methylation rates based on sulfate reduction rates with reasonable success. Recently, King *et al.* (2000) determined that phylogenetic SRB strains methylate mercury at highly variable rates.

Salt marshes are among the most productive ecosystems on Earth and they serve as sources, sinks, and filters for natural and anthropogenic compounds. In the southeastern U.S., marshes are dominated by *Spartina alterniflora* marsh grass. *Spartina* has the capability of surviving in highly anoxic environments and its activities strongly impact sulfate-reducing bacteria (Hines *et al*., 1999; Rooney-Varga *et al*., 1997). In addition, most research has gone into studying belowground plant activities since the majority of net productivity has been attributed to plant roots and rhizomes (Howes and Teal, 1985). Moreover, the rhizosphere is an active zone for bacterial productivity (Hines *et al*., 1999). Therefore, impacts of *Spartina alterniflora* root activity on SRB community structure and impacts on mercury methylation need to be further assessed.

Problem Statements

There is limited information regarding the community structure of sulfate-reducing bacteria (SRB) that methylate mercury in salt marsh systems. Early studies attributed mercury methylation to *Desulfovibrio desulfuricans*. However, some groups of sulfate-reducing bacteria can methylate mercury at higher rates than others. King *et al*. (2000) demonstrated that acetate-utilizing sulfate-reducing bacteria (e.g. the family *Desulfobacteriaceae*) are capable of methylating mercury at higher rates compared to non-acetate utilizers (e.g. the family *Desulfovibrionaceae*) in pure culture. Therefore, one goal of this project is to elucidate the SRB community structure responsible for mercury methylation in salt marsh systems.

Previous laboratory studies and field observations have demonstrated that the activity of *Spartina* influences the activity and composition of bacterial populations (SRB) that methylate mercury in salt marsh sediment. However, relationships between *Spartina* growth, microbial activity, sediment chemistry and mercury methylation in *contaminated* salt marsh sediment have not been adequately explored. Previous studies have correlated sulfate reduction rates and cell abundance with mercury methylation (Devereux *et al*., 1996; King *et al*., 1999, King *et al*., 2000), but they did not include effects of plant activities. Therefore, another major goal of this project is to determine the impact of *Spartina alterniflora* on the complex distribution of sulfate-reducing bacteria and subsequently influence mercury methylation in contaminated salt marsh systems.

Objectives

The project hypothesis that is addressed is that plants and microbes are primary regulators of mercury methylation in salt marsh systems. Biochemical and molecular techniques have been utilized to quantify activities of sulfate-reducing bacteria and *Spartina alterniflora* over a seasonal growth cycle in an experimental mesocosm system. The objectives of this project are:

(1) Elucidate seasonal dynamics of the composition of microbial consortia involved in mercury methylation using SRB group-specific 16S rRNA-targeted oligonucleotide probe technology.

(2) Qualitatively establish the dynamic relationship between plant activities and the microbial community structure in the salt marsh sediment over a seasonal cycle.

(3) Compare effects of contamination and vegetation on mercury methylation by comparing biogeochemical measurements, rate measurements, and microbial distribution between the pristine, contaminated vegetated, and contaminated unvegetated mesocosms.

CHAPTER II
LITERATURE REVIEW

Mercury in the Environment

Mercury is a well-known pollutant that exists naturally in the air, water, and sediment. Its chemical properties allow it to be ubiquitous and persistent in the environment. Human activities also add to the total input of mercury into the environment, most of which is released into the atmosphere before settling into the water and sediment. Once deposited, mercury can be cycled through the aquatic and terrestrial environments or be re-emitted back into the atmosphere (EPA, 1997).

Properties and Uses of Mercury

Mercury generally exists in three forms or oxidative states: elemental mercury (Hg (0)), mercuric (Hg (II)), and mercurous (Hg (I)). The most common form of mercury is the elemental form. Elemental mercury is a silver liquid at room temperature and is very volatile (V.P.=1.6×10^{-4} kPa). Therefore, mercury typically exists in the gaseous form in the atmosphere. Organic methylmercury [CH_3Hg^+] and dimethylmercury [$(CH_3)_2Hg$] are formed from the complexation of mercuric and mercurous ions with organic matter and from the biological conversion of mercuric ion (mercury methylation). Additionally, mercuric ions can complex to anions to form inorganic [$HgCl_2$, $Hg(OH)_2$ and HgS]

compounds (EPA, 1997). Compared to other metals, mercury has a stronger potential to from covalent bonds rather than ionic bonds.

Mercury's physical and chemical characteristics make it useful in a variety of industrial processes. For example, mercury has high surface tension and constant volume expansion, which make it an effective medium in thermostats, navigational equipment and other measuring devices (Stein *et al*., 1996). Mercury is an excellent bacteriacide and fungicide for wood processing, paint products, and agriculture due to its high toxicity (EPA, 1997). Mercury is also used as a catalyst in the production of chlorine and caustic soda in chlor-alkali plants (EPA, 1997) and in the production of gold (Drake, 1998; EPA, 1997). In addition, mercury is used in the production of a number of consumer products, such as dental amalgams, cosmetics, soaps, detergents, batteries, fluorescent lights, electrical devices, thermometers, pharmaceuticals, and in paints and dyes (Rood, 1996; Stein *et al*., 1996; Perry, 2001).

Sources of Mercury in the Environment

Mercury is one of the most toxic heavy metals found in the environment, but the element exists naturally and ubiquitously in rocks, air, water, soils, and volcanic dust (Stein *et al*., 1996). Total global input of mercury to the environment, which includes natural, anthropogenic, and re-emission from the global pool, is approximately 5,500 tons per year (EPA, 1997). The U.S. alone contributed approximately 158 tons (143 Mg) of mercury in 1994-1995, or three percent of the annual global mercury input (EPA, 1997). Natural inputs of mercury include volcanic ash, and degassing from the land and ocean

(Rood, 1996). Anthropogenic inputs of mercury currently comprise approximately half of all mercury entering the world. Anthropogenic mercury discharges of 16,829 kg/yr in 1973 and 40,234 kg/yr in 1988 were reported (Rood, 1996). Hence, mercury levels appear to be increasing. The majority of anthropogenic mercury input into the ecosystem is from combustion processes, such as the burning of fossil fuels, incineration of medical and municipal waste, wastewater discharge, mining, and agricultural activities (Rood, 1996; EPA, 1997). As a result, EPA (1997) required a 50 % reduction in emissions from municipal waste combustors and medical waste incinerators from 1995 levels.

Mercury Cycling and Attenuation in the Environment

Global cycling of mercury can be attributed to both natural and anthropogenic activities. Mercury in the atmosphere can exist in its ionic, elemental, or particulate form and its stability permits widespread and long-term persistence in the environment. Air borne mercury primarily exists in the gas phase, except mercury present in a plume from an industrial source where particle-phase mercury is concentrated (Stein *et al*., 1996). Once elemental mercury volatilizes into the atmosphere, it can remain there for three months to two years (Munthe and McElroy, 1992) and disperse widely for thousands of miles (EPA, 1997). Due to its low solubility, elemental mercury is not released from the atmosphere during rainfall events, but it can eventually be oxidized by ozonation (Schroeder *et al*., 1991; Stein et al., 1996) or by photo-oxidative processes (Munthe and McElroy, 1992) to form ionic mercury, Hg^{2+}. Mercuric mercury and methyl mercury are

both soluble in water and thus wash out with rainfall, which constitutes the major form of mercury removal from the atmosphere (EPA, 1997).

The sediment serves as a primary sink for mercury due to mercury's strong affinity to organic and sulfidic substrates in marine environments (Rood, 1996). Under aerobic conditions, mercury species strongly bind to organic matter and form organomercurial compounds (methylmercury and dimethylmercury). Under anaerobic conditions, the formation of insoluble mercuric sulfides is possible (Lindberg and Harriss, 1974). Mercury sorption is highly dependent on pH, salinity, temperature, amount of organic carbon, and sulfide concentration. For example, at low chloride concentrations, mercury sorption to organic matter was unchanged between pH 4 and 6 and decreased at pH values higher than 6. At high chloride concentrations, the opposite occurred (Barrow and Cox, 1992). In addition, high sulfide concentrations and low redox potentials in the sediment will reduce the availability of inorganic mercury (Gilmour and Henry, 1991). Under these conditions, divalent mercury is transformed to cinnabar (HgS), which has extremely low water solubility ($K_{sp} = 10^{-53}$) (Bodek *et al*., 1988). Therefore, reducing sediments with high sulfide concentrations may serve as a sink and immobilize mercury. However, oxygen penetration in the overlying water or at the root tips will resolubilize the mercury bound to sulfide (Stein *et al.*, 1996).

Mercury is transferred to the aquatic environment by precipitation and terrestrial runoff. The aqueous solubility of elemental mercury is extremely low (2.8×10^{-7} mol/L or 56 μg/L). In the presence of oxygen or other potential oxidants, elemental mercury can be quickly oxidized into divalent mercury (Stein *et al*., 1996). Although mercuric ion

solubility is very low (39 μg/L), its solubility is enhanced by complexation with anionic species (Bodek *et al.*, 1988). Acidic conditions also promote the formation of soluble mercuric complexes ($HgCl_2$ and CH_3Hg), but more basic conditions promote the formation of volatile mercury complexes (Hg^0 and $(CH_3)_2Hg$) (Bodek *et al*., 1988; Stein *et al*., 1996; WHO, 1976; WHO, 1990). In high salinity environments, mercuric chloride complexes become the dominant species and also increase mercuric ion solubility (Bodek *et al.*, 1988). In addition, the presence of humic and fulvic acids in the water column may increase mercury bioavailibility and persistence in the aquatic phase and decrease settling of mercury to the sediment or volatilization of mercury to the atmosphere (Miskimmin *et al.*, 1992).

Mercury in the Biota

Methylmercury is the most toxic form of mercury and comprises 90-99 % of the total mercury in biota (Faust and Osman, 1981). Due to its lipophilic properties, bioaccumulation of methylmercury up the food chain is a concern for human health (Stein *et al*., 1996). The majority of methylmercury exposure to humans occurs through the ingestion of contaminated fish, other animals and plants. Methylmercury targets the central nervous system and renal systems and causes neurological disorders, such as "mad hatters" disease, also known as "Minamata disease" (EPA, 1997). The term "mad as a hatter" originated from the behavior of felt-hat makers who were overexposed to mercury during the 19th century (Perry, 2001).

Elemental mercury vapor can be inhaled and absorbed to the lungs and subsequently to the bloodstream (EPA, 1997). However, if elemental mercury is oxidized to mercuric ion, its mobility through the placental and blood-brain barriers is impeded (EPA, 1997). Inorganic mercury penetration into the gastrointestinal tract varies with the particular salt present in the blood (EPA, 1997). In contrast, methylmercury is readily absorbed by the gastrointestinal tract and easily penetrates placental and blood-brain barriers (EPA, 1997). Consequently, methylmercury is not readily demethylated and has a relatively long half-life in humans, ranging from 44 to 80 d (EPA, 1997).

One particular incident in the 1950s in Minamata Bay, Japan sparked interest and concern in the effects of methylmercury on human health. An industrial spill of waste sludge tainted with methylmercury caused 900 deaths and more than 2,000 cases of central nervous system damage (Hosokawa, 1995). These events were attributed to the ingestion of contaminated fish and shellfish that bioaccumulated methylmercury from waste sludge emitted from a local chlor-alkali plant (Hosokawa, 1995; EPA, 1997). Infected people reported symptoms of impaired vision, numbness in the extremities, speech and hearing impairment, incoordination of movement, and hallucinations (EPA, 1997).

Another incident of methylmercury poisoning occurred in Iraq prior to 1960 and again in the early 1970s (EPA, 1997). In these cases, grain seeds treated with mercury-containing fungicide resulted in severe mercury poisoning. Although the duration of methylmercury poisoning was shorter, the effects were much worse. During the 1970s episode, more than 6,500 people were admitted to the Iraqi hospital and 459 fatalities

resulted (EPA, 1997). Methylmercury continues to be a problem in many parts of the world. Even in Canada, results of a twenty-year testing program that tested methylmercury levels in 514 native communities suggested that many people were at risk for mercury poisoning (Wheatley and Paradis, 1996). Consequently, the adverse effects on fetal development are considerably more discouraging.

The animals located at the top of the food chain are most affected by methylmercury contamination due to bioaccumulation. Predator fish, such as shark and swordfish, eat or forage on smaller fish and may contain 10,000 to 1 million times the concentration of methylmercury in the surrounding water (WHO, 1976; WHO, 1990; USDHHS, 1992). Effects on wildlife include, death, reproductive impairment, impaired growth and development, and behavioral abnormalities (EPA, 1997). Fish show toxic signs such as loss of appetite, dark color, rolling from side to side, and bending at rest (Matida *et al*., 1971). Plants affected by mercury exposure show symptoms of plant senescence, growth inhibition, decreased chlorophyll content, leaf injury, and root damage (EPA, 1997).

Mercury Attenuation in the Environment

Mercury reductions can be initiated by controlling emissions from anthropogenic sources and by minimizing the bioavailibility of mercury. Mercury can be naturally attenuated by complexing mercury with sulfide, producing mercury sulfide (HgS) or cinnabar and thereby precipitating mercury out into the sediment. The sediment serves as the primary sink for mercury and holds approximately 95 % of the total mercury released

into the environment (EPA, 1997). However, resolubilization of HgS by bacteria can remobilize some of this mercury. An alternative way mercury can be attenuated is to convert the more toxic forms of mercury, methylmercury and mercuric ion, to a less toxic and volatile form, elemental mercury. The atmosphere acts as a sink for elemental mercury since its low solubility prevents it from being released during rainfall events (Munthe and McElroy, 1992). Mercury ends up in the atmosphere from anthropogenic emissions and on a smaller scale, from vascular plant emissions. Leonard *et al*. (1998a and 1998b) demonstrated that subsequent to uptake, five species of plants with differing physiological attributes from different ecological settings were capable of volatilizing mercury to the atmosphere.

Current Mercury Contamination Research

Although mercury pollution is a global issue, several researchers have implemented investigative studies or remedial plans to deal with mercury issues in specific areas that have suffered significant mercury contamination. These concerns are manifested primarily by the issuance of fish consumption advisories in the majority of U.S. because of high levels of mercury in game fish. Examples of these cases include the Great Lakes and the Everglades.

Mercury levels in predatory fish in the Great Lakes have been significantly high and display levels that exceed governmental advisories for safe consumption (Amyot *et al*., 1999). As a result, the Great Lakes Research Consortium was assembled to dedicate collaborative research and education on the Great Lakes ecosystem. The Consortium

publishes research in the *Great Lakes Research Review* on topics such as the fate and transport of toxic contaminants, fisheries issues, and effects of toxics issues. One study by Amyot *et al*. (1999) estimated that atmospheric deposition accounted for 75 % of Hg inputs in Lake Michigan. Therefore, control of industrial sources could potentially significantly reduce the mercury contamination problems in the Great Lakes.

The Great Lakes Water Quality Agreement of 1978 was implemented to "virtually eliminate" persistent toxic substances from the Great Lakes Basin. The Great Lakes Binational Toxics Strategy, signed on April 7, 1997, by U.S. EPA addresses this commitment by setting reduction targets for an initial list of pollutants, including mercury, PCBs, DDT, chlordane, and dioxins/furans. The Pollution Prevention Act of 1990 expanded this policy to the national level. Congress declared as national policy that pollution should be prevented or reduced at the source whenever feasible; pollution that cannot be prevented should be recycled. If pollution cannot be prevented or recycled, it should be treated in an environmentally safe manner. Disposal or other release into the environment should be used as a last resort. Therefore, this plan intends to alleviate the mercury problem by going to the root of the source and thereby preventing additional pollution problems in the future. Hence, regulatory compliance is one way of reducing mercury in the environment because it is a strong motivator for pollution sources to implement pollution prevention programs.

The Everglades have suffered great losses in fish and wildlife due to mercury contamination and bioaccumulation. The U.S. Geological Survey is conducting an investigative study of how mercury is contaminating the Everglades by identifying the

hydrologic, biologic, and geochemical processes controlling mercury cycling in the Everglades. Recent observations demonstrate that seasonal variations in total mercury concentrations in surface water are primarily controlled by rainfall, which is the dominant source of Hg to the Everglades. However, the trends are highly variable, suggesting that mercury deposition from the atmosphere is considerably random (Krabbenhoft, 1996). In the sediment, MeHg production is most significant at the sediment surface and is driven by microbial sulfur cycling and dissolved organic carbon (Gilmour *et al*., 1992 and 1998). According to Krabbenhoft (1996), the extent and distribution of MeHg is attributed to excess sulfate from agricultural runoff, which stimulates sulfate-reducing bacteria, the primary methylators of mercury.

New Technologies in Mercury Research

Phytoremediation is a potentially viable approach to sequestration and removal of mercury. Meagher *et al*. (2000) have successfully engineered a modified bacterial mercuric ion reductase gene called *mer*A and an organomercurial lyase called *mer*B. The MerA enzyme reduces ionic mercury (Hg^{2+}) to less toxic elemental mercury (Hg^0). Hg^0 can then volatilize into the atmosphere and remain sequestered there for years (EPA, 1997). The MerB enzyme encodes an organomercurial lyase that converts methylmercury to methane and Hg^{2+} (Bizily *et al*., 1999). Expression of *mer*B alone can confer MeHg resistance, but the expression of both *mer*A and *mer*B together prevents biomagnification of MeHg and the accumulation of ionic mercury (Meagher *et al*., 2000). Both genes have been successfully expressed in *Aradopsis* plants, as well as the canola

and tobacco plant lines. These plants can function normally on medium with high levels of Hg^{2+} (25-250 μm) that is normally lethal to plants (Meagher *et al*., 2000). Hence, the use of plants for the remediation of mercury-contaminated sites could potentially be an invaluable strategy for controlling the most toxic forms of mercury in the environment.

Constructed wetlands or experimental mesocosms can also be used to evaluate mercury transformation processes under a controlled state. Constructed wetlands are often used to evaluate pollutant removal efficiency and how pollutant transformations are impacted by physical, chemical, and biological changes. This project uses a state-of-the-art mesocosm facility to study the biogeochemical and microbial processes involved in mercury methylation in a salt marsh system. These processes will be studied over a seasonal time scale since this cycle reflects the effect of changes in temperature, salinity, pH, tidal flow, sulfate, dissolved sulfide, DOC, and bulk phase carbon. The results of this study will provide basic scientific data in areas that are not well understood, including the role of *Spartina alterniflora* marsh grass on mercury methylation and demethylation and the community structure of the microorganisms involved in mercury transformation.

In summary, mercury is highly persistent in the environment and is difficult to attenuate naturally. There are still many unknowns concerning mercury transformation and current strategies for attenuating mercury are difficult to implement. The use of genetically engineered plants for the remediation of pollutants is still a controversial issue due to lack of public knowledge. Undoubtedly, more research is needed in understanding the controls for mercury methylation and demethylation before remediation strategies can

be implemented. Constructed wetlands or experimental mesocosms may bring insight into the unknowns concerning mercury transformation processes, including the biological and chemical drivers of mercury transformation. More importantly, mesocosms allow examination of these processes to take place *in situ*, without significantly altering the natural state of the environment. The following sections provide background information on salt marsh systems and sulfate-reducing bacteria, which are principal drivers for mercury methylation and demethylation.

Salt Marsh Ecosystems

Salt marshes are the most productive and dynamic ecosystems on earth (Howarth, 1993). They exist between the open ocean and the coastline and are impacted by dynamic tidal movement. Along the eastern coast of the U.S., salt marshes are flooded with salt water twice a day. Lower marshes have more frequent and irregular flooding (Howarth, 1993). Tides bring in fresh nutrients daily while marsh grass traps these nutrients along with detritus, providing abundant food for microorganisms. Salt marshes on the eastern U.S. coast are dominated by vascular marsh grasses called *Spartina alterniflora*. These marsh grasses participate in cycling of nutrients, carbon, oxygen, and metals, including mercury. Therefore, Sp*artina alterniflora* has a strong influence on the microbial community structure and biogeochemistry in the salt marsh.

Organic matter input by primary production of salt marsh grass is estimated to be between 460 to 3200 g C/m^2/yr (Giblin and Wieder, 1992; Schubauer and Hopkinson, 1984). Surface algae contribute 80 to 190 g C/m^2/yr (Pomeroy *et al*., 1981), and sulfur-oxidizing bacteria fix another 275 to 500 g C/m^2/yr in salt marshes. More than half of total primary production in salt marshes is produced belowground in roots and rhizomes of salt marsh grasses (Pomeroy *et al*., 1981; Good *et al*., 1982; Schubauer and Hopkinson, 1984). However, this is still an underestimation since excretion of dissolved organic matter and fermentation products were not included in the estimate (Howarth, 1993). Presumably, the large amount of organic matter produced in salt marsh systems stimulates high microbial activity.

Aerobic Oxidation in Salt Marsh Sediments

During drainage and low tide, air enters the pore spaces (void space where air can enter) in salt marsh sediment as a result of lateral drainage of porewater to intertidal creeks and during evapotranspiration by salt marsh grasses (Howarth and Giblin, 1983). Oxygen penetration into sediment impacts both microbial and chemical processes in the sediment surface and the grass root and rhizosphere. Oxygen initially diffuses into the hollow channels of the grass's vascular system (Teal and Kanwisher, 1961). The depth of oxygen penetration varies from marsh to marsh and depends on the frequency of flooding, sediment porosity and distance to creeks (Howarth, 1993). For example, Howes *et al*. (1991) reported that, in Great Sippewissett salt marsh in Massachusetts at 5 m from the creek bank, gas-filled pores reached depth of 10 cm 12 hr after high tide subsided. In a South Carolina salt marsh, King (1988) reported oxygen penetration to only 2 to 5 mm depth below the surface.

Oxygen present in air pockets in salt marsh sediments stimulates bacteria capable of aerobic respiration. Approximately 44 % of carbon dioxide production in a Massachusetts salt marsh was attributed to aerobic respiration (Howes *et al.*, 1984). Of the total amount of oxygen consumed, half was consumed by aerobic respiration and half was consumed for the oxidation of sulfide compounds (Howarth and Merkel, 1984). However, oxygen uptake differs between different marsh systems due to differences in the frequency of tidal flooding and sediment porosity. Aerobic respiration evidently occurs at the sediment surface and to a smaller extent, in the rhizosphere of grasses (Howarth, 1993). Howarth and Hobbie (1982) measured rates of oxygen uptake by

sediments in various marshes from Nova Scotia to Louisiana to be between 5 to 66 mol $O_2/m^2/yr$. Assuming that half the consumption of oxygen goes to aerobic respiration, then approximately 2.5 to 33 mol $O_2/m^2/yr$ can oxidize between 30 to 400 g $C/m^2/yr$ (Howarth, 1993).

The diffusion of oxygen through marsh grass roots to the sediment and from air to surface sediment can impact sulfate and sulfide chemistry. Several reports suggest that sulfide oxidation may be important because of two observations. First, sulfide generation rates are much higher than reduced sulfur accumulation rates in sediments (Chanton *et al*., 1987; Berner and Westrich, 1985). Second, gross rates of sulfate reduction and sulfate concentrations are much higher in the sediment than the diffusive flux of sulfate entering the sediment (Urban *et al*., 1994). Therefore, another source of sulfate is needed to maintain such high rates of sulfate reduction at the sediment surface. Sulfide oxidation near the sediment surface is controlled by evapotranspiration, the availability of organic substrates for sulfate reduction, and air entry to due to sediment desaturation (Boulegue *et al*., 1982; Dacey and Howes, 1984; Morris and Whiting, 1985, King, 1988). *Spartina alterniflora* roots are known to oxidize sulfide as a detoxification strategy since sulfide can stunt growth, and inhibit important plant enzymes (Lee *et al*., 1999). Bioturbation by fiddler crabs and snails may also contribute to the oxidation of chromium reducible sulfur (King *et al*., 1982; Howarth and Giblin, 1983). Sulfide depletion evident at lower depths may be the result of plant root uptake (Carlson and Forrest, 1982) or sulfide complexation with iron or manganese oxides (Aller and Rude, 1988) or metals, such as

mercury. Jorgenson (1990) introduced the importance of thiosulfate as a main product of sulfide oxidation and as a shunt between oxidative and reductive pathways.

A quantitative framework for calculating sulfide oxidation rates has not been developed, but it appears that sulfide oxidation may be just as significant as sulfate reduction in salt marsh sediment. Urban *et al*. (1994) hypothesized that sulfide oxidation occurs nearly as rapidly as sulfate reduction based on nonlinear rates of sulfate reduction and calculated turnover times of sediment sulfide pools. Jorgensen (1977) postulated that 10 % of all sulfide was precipitated by metal ions within the anoxic sediment, while the rest was reoxidized at the surface. The difficulty in studying sulfide oxidation has been attributed to the complexity of understanding the chemical pathways and intermediates involved. Isotopic exchange reactions between free sulfide, iron sulfide, polysulfides, and elemental S complicate methodical investigations (Fossing and Jorgensen, 1990). This project will introduce a mass balance approach for estimating sulfide oxidation rates based on sulfate reduction rates, porewater sulfate concentrations, and velocity of water that flows through the sediment during drainage (see chapter on discussion).

Anaerobic Processes in Salt Marsh Sediment

Instead of using oxygen as the terminal electron acceptor, a number of other substrates are used in order of their redox potential by anaerobic bacteria. The following electron donors are listed from most energetically favorable to least energetically favorable: oxygen, nitrate, manganese, iron, sulfate, and carbon dioxide (Berner, 1982; Lannbroek, 1990; Ponnamperuma, 1972). Theoretically, bacteria use the most

energetically favorable substrate available. However, in non-competitive communities or environments where other factors control bacterial community structure, this idealized hierarchy does not exist (Howarth, 1993). For example, sulfate reduction has been reported to take place in the presence of low levels of oxygen (Wakao and Furusaka, 1976; Jorgensen, 1977; Bak and Pfenning, 1991; Jorgensen and Bak, 1991).

Dissimilatory nitrate reduction would be the major process after aerobic respiration of oxygen, but nitrate reduction is not significant in salt marshes since nitrate levels are relatively low (Howarth, 1993). Therefore, the consumption of carbon by nitrate reduction is only approximately 3 to 10 g $C/m^2/yr$ (Delaune and Patrick, 1980; Haines *et al*., 1977; Kaplan *et al*. 1979). Similarly, iron and manganese reduction are not significant processes relative to sulfate in porewaters of salt marsh sediment In the presence of hydrogen sulfide, iron is removed before it can be assimilated by iron-reducing bacteria (Jacobson, 1990). However, if reduction and re-oxidation are closely coupled, rapid cycling of these metals could occur without significant build-up of porewater concentrations. Additionally, biotic reduction of Fe(III) may be more significant than once thought (Kostka *et al*., 2002). Lovely (1987) and Lowe *et al*. (2000) observed that a disappearance of iron-reducing bacteria stimulates the propagation of sulfate-reducing bacteria (SRB), indicating that, in the presence of reducible Fe(III), iron-reducers may outcompete SRB for growth substrates.

Sulfate reduction is by far the dominant final (terminal) electron acceptor in salt marsh sediment despite its ranking on the energetic scale. Over 50 % of all organic matter in salt marsh sediment is consumed by dissimilatory sulfate-reducing bacteria

(Gibson, 1990; Jorgensen, 1977; Jorgensen, 1982). Sulfate reduction rates range between 6 to 75 mol S/m^2/yr, which consumes 144 to 1800 g C/m^2/yr (Giblin and Wieder, 1992). In the Great Sippewissett Marsh in Massachusetts, sulfate reduction consumed 1800 g C/m^2/yr (Howarth and Teal, 1979). In comparison, a salt marsh on Sapelo Island in Georgia consumed 850 g C/m^2/yr (Howarth and Merkel, 1984). Sulfate reducing bacteria degrade low molecular weight alcohols and fatty acids. More complex organic compounds are degraded by fermenting bacteria, and in turn provide more substrates for sulfate-reducers (Howarth, 1993).

Methanogenesis plays a smaller role in salt marsh sediment, consuming only 0.4 to 40 g C/m^2/yr (Bartlett *et al*., 1987; Howarth and Hobbie, 1982; Howes *et al*., 1985; King and Wiebe, 1978). It was previously postulated that sulfate reducers outcompeted methanogens for substrates, but now it has been discovered that anaerobic methane oxidation may limit methanogenesis (Ivanov *et al*., 1989). In other words, the relatively low fluxes of methane out of sulfate-rich marine sediments are a result of methane oxidation rather than inhibition of methane formation.

Mercury Methylation in the Environment

Although methylmercury can be formed through both abiotic and biotic processes, the focus of this project is on biologically mediated mercury methylation. Sulfate-reducing bacteria are the principal methylators of mercury (Andersson *et al*., 1990;

Compeau and Bartha, 1985; Compeau and Bartha, 1984; Blum and Bartha, 1980; Gilmour and Capone, 1987). The biological conversion of inorganic mercury to methylmercury in sediment is described in the following section in detail.

Factors affecting Methylmercury Production

Mercury methylation and demethylation are mainly microbially driven processes. These transformations occur in water, sediment, air, and biota (Figure 2.1). Mercury methylation can occur in the water column, at the sediment-water interface, and in the sediment. In all phases, elemental mercury must first be converted to divalent mercury (Hg^{2+}) since divalent mercury is the precursor to the formation of methylmercury (Stein *et al*., 1996). Mercury methylation results in the formation of monomethylmercury and dimethylmercury. Under acidic conditions and when mercury concentrations are high, monomethylmercury production is favored (Stein *et al*., 1996), while under low mercury concentrations and alkaline conditions, dimethylmercury production is favored (Nriagu, 1979; Craig and Moreton, 1984).

Mercury methylation rates are typically highest at the top few centimeters of sediment and decrease with depth. It has been postulated that elevated levels of mercury methylation occur at the upper sediment zone due to the presence of active bacterial populations, adequate temperatures, and abundance of organic matter (Stein *et al*., 1996; Winfrey and Rudd, 1990).

A sufficient amount of organic matter must be present for mercury methylation to occur. Compeau and Bartha (1984) demonstrated that at the sediment/water interface, organic matter is high, and thus mercury methylation rates are high and both decrease

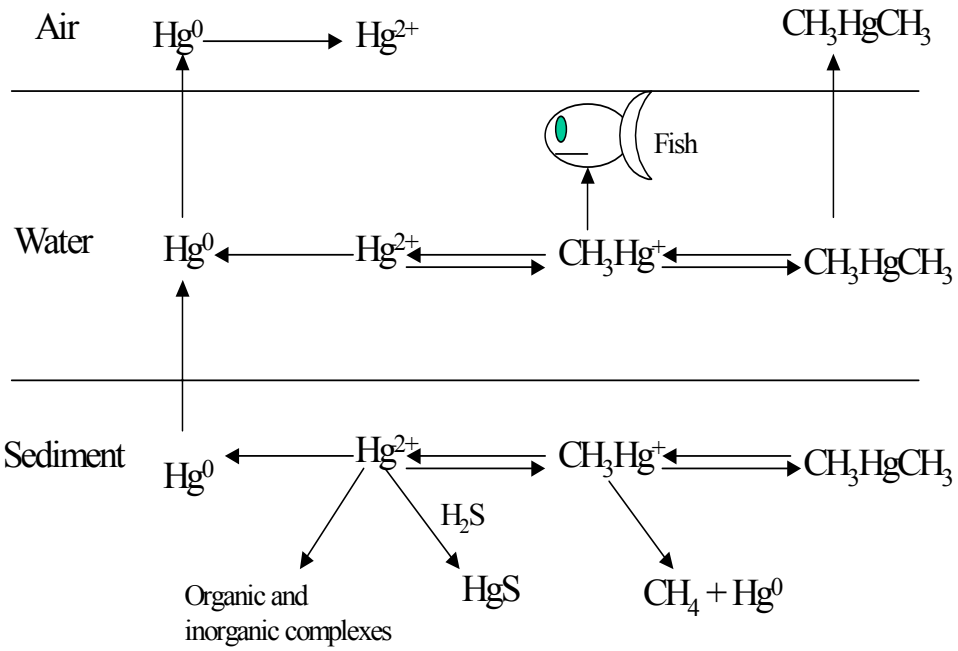

Figure 2.1 Mercury transformation in the environment (adapted from Madigan *et al*., 2000).

with depth. In addition, mercury complexing with organic matter would provide longer exposure time for methylating bacteria.

Mercury methylation is also affected by pH, temperature, electron potential and salinity. At lower pH, methylation rates increase because the increase in number of protons liberates divalent Hg from complexes, making them available for methylation (Andersson *et al*., 1990; Miskimmin *et al*., 1992; Stein *et al*., 1996). In addition, higher temperatures promote faster methylation rates (Zilloux *et al*., 1993). A lower electron potential also promotes mercury methylation rates because a reducing environment is conducive to sulfate reducing bacteria. For example, an electrode potential of –220 mV results in a maximum production of methylmercury, while an electrode potential of +110 mV results in a minimum value for methylation (Compeau and Bartha, 1984). Lastly, microbial methylation is inversely related to salinity in salt marsh sediments because Blum and Bartha (1980) observed highest mercury methylation at 4.0 ppt and minimum mercury methylation at 25.0 ppt.

Since sulfate-reducing bacteria are the principal methylators of mercury (Andersson *et al*., 1990; Compeau and Bartha, 1985; Compeau and Bartha, 1984; Blum and Bartha, 1980; Gilmour and Capone, 1987), sulfate concentrations directly impact microbial methylation activity. Sulfate concentrations in the ocean are typically 28 mM or 900 mg/L (Holland, 1978). In lakes, sulfate concentrations range between 0.01-0.02 mM (320-640 μg/L as S). Therefore, mercury methylation is more significant in salt marshes than in freshwater sediment (Gilmour and Henry, 1991). Gilmour and Henry (1991) postulate that mercury methylation is optimum when sulfate concentrations are between

200-500 μM. Sulfate concentrations greater that 500 μM inhibit methylation since large concentrations of sulfide would be produced and complex with mercury, making the metal unavailable for methylation. However, high concentrations of sulfate do not inhibit mercury methylation when sulfide oxidation is significant (see results in Chapter 4).

The relationship between sulfate reduction rates and mercury methylation rates has been examined. Recently, King *et al*. (1999) developed a quantitative framework for predicting mercury methylation rates based on sulfate reduction rates. The relationship was affirmed using laboratory sediment slurries and whole sediment cores. Both sulfate reduction and mercury methylation are influenced by temperature, carbon substrates and mercury bioavailability (King *et al.*, 1999). In addition, the quantitative relationship is based on the activity and community composition of sulfate-reducing bacteria (King *et al.*, 2000; King *et al.* 2001).

Although mercury methylation is a microbial-mediated process, very little research has looked at the impact of vegetation activities towards these microbial communities and the role plants play in mercury transformation processes. Seasonal changes that impact *Spartina alterniflora* growth patterns will inevitably influence sulfate reduction and mercury methylation. Weber *et al*. (1998) demonstrated that concentrations of elemental mercury, monomethylmercury, and dimethylmercury varied seasonally with *Spartina* growth. During active growth of *Spartina*, demethylation outcompeted methylation since methylmercury production was at a minimum. During the reproductive phase of *Spartina*, methylation prevailed over demethylation. Consequently, *Spartina* activities influence the microbial consortia responsible for mercury methylation and demethylation,

but a good understanding of these interactions is still rather limited. Therefore, this project intends to develop a mechanistic understanding of the controls of plant systems on microbial mediated Hg transformation in salt marsh systems.

Characteristics of Sulfate-Reducing Bacteria

Early investigations into mercury methylation revealed that anaerobic sediments produced substantially greater amounts of methyl mercury compared to aerobic sediments (Jensen and Jernelov, 1969; Olson and Cooper, 1976). Inhibition studies using bromoethanesulfonate, a specific methanogen inhibitor, ruled out methanogenic bacteria as primary methylators because methylmercury production increased with inhibitor additions (Compeau and Bartha, 1984). Methanogens often compete with sulfate-reducing bacteria for substrates, and results from the inhibition study reflected a reduction in competition for substrates. In contrast, when molybdate was used to inhibit sulfate reduction, mercury methylation was reduced by 95 % (Compeau and Bartha, 1985). Enrichment cultures and pure cultures of *Desulfovibrio* also demonstrated the ability to methylate mercury in sulfate-rich environments (Compeau and Bartha, 1995; Pak and Bartha, 1998a; 1998b), but pure cultures of methanogenic bacteria could not methylate mercury (Pak and Bartha, 1998a).

Speciation and Phylogeny of Sulfate-Reducing Bacteria (SRB)

Dissimilatory sulfate-reducing bacteria (SRB) use sulfate as the terminal electron acceptor and consequently convert sulfate to sulfide. SRB typically inhabit the anoxic zones of sediment where sulfate is plentiful (Gilmour and Henry, 1991), such as subsurface zones of lakes and anoxic sediments. SRB are highly diversified in marine sediments where sulfate is not limiting (17-28 mM). SRB are found in a variety of environments, including anaerobic digestors, freshwater sediment, and rice paddies (Watanabe and Furusaka, 1980; Gilmour *et al*., 1992). Some members of SRB are also found in oxic freshwater zones and oxic marine sediments (Bak and Pfenning, 1991; Jorgensen and Bak, 1991), as well as anoxic microniches within oxic environments (Jorgensen, 1977).

Currently, there are nineteen defined genera of dissimilatory sulfate-reducing bacteria (Rooney-Varga *et al*., 1998). Dissimilatory sulfate-reducing bacteria are present in three distantly related groups: Gram-positive bacteria, proteobacteria (Gram-negative mesophilic bacteria), and thermophilic sulfate reducing bacteria in the archaeal domain (Devereux and Stahl, 1993). The SRB studied in this project are members of the Gram-negative mesophilic bacteria and restricted to one of four subdivisions of the delta proteobacteria (Devereux and Stahl, 1993). The genera are also divided into two families. The *Desulfovibrionaceae* family includes *Desulfovibrio* and *Desulfomicrobium* genera. These members can utilize lactate, pyruvate, fumarate, propionate, ethanol, and other organic acids. The *Desulfobacteriaceae* family includes, *Desulfobulbus*, *Desulfobacter, Desulfococcus, Desulfosarcina, Desulfobacterium* and *Desulfonema*

genera. Members of this family use similar substrates as those in the *Desulfovibrionaceae* family, except, members of the *Desulfobacterium, Desulfococcus*, and *Desulfobacter* genera can also use acetate as a sole carbon and electron source (Rooney-Varga *et al*., 1998). The evolutionary relationship for dissimilatory sulfate-reducing bacteria was derived from comparison of 16S rRNA gene sequences (Figure 2.2).

Members of the genera *Desulfovibrio* and *Desulfobulbus* inhabit both freshwater and marine water habitats (Widdel, 1988; Bak and Pfenning, 1991). *Desulfobacter, Desulfobacterium, Desulfosarcina,* and *Desulfonema* members are primarily found in marine or brackish water (Widdel, 1988). *Desulfobacter* appears to be the main utilizer of acetate in brackish and marine sediments (Widdel, 1988), but it does not appear to grow well on other compounds (Devereux and Stahl, 1993).

Identification of SRB using 16S rRNA Oligonucleotide Probes

Previous methods of understanding bacterial groups and community structure were limited to what could be cultured in the laboratory and by enrichment and isolation techniques. The most obvious drawback in culture-based techniques is that only 0.3 % of the total number of cells in soil that are observed microscopically are culturable in the laboratory (Amann *et al.*, 1995). In contrast, the use of nucleic acid techniques allows for the specific identification of phylogenetic groups in a particular environment. Therefore, organisms that are routinely cultivated are not necessarily representative of what is observed using molecular techniques.

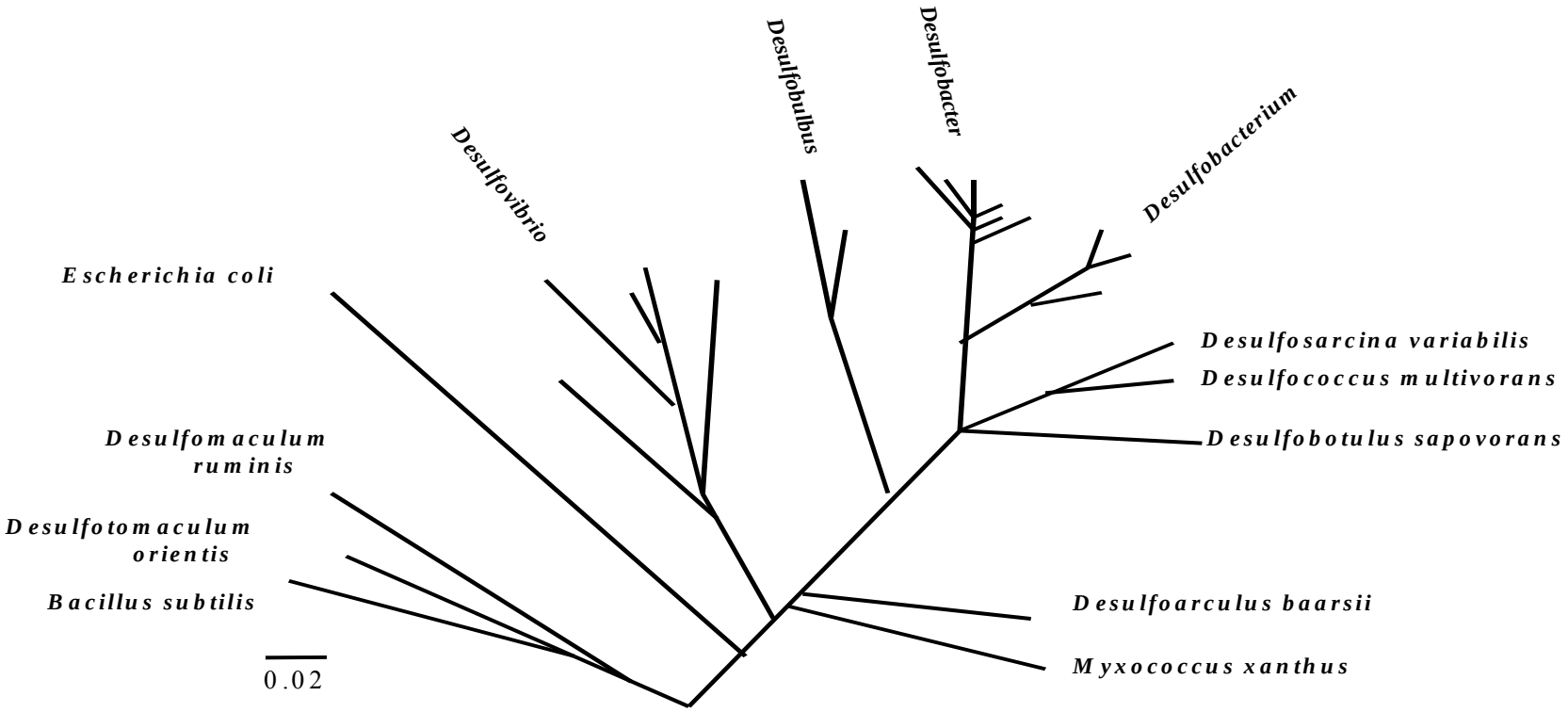

Figure 2.2 Phylogenetic groups of sulfate-reducing bacteria (from Devereux *et al*., 1992).

DNA extraction techniques are generally used to detect the presence of bacterial populations, but RNA extraction techniques are used to investigate biochemical and biological activity since ribosome content is an indication of microbial metabolic activity (Wagner, 1994). Most RNA protocols target the 16S rRNA gene due to its abundance in living organisms (Giovannoni *et al.*, 1988) and its usefulness in tracking phylogenetic relationships between all classifications of living organisms. The 16S rRNA gene consists of conserved and non-conserved (species-specific) regions or sequences (Devereux and Stahl, 1993; Embley and Stackerbrandt, 1996). Sequence comparisons of the 16S rRNA gene revealed unique differences between different microbial phylogenetic groups (Olsen *et al*., 1986; Pace *et al*., 1986). The ability to distinguish bacterial ancestry has been useful in identifying bacteria in environmental studies. For example, the first use of 16S rRNA-targeted sequence comparisons was in rumen ecology (Stahl *et al*., 1988).

Oligonucleotide probing has been used to quantify microbial activity (Embley and Stackerbrandt, 1996). A high concentration of ribosomes is indicative of high protein synthesis, and therefore indicates an active metabolism by microorganisms. The probes are complementary to the conserved tracts of the 16S rRNA unique to each bacterial phylogenetic group. Probes are labeled with either radioactive [γ-^{32}P] ATP or with fluorescence (DeLong *et al.*, 1989; Giovannoni *et al*., 1990; Devereux *et al*., 1992; Embley and Stackerbrandt, 1996; Frischer *et al*., 1996). However, caution should be taken with obtaining quantitative data from probe signals since some inactive cells contain an abundance of rRNA (Embley and Stackerbrandt, 1996).

Traditionally, hybridization studies require the extraction of RNA from environmental samples. Prior to hybridization with 16S rRNA-targeted oligonucleotide probes, RNA is isolated from sediment by direct phenol extraction and purified using Sephadex gel columns (Devereux *et al*., 1992; Moran *et al.*, 1993). However, the procedure is tedious and time-consuming and a great deal of extracted RNA is lost due to enzymatic RNases during extraction (Ogram *et al*., 1995). Frischer *et al*. (2000) successfully employed the use of whole cell extracts for sediment hybridization studies. This procedure extracts whole cells from environmental samples using homogenization, detergents, and dispersants and takes less time to perform than RNA extraction. The efficiency of the whole cell protocol, relative to DAPI epifluorescence counting, ranged from 91 to 102 % and the average recovery was 95.7 $\pm$ 3.7 % (Frischer *et al*., 2000). In general, results from whole cell and direct RNA extractions were comparable and therefore, this project will employ the whole cell extraction procedure prior to hybridization with radioactively labeled 16S rRNA oligonucleotide probes.

The application of 16S rRNA sequencing has been applied to studying SRB community structure as well. Devereux *et al*. (1989, 1990, 1992, 1993) designed six SRB-specific 16S rRNA-targeted oligonucleotide probes and were used to assess the diversity of the sulfate-reducing populations in salt marsh sediments. In addition, these probes have been used to assess mercury methylation activity of SRB (Devereux *et al*., 1996; King *et al*., 2001). The SRB-specific probes derived from Devereux *et al*. (1992) were used in this project and are listed in Table 2.1. Each probe is assigned an identification code; for example, probe 660 is specific for *Desulfobulbus*. In addition,

acronyms DBACTER, DSBM, DSB, DSV, and DSC will be used throughout this report for *Desulfobacter, Desulfobacterium, Desulfobulbus, Desulfovibrio*, and *Desulfococcus* phylogenetic groups.

Mercury Methylation and Demethylation by Sulfate-Reducing Bacteria

Solid phase mercury (II) is biologically available for microbial mercury methylation, although the biochemical pathways that result in mercury methylation remain somewhat unclear. Some studies have suggested that tetrahydrofolate, methylcobalamin enzyme and a corrinoid protein carrier are involved with the transfer of the methyl group from serine or pyruvate to mercury, shown in Figure 2.3 (Berman *et al*. 1990; Choi *et al.* 1994a & b). Radiolabeled carbon in serine or pyruvate is first donated to a tetrahydrofolate carrier (Berman *et al.*, 1990). Choi *et al*. (1994 a & b) proposed that methylcobalamins and corrinoid protein carriers facilitated the transformation of the methyl-tetrahydrofolate group to methylmercury. In studies tracing carbon flow in mercury methylation of *Desulfovibrio desulfuricans*, approximately 95 % of mercury methylation activity was attributed to serine and only 21 % to pyruvate (Berman *et al*., 1990). However, it is unknown whether all sulfate-reducers have these enzymes or whether only a few possess the enzyme and are capable of mercury methylation.

In contrast, mercury demethylation may occur through an organomercurial lyase (OML) pathway in which a covalent carbon-mercury bond is cleaved enzymatically by organomercurial lyase enzyme that codes for the *mer*B operon (Figure 2.4 a). This

Table 2.1 SRB-specific probes used in microbial community characterization.

16 S rRNA probes used for identification of SRB phylogenetic groups				
Probe #	Probe Name	Specificity	Probe sequence (5' to3')	Reference
Univ 342	UNIV 342	All eubacteria	CTG-CTG-CSY-CCC-GTA-G	Vescio & Nierzwicki-Bauer (1995)
129	DBACTER	*Desulfobacter*	CAG-GCT-TGA-AGG-CAG-ATT	Devereux *et al* . (1992)
221	DSBM	*Desulfobacterium*	TGC-GCG-GAG-TCA-TCT-TCA-AA	Devereux *et al* . (1992)
660	DSB	*Desulfobulbus*	GAA-TTC-CAC-TTT-CCC-CTC-TG	Devereux *et al* . (1992)
687	DSV	*Desulfovibrio*	TAC-GGA-TTT-CAC-TCC-T	Devereux *et al* . (1992)
814	DSC	*Desulfococcus*	ACC-TAG-TGA-TCA-ACG-TTT	Devereux *et al* . (1992)
		Desulfosarcina		
		Desulfobotulus		

pathway produces methane as the sole carbon product (Robinson and Tuovinen, 1984; Nakamura *et al*. 1990). Alternatively, Oremland *et al*. (1991) suggested that methylmercury can be transformed through an oxidative demethylation (OD) pathway, in which methylmercury serves as an analog for a single-carbon substrate, producing carbon dioxide as the sole carbon product (Figure 2.4 b). The resulting mercuric ion, Hg^{2+}, is reduced to elemental mercury through an enzyme-mediated mercuric reductase pathway, which involves a *mer*A enzyme (Barkay *et al*. 1991). Studies on these demethylation pathways have been expanded to include the use of transgenic plants that express and modify the bacterial *mer*A and *mer*B genes. Plants which contain the *mer* genes could potentially convert toxic mercury (divalent mercury and methylmercury) to the less toxic, elemental mercury and provide another approach to the remediation of mercury (Rugh *et al*., 1996).

$$\text{Pyruvate} + \text{THF} \rightarrow \text{CH}_3\text{-THF} + \text{CO}_2$$

$$\text{CH}_3\text{-THF} + \text{Co-Corrinoid} \xrightarrow{\textit{Methyltransferase I}} \text{CH}_3\text{-Co-Corrinoid}$$

$$\text{CH}_3\text{-Co-Corrinoid} + \text{Hg}^{2+} \xrightarrow{\textit{Methyltransferase II}} \text{Co-Corrinoid} + \text{MeHg}^{+}$$

Fig 2.3 Mercury methylation pathways

a. Organomercurial lyase (OML) pathway: $CH_3Hg^+ \rightarrow \mathbf{CH_4} + Hg^{2+}$
b. Oxidative (OD) Pathway: $CH_3Hg^+ \rightarrow \mathbf{CO_2} + Hg^{2+}$

Fig 2.4 Mercury demethylation pathways

Although it has been accepted that sulfate-reducing bacteria help mediate mercury transformation in estuarine sediments, not much is known about the community structure and abundance of bacteria concerning these processes. Early investigations into characterizing the community structure involved anaerobic enrichment and isolation procedures (Compeau and Bartha, 1985; Choi and Bartha, 1994; Pak and Bartha, 1998a). These studies proposed that *Desulfovibrio desulfuricans* was the predominant methylator of mercury when sulfate is limiting and when electron donors, such as acetate, lactate, and pyruvate, are available. However, a preponderance of evidence has indicated that microorganisms capable of sulfate reduction are currently thought to be more phylogenetically diverse than once thought (Rooney-Varga *et al.* 1997). Current molecular methods, including 16S ribosomal RNA (rRNA) sequence-based methodologies, have facilitated identification and characterization of microorganisms that participate in methylation and demethylation in estuarine sediments. *Desulfobacter* and *Desulfococcus* sp. have also been identified by 16S rRNA sequence methodologies as SRBs capable of methylating mercury (Devereux *et al*. 1995). Recent data suggest that members of the *Desulfobacteriaceae* family are better methylators than other SRB groups when acetate is available (Hines *et al*., 1999; King *et al.*, 2000).

In contrast, information is very limited regarding bacterial populations involved in demethylation of mercury. M. Shariat *et al*. (1979) tested forty strains of bacteria capable of demethylating methylmercuric chloride. Over 60% of mercury demethylation occurred in aerobic organisms, including *Serratia marcescens, Nitrobacter freundii,* and *Pseudomonas fluorescens*. Of the four anaerobes tested, only *Desulfovibrio*

desulfuricans, demonstrated demethylation capabilities. In addition, 20-84% demethylation occurred under aerobic conditions, while only 32% demethylation occurred during anaerobic screening of *Desulfovibrio desulfuricans* (Shariat *et al*., 1979).

Oremland *et al*. (1991) suggest that SRB and methanogens are involved in oxidative demethylation of methylmercury. Their findings propose that sulfate-reducers dominate estuarine sediments, while methanogens compete with sulfate-reducers in freshwater sediments (Oremland *et al*., 1991; 1995). However, mercury resistant bacteria that specifically use the organomercurial lyase pathway have not been isolated. On the other hand, several bacterial isolates that do not contain the necessary *mer* genes have demonstrated the ability to volatilize mercury (Reyes *et al*., 1999). Therefore, other pathways may exist which provide possible mechanisms of mercury detoxification in marine microbial communities.

Influence of *Spartina alterniflora* on Microbial Community Structure and Biogeochemistry in Salt Marsh Systems

Microbial activity in estuarine sediments is influenced by local vegetation activities. *Spartina alterniflora* marsh grass populates extensive regions of the eastern and gulf coasts. Studies indicate that *Spartina* concentrates mercury from the sediment into its aboveground parts (Newell *et al.,* 1982). In addition, it has been reported that *Spartina* influences metal cycling and speciation in sediments belowground. Methylation activity is highest at the root zone, or rhizosphere, where carbonaceous nutrients are present in root-exudates (Howes *et al.,* 1981). Sulfate-reducing bacteria methylate

mercury year round, but an accumulation of monomethyl mercury only occurs after senescence of the annual crop in the fall (Weber *et al*., 1997). Presumably, during the growth season of *Spartina*, demethylation outcompetes methylation, and thereby prevents the accumulation of methyl mercury (Weber *et al*., 1997). Methyl Hg availability is affected by sulfate reduction and by the presence of vegetation. Moreover, *Spartina* root tips have substantial capacity to oxidize sulfide in both low- and high-sulfide environments, thereby preventing sulfide accumulation (Kraus and Doeller, 1999). Very little quantitative information regarding sulfide oxidation is available in the literature. Therefore, a better understanding of how *S. alterniflora* influences microbial diversity and biogeochemistry of marine sediments is a fundamental objective.

Sulfate Reduction Coupled to Mercury Methylation

The chemical mechanisms controlling Hg speciation have been reviewed (Compeau and Bartha, 1985; Gilmour and Henry, 1991). Based on these studies, mercury methylation is coupled to sulfate reduction catalyzed by sulfate reducing bacteria (SRB). Several factors may influence the activity of SRB populations including: salinity, pH, alkalinity, sulfate, sulfide, dissolved organic carbon, and the bioavailibility of ionic mercury (Gilmour and Henry, 1991).

King *et al*. (1999) established a quantitative framework for the coupling of sulfate reduction to mercury methylation in salt marsh sediments. Sediment cores obtained from a salt marsh located on Skidaway Island in Savannah, Georgia revealed similar trends in sulfate reduction rates and mercury methylation rates (Figures 2.5 and 2.6). A

preliminary model was used to quantitatively define the relationship between sulfate reduction rates (SRR) and mercury methylation rates (MMR):

$$\frac{d[CH_3Hg^+]}{dt} = f^* \frac{-d[SO_4^{2-}]}{dt} * \frac{[Hg^{2+}]}{K_{Hg^{2+}} + [Hg^{2+}]}$$

where MMR = $d[CH_3Hg^+]/dt$

SRR = $-d[SO_4^{2-}]/dt$

In this model, methylation rates are dependent on mercury concentration, a mercury half-saturation constant, and the ratio of the rate of mercury methylation to sulfate reduction, *f*. An f_{max} term was used to define the ratio of MMR and SRR at mercury saturation:

$$f_{max} = \frac{MMR}{SRR}$$

The resulting equation is:

$$f_{max} = f^* \left\{ \frac{[Hg^{2+}]}{\left(K_{Hg^{2+}} + [Hg^{2+}] \right)} \right\}$$

King *et al.* (1999) confirmed this relationship in laboratory sediment slurries and in whole sediment cores. Values for f* were derived for each SRB phylogenetic group using pure cultures. These values are represented in Figure 2.7. There was a 100-fold difference between f* values determined for genera *Desulfobacterium* and genera – *Desulfovibrio*. Acetate-utilizing *Desulfobacterium* members methylated Hg at much higher rates than non-acetate-utilizing *Desulfovibrio* members. Therefore, the ability to

use acetate for carbon metabolism is a significant factor in determining the incidence of mercury methylation among different phylogenetic groups.

In summary, mercury methylation is closely linked to sulfate reduction and both processes are primarily controlled by microbial and plant activities. However, not much is known about how these drivers influence each other and the specific impacts both have on mercury methylation. This project intends to provide more viable information on these processes.

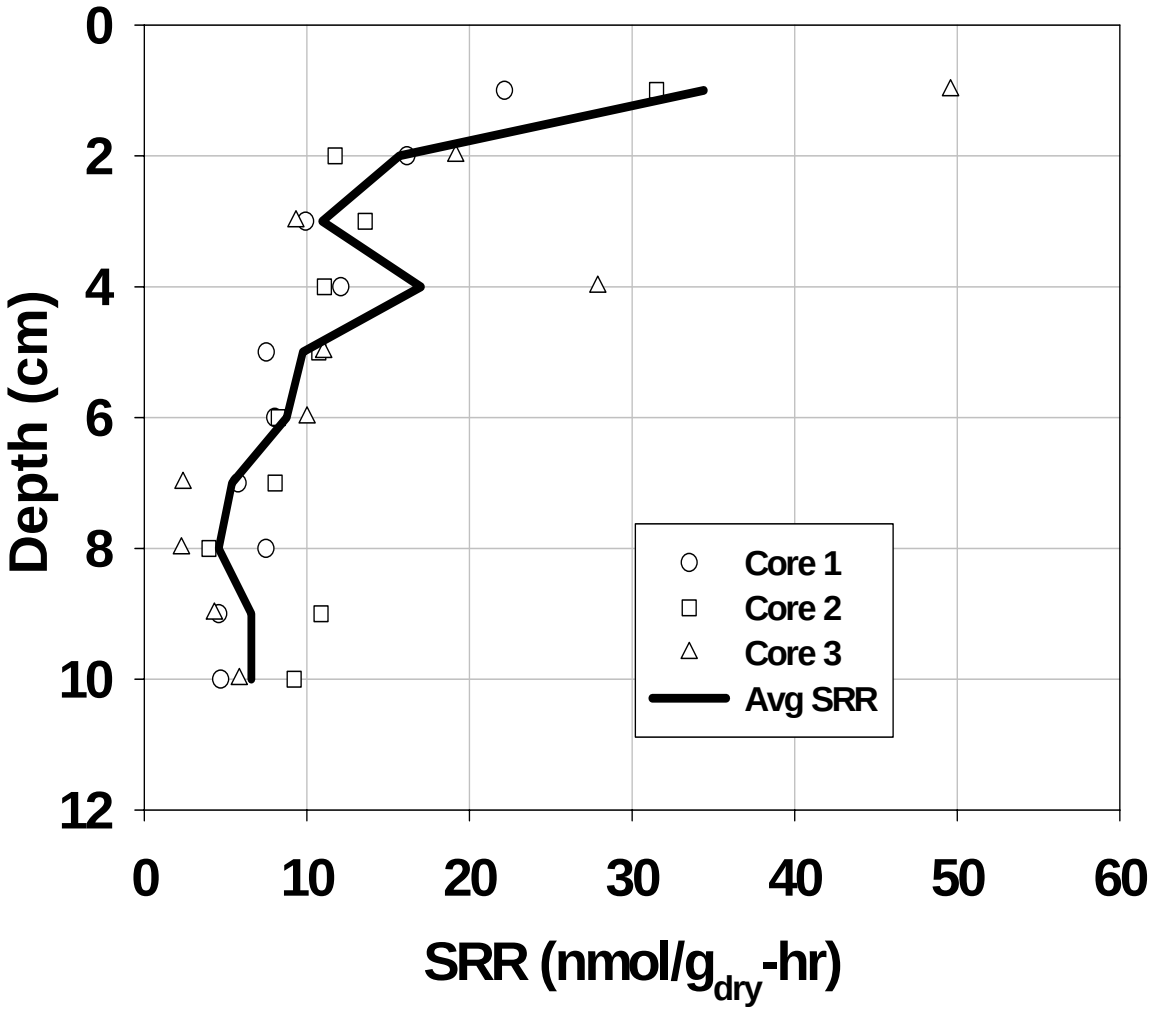

Figure 2.5 Sulfate reduction rates (SRR) in sediment cores from tidal marshes at the Skidaway Institute of Oceanography (King *et al*., 2001).

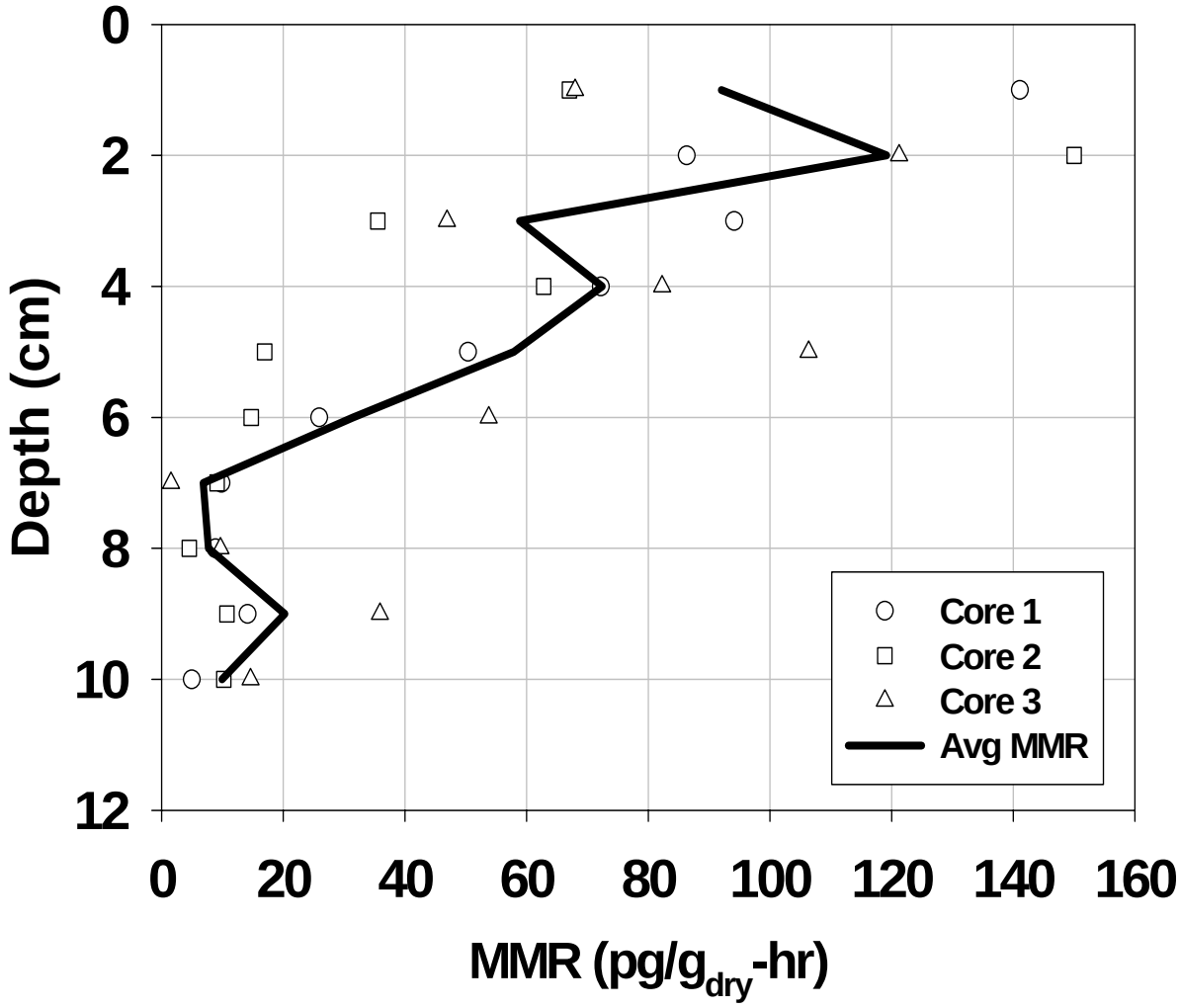

Figure 2.6 Mercury methylation rates (MMR) in sediment cores from tidal marshes at the Skidaway Institute of Oceanography (King *et al*., 2001).

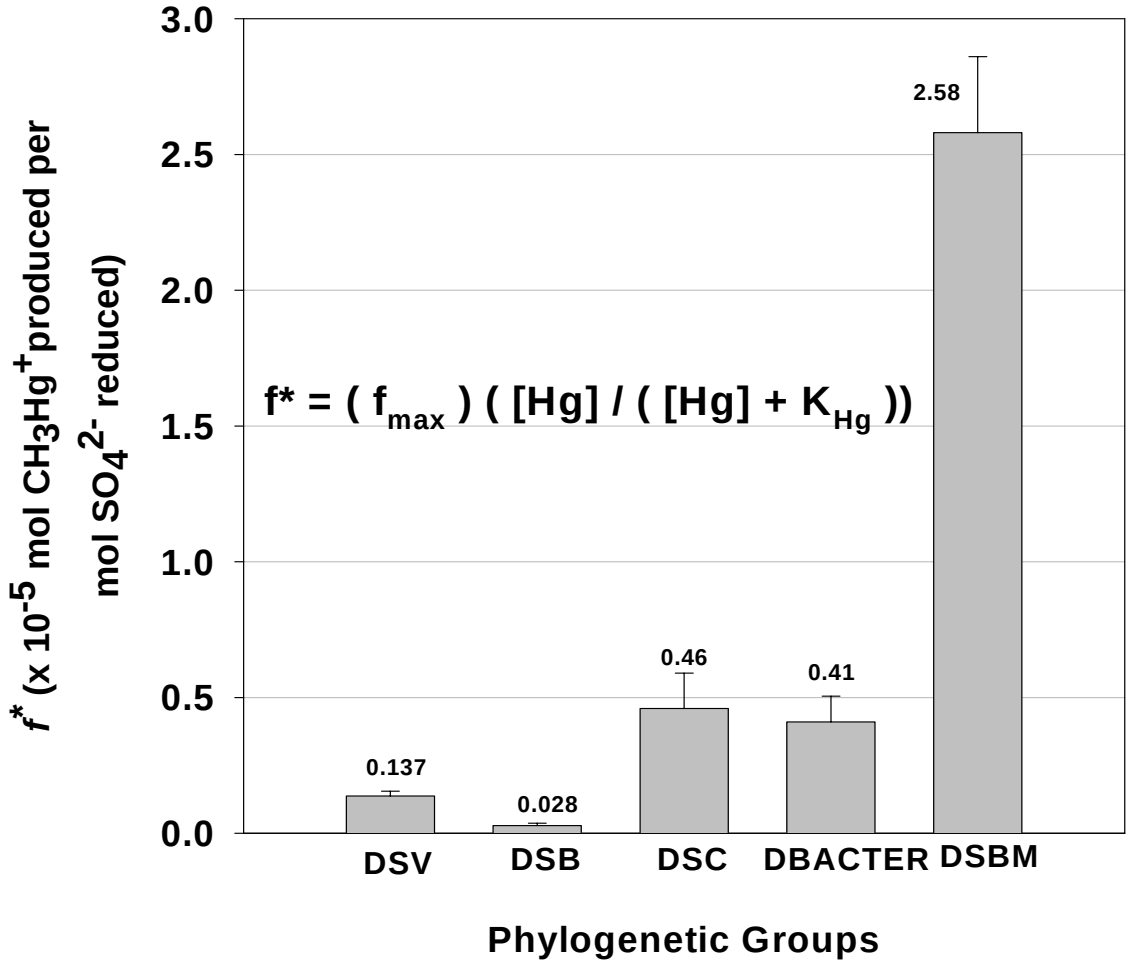

Figure 2.7 Values of f* for sulfate-reducing bacteria phylogenetic groups (King, 1999).

CHAPTER III
MATERIALS AND METHODS

Site description

The research was conducted in the Bioremediation and Environmental Research Mesocosm (BERM) facility located in Savannah, Georgia at the Skidaway Institute of Oceanography. This facility consists of a greenhouse, several mesocosms, and a laboratory. Three mesocosm cells (Figure 3.1) were established with the following sediment characteristics: pristine vegetated (M1); contaminated and vegetated (M2); contaminated and unvegetated (M3). Pristine sediment was obtained from Priest's Landing (Grove's Creek) on Skidaway Island, Savannah, Georgia. "Pristine" in this report means that the sediment was not intentionally contaminated with mercury. It does not mean that the sediment does not contain any mercury in the conduct of the experiment nor from previous anthropogenic activities affecting the sediment. "Contaminated" sediment, containing approximately 10 mg/kg mercury, was obtained from the perimeter of a highly contaminated Superfund site (LCP Chemicals site), located in Brunswick, GA. The site once held a chlor-alkali plant, which operated until 1994, where chemical wastes were disposed on-site into adjacent marsh dominated by *Spartina alterniflora* and *Juncus romerianus*. Mercury levels range from parts per thousand near the site and to parts per million in the marsh.

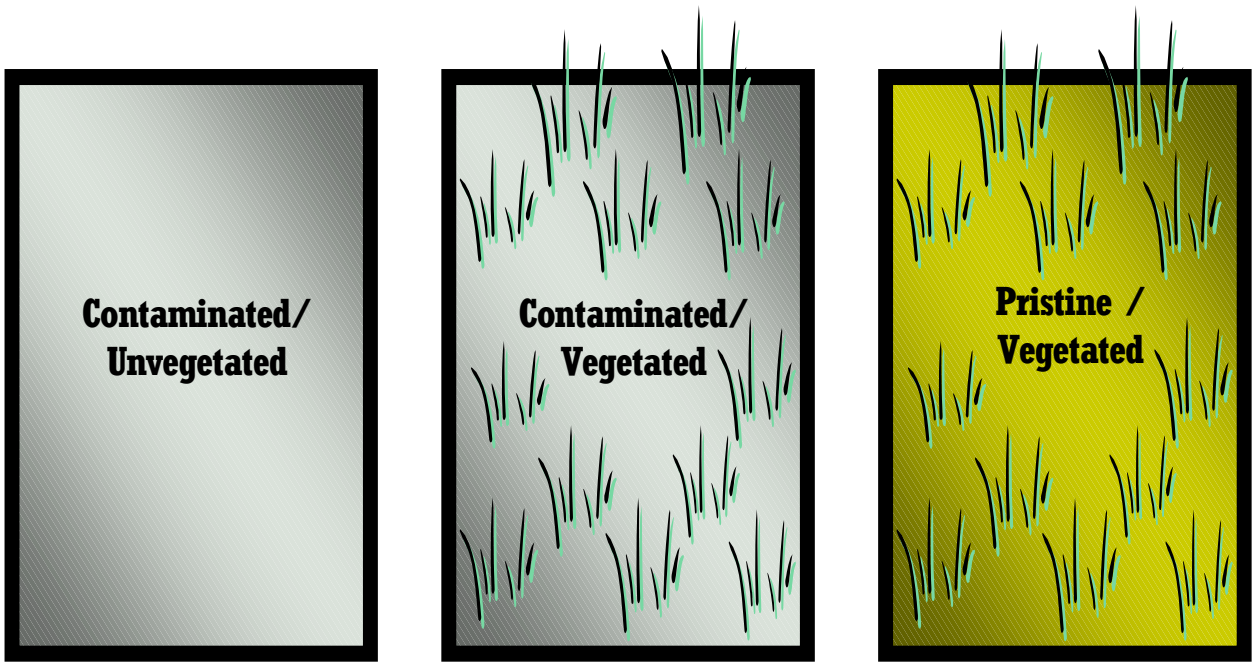

Figure 3.1 Schematic of BERM mesocosms.

Bioremediation and Environmental Research Mesocosms

The Bioremediation and Environmental Research Mesocosm (BERM) facility was the primary sampling site for this study. Each mesocosm cell is approximately 3.05 m (10 ft.) long, 1.52 m (5 ft.) wide, and 1.52 m (5 ft.) in depth. Each mesocosm contains approximately 97 cm (38 in.) of sediment and 15.2 cm (6 in.) of drainage stone underneath the sediment. An erosion-control cloth (0.15-mm–thick) was placed between the sediment matrix and a fiber-reinforced polyethylene sheeting (0.15-mm –thick).

Influent and effluent filtered seawater was controlled by a piping system as shown in Figure 3.2. The Skidaway River, which is located approximately 810 ft (247 m) from the facility, was the source of water for the BERM facility. The river water had salinities ranging from 29 to 36 ppt during the summer of 2000, which were uncharacteristically high due to very little rainfall. Water is pumped continuously at the river boat dock, through a boat-dock filter, and through a vertical rock filter at the BERM before it reaches a concrete holding tank. From the concrete tank, the water is distributed to several elevated reservoir tanks (5000-L capacity). These tanks are situated at 2.1 m (6.75 ft.) above the mesocosms to maintain a constant head via an overflow orifice.

Time-activated programmable logic controllers (PLCs) regulate the flow of water in the mesocosms and essentially control the tidal cycles. Figure 3.3 shows the actual time segments in the tidal cycle. A tide cycle of 12.75 hr has been programmed and used to equilibrate each mesocosm since Fall 1999. Each mesocosm is regulated by a separate PLC, each of which controls the influent and the underdrain PLC valves. When influent

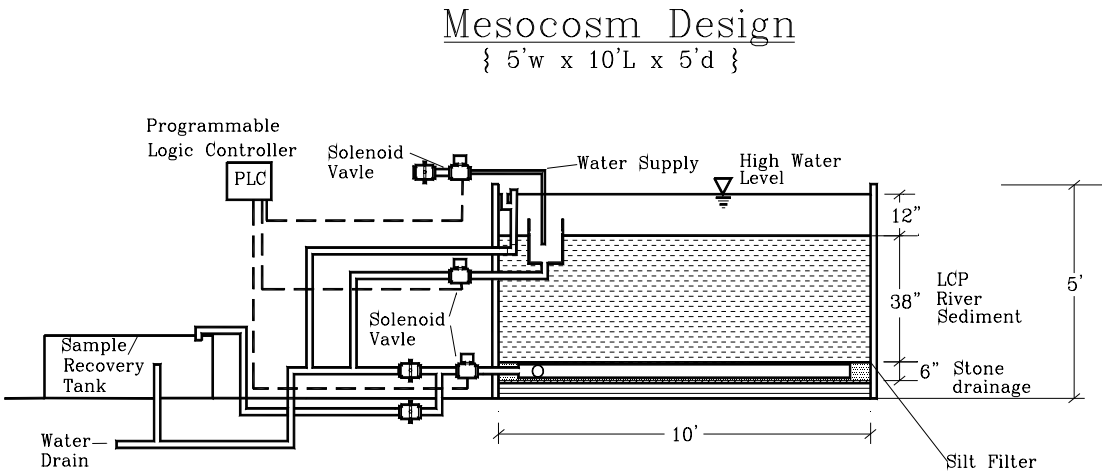

Figure 3.2 Schematic of the piping system and electronic control system for the BERM.

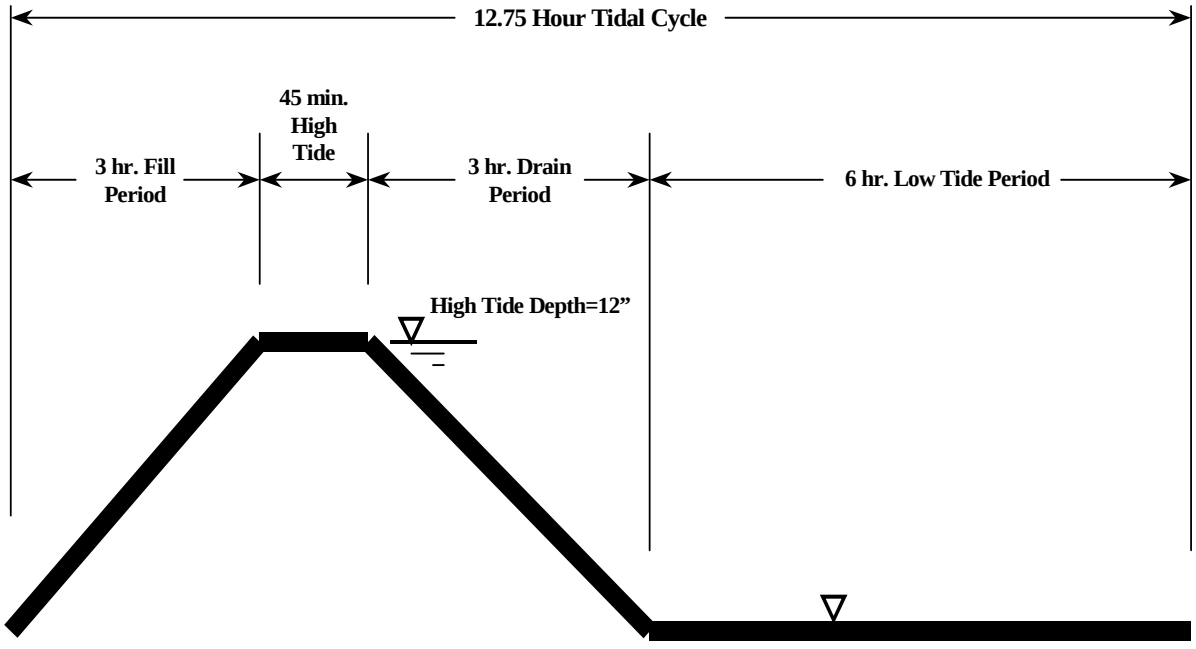

Figure 3.3 Schematic of tidal cycle in BERM mesocosms.

PLC valves are open, influent water travels by gravity to the mesocosms and floods the sediment.

A 0.64-cm diameter orifice was drilled in a pipe slip cap and attached to the end of the influent line. This orifice is connected to a manual gate valve to control influent flow rates. This orifice size was chosen to obtain the desired flow rate and tidal flooding period. Influent water flows into a 30.5-cm diameter plastic bucket for energy dissipation. The bucket is approximately 0.6 m deep, with half of this depth below the sediment elevation. As the bucket fills, water flows through a series of 2.5-cm diameter orifices at the sediment surface, which allows for simulation of a smooth incoming tide along the surface of the marsh.

Each mesocosm features two separate drainage systems. Surface drainage occurred through the same bucket previously discussed. In surface drainage, water re-enters the bucket through the orifices at sediment elevation. Once in the bucket, water exits the mesocosm through a 10.2-cm diameter hole at the bottom; a manual gate valve and a PLC valve control the flow through this orifice. This surface mechanism allows the mesocosm to drain without any significant drainage through the sediment or through any potential cracks developing between the mesocosm sides and the sediment. The PLC valve for surface drainage of all three mesocosms is controlled by a single PLC (#4) which is different from the other PLCs (#1, #2, #3). Once the PLC valve opened for surface drainage, effluent flow rate from each mesocosm was controlled not by the diameter of the outlet pipe, but rather by partially closing the manual gate valve in order

to restrict outflow. The manual gate valve in each of the three mesocosms was manipulated to achieve the desired tidal drainage period.

For each mesocosm, effluent from the surface drainage system can be directed back to the river or to an effluent holding tank (6,000-L capacity) for evaluation and treatment if required. A T-section in the effluent piping system with a gate valve allowed for selection of outflow destination; for this study, surface drainage was directed back to the river.

Each mesocosm also featured a bottom drainage system, also known as the Underdrain. The underdrain consists of a grid of perforated PVC pipe located within the drainage stone at the bottom of each mesocosm. This system in effect flushes porewater from the sediments and drainage stone. Water that had drained through the marsh sediment could be collected for study. A mass balance on pertinent sediment and porewater parameters could be conducted with samples from this bottom drainage. Three PLCs (#1, #2, #3) and a set of PLC valves governed flow through the underdrain.

Just as with the surface drainage mechanism, effluent from the underdrain could be directed back to the river or to an effluent holding tank for evaluation and treatment. A T-section in the effluent piping system with a gate valve allowed for the selection of outflow destination; for this study, bottom drainage was directed to the effluent holding tank.

An overflow weir system allowed for drainage when the mesocosm water depth reached the maximum tidal depth. This system consisted of a 7.62-cm -diameter vertical primary overflow pipe at the maximum tidal depth (approximately 30.5 cm) above

sediment elevation. An additional 7.62-cm diameter emergency overflow pipe is located adjacent to, and 2.5 cm above, the primary discharge pipe. This emergency pipe is used in the event that the primary overflow became clogged. Overflow water could be directed back to the river or to an effluent holding tank for evaluation and treatment. A T-section in the effluent piping system with a gate valve allowed for the selection of outflow destination. For this study, overflow was directed back to the river.

The surface drain and the two overflow pipes were protected from foreign materials and clogging by a retrofit system. This consisted of an oversized-diameter perforated bucket or pipe around each unit. Any material that could potentially obstruct the outlets was impeded by the perforations in the retrofit pipe. It should also be noted that PLC valves, although timed, could be taken apart and opened or closed manually, if necessary.

Sample Collection

To monitor the seasonal cycle in salt marsh sediments, three major sampling events were performed in July 2000, February 2001, and May 2001. Intact sediment cores were collected from each mesocosm using small coring devices made of Lexan (15-cm length, 2-cm i.d). The core barrels have 1-mm diameter portals drilled into them at 1-cm intervals. These holes were sealed with silicone sealant to maintain anaerobic conditions but also to allow syringe needles to pass through for injections. Sediment cores over a seasonal cycle were obtained and immediately transported to the laboratory. Cores were then anaerobically divided into 2-cm increments in a glove bag. The following analyses were delivered for each core sample:

1) Sulfate and Sulfide Analysis: Single core per mesocosm
2) Sulfate Reduction Analysis: Triplicate cores per mesocosm
3) Total Mercury Analysis: Duplicate cores per mesocosm
4) Density/Porosity: Single core per mesocosm
5) Microbial Analysis: Duplicate cores per mesocosm

Core sediment was used for sulfate reduction rates, density and porosity and microbial analyses. For sulfate, sulfide, and total mercury analysis, porewater was extracted from core sediment as described below.

Porewater Extracted from Cores

All cores for sulfate, sulfide, and Hg analysis were divided into 2-cm increments (0-2, 2-4, 4-6, 6-8, 8-10 cm depths) and placed in separate centrifuge tubes inside a glove bag. The tubes were centrifuged at 4,200 x g (5000 rpm) for 10 min (Eppendorf Centrifuge Model #5416) and porewater was filtered through a 0.2 µm acid cleaned (6N HCl) nylon filter under anaerobic conditions. The porewater was partitioned as follows:

1) Sulfate Analysis: A volume of 500 µL porewater sample was acidified with 4 µL concentrated HCl. The samples were stored at 4 ºC until analysis.
2) Sulfide Analysis: A volume of 250 µL of porewater sample was fixed with 100 µL 20% zinc acetate (ZnAc). Samples were stored at 4 ºC until analysis.
3) pH: For any remaining porewater sample, 250 to 500 µL was used for measuring pH using a pH electrode (VWR Scientific) under anoxic conditions.

4) Total Hg Analysis: All of the porewater collected (at least 2 mL) from the each Hg core was acidified to 0.2 % with 18N H_2SO_4 and stored at 4 ºC until analysis. It was determined from a separate experiment that the volume of sample had a huge impact on the resulting concentration of total Hg (discussed in later section).

Porewater Extracted from Sippers

Sediment porewater was also collected using *in situ* sipper systems. The sipper stakes are constructed of high-density polyethylene (HDPE) and have a porous HDPE collar located at the required sampling depth (Short *et al*. 1985). Sippers and glass syringes were routinely cleaned with 6N HCl sufficiently to rid of mercury contamination prior to sampling. Porewater from sippers were collected at 3-, 6-, and 10-cm depths. Porewater was extracted from the sipper into argon-flushed glass syringes by applying a mild vacuum and replacing the extracted volume with ultra high purity (UHP) argon passed through a gold trap. A gold trap consisted of gold-coated sand in a quartz tube and prevented Hg contamination from the air from getting into the porewater sample. Pore water is then filtered through a 0.2 µm nylon filter. Porewater extracted from acid-cleaned sippers (in 6N HCl) was collected for colorimetric analysis of sulfate and sulfide, and for cold-vapor atomic fluorescence analysis of methyl mercury. Approximately 500 µL and 250 µL of porewater from each sample were placed in 2-mL gas-tight vials (Fisher Scientific) for sulfate and sulfide analysis, respectively. Porewater from sippers was not used for total Hg analysis because contamination problems arose and could not be prevented.

At least 3 mL of porewater was extracted from separate sippers for methyl mercury analysis. Methyl mercury samples were acidified to 0.2% using 18N H_2SO_4 and stored at 4 ºC until analysis.

Water was also collected from the inlet and outlet tanks by placing tubes under the inlet and outlet stream, or with a sipper. These samples were collected for colorimetric analysis of sulfate and sulfide.

Physical Characteristics of the BERM mesocosms

Sediment Density and Porosity

Duplicate sediment cores were taken from each mesocosm and sectioned into 2-cm increments into a plastic syringe. Each lift was homogenized using a small metal spatula. From this homogenized sediment, duplicate density/porosity samples were taken.

Syringes were cut to have a flat open end so that a known volume of wet sediment could be measured and extracted from the syringe. Wet sediment was inserted into a 3-mL plastic syringe. One cubic centimeter of wet sediment was extracted into pre-weighed polyethylene scintillation vials. The wet weight of the sediment was determined by weighing the sediment-filled scintillation vial and subtracting the vial weight. Dry sediment fraction was determined by drying the known volume of sediment at 75°C for 48 hr in an oven. Saturated bulk density (g/cm^3) was calculated by the following equation:

$$\rho_b = \frac{\text{wet weight of sediment}}{\text{sediment volume}}$$

Since the mesocosm sediments are waterlogged, saturation is assumed to be 100 percent. The porosity is based on the dry weight and wet weight of the sediment and based on mass and density of Skidaway River water (density = 1.02 g/cm^3) that occupied the void volume of sediment as shown below:

$$\Phi = \frac{\text{void volume}}{\text{total sed. vol.}}$$

The particle density of the sediment was based on the following equation:

$$\rho_p = \frac{(X_p * \rho * \rho_w)}{\rho_w - (\rho * X_w)}$$

X_p = mass fraction of dry particle (g/cm^3)

X_w = mass fraction of water (g/cm^3)

ρ = wet density (g/cm^3)

ρ_p = particle density (g/cm^3)

ρ_w = density of Skidaway River water (g/cm^3)

Underdrain Effluent Volume

The volume of effluent was measured from each mesocosm by placing a 250 L drum under the outflow of the under-drainage pipes. The effluent from the outlet pipes was collected during underdrainage of the individual mesocosms. The measurements were recorded during each sampling event.

Temperature

Sediment temperature was recorded in all mesocosms using a mercury thermometer during each sampling period. An average temperature measurement was taken at a 5 cm depth since temperatures within the top 10 cm of the sediment did not vary significantly. The temperature only varied between 1-2 °C throughout the day, and the temperature differences between the sediment and the overlying water only varied by < 1 °C.

Salinity

Salinity of surface water was determined using a refractometer (Fisher-Scientific #13-946-27, salinity meter with automatic temperature compensation). The refractometer was calibrated with de-ionized water and considered to have a salinity of zero. A few drops of water were placed on the refractometer prism surface using a plastic pipette. The reading was allowed to stabilize for 15 sec and recorded. After each reading, the prism was cleaned with deionized water and wiped dry with a sterile tissue.

Above-ground *Spartina* Biomass Analysis

Since 1998, three indicators of plant growth in the vegetated mesocosms were observed: the height of the tallest shoot for each *Spartina* plant, the number of shoots per plant, and the number of plants in the mesocosm. By 2000, these parameters had reached a near maximum. The number of shoots and the number of plants were too numerous to count, but the height of the tallest shoot was regularly measured during the third year of this project. The shoot heights were measured using a ruler.

Mesocosm Restoration and Maintenance

Sampling with core barrels and sippers caused a moderate amount of disturbance in the mesocosm sediments. Holes had to be refilled with sediment to prevent further intrusion to the BERM mesocosms. Sampling holes were filled by gently applying pressure around the hole, pushing out any water that had accumulated in the open hole. The mesocosm repair was conducted no longer than a day after sampling in order to allow for maximum equilibration time before the next sampling.

Algal mats and any plant growth in the unvegetated mesocosm were removed to maintain the mesocosm in an unvegetated state. Algal mats grew rapidly during the summer months of May-September. To remove algal mats, a jagged edge paint scraper was applied lightly across the sediment surface. Algal mats that grew in the reservoir tank were removed with a skimmer. When pipes became clogged and pressure loss was evident in the influent line, foreign matter was forced out by manually opening the pipe joints and applying water pressure from a garden hose inside the pipes. The algae was collected in plastic bags, weighted, and frozen until analysis. For unwanted plant growth in the unvegetated mesocosm, shoots were removed gently from the sediment.

Porewater Geochemistry Experimental Methods

pH Analysis

A pH electrode (Orion # 8175BN Sure Flow Semi-Micro Ross Combination pH Electrode) and a pH meter (Orion Model 611 pH/millivolt Meter) were used to determine the pH of sediment porewater. The electrode was calibrated using 4.0, 7.0 and 10.0 pH buffer solutions. The electrode was placed directly into the filtered porewater sample and the reading was stabilized after one minute.

Porewater Sulfate Analysis

The turbidometric method for sulfate measurement is outlined in Tabatabai (1974). This method measures turbidity formed from mixing barium chloride gelatin with an acidified water sample and correlates turbidity with sulfate concentration.

Barium chloride gelatin reagent was prepared by dissolving 1.5 g solid gelatin in 500 mL of de-ionized water at 70°C using a graduated cylinder and mixing on a hot stir plate until dissolved. The gelatin solution was stored in a plastic bottle for 24 hr at 4°C before use. One gram of solid barium chloride monohydrate was dissolved in the gelatin solution to a volume of 100 mL and the solution was incubated at room temperature for one hour. Barium chloride gelatin is good for one week. Sulfate standards were made at concentrations of 10, 20, and 30 mM using Na_2SO_4 and stored in the refrigerator at 4°C. Standards are good for up to one year. Each polypropylene tube was filled with 10 mL of distilled water, 500 µL 1N HCl, and 40 µL of acidified sample. In time increments of 30

sec, 50 µL of barium chloride gelatin were added to each sample. The sample was covered with parafilm and mixed gently. After 30 min of incubation at room temperature, each sample absorbance was recorded at 420 nm using 4 cm quartz cells in a spectrophotometer. A detection limit of 0.48 mM was ascertained. The sulfate standard curve generally had r^2 values greater than 0.9975.

Dissolved Sulfide Analysis

The method for measuring dissolved sulfide is outlined in Cline (1969). An appropriate amount of Cline reagent is added to the sample and the measured absorbance is correlated to dissolved sulfide concentration. Cline reagent was prepared by dissolving 2.0 g of diamine and 3.0 g of ferric chloride in 6N HCl for a total volume of 500 mL. Solution should be a deep yellow and refrigerated at 4°C until use. Dissolved sulfide reacts with the Cline reagent to produce a blue color.

Standard solutions were prepared anoxically using sodium sulfide and water was purged with nitrogen gas. Two 500-mL bottles were filled with distilled water and bubbled with N_2 gas for 1 hr. A small Na_2S crystal was cleaned with distilled water and dried with a sterile tissue. The crystal was weighed and immediately placed in one of the bottles of anaerobic water. Sulfide standards were prepared in concentrations of 2.5 µM, 5 µM, 15 µM, and 30 µM using 300 µL of 20% ZnAc; i.e., 100 µL of 20% ZnAc per 250 µL standard.

Distilled water was added to the samples to bring the solution up to 1 mL. Cline reagent was added to the acidified samples and standards at a ratio of 80µL to 1 mL of

sample or standard. Some samples were diluted when the resultant concentrations were out of standard curve range. After 15–20 min, the absorbance was read at 670 nm using 1 cm cells. A detection limit of 0.25 mM was ascertained and standard deviation of 3.0% was determined based on data by Cline (1969). Standard curves usually had r^2 values greater than 0.994.

Sulfate Reduction Rate Measurement

The technique of determining sulfate reduction rates using a radioactive tracer ($^{35}SO_4^{2-}$) using a two-step method has been described by Fossing and Jorgenson (1989) and King *et al*. (1999). The core barrels used in sampling have 1-mm holes drilled into them at 1 cm intervals. These holes are sealed with silicone to maintain anaerobic conditions but also allow syringe needles to pass through for injections.

Prior to analysis, a solution of chromium (Cr^{3+}) was reduced to reactive Cr^{2+} by percolating 200 g $CrCl_3 \cdot 6H_2O$ in 0.5N HCl to a volume of 750 mL through reduction with "mossy zinc" granules. Zinc granules were first washed with 6N HCl and then twice with distilled water. The granules were then placed in a bottle and the Cr^{3+} solution was poured into the bottle. The mixture is bubbled with N_2 gas until there is a color change from dark green to bright blue, which indicates a reduction in chromium.

Immediately after sampling, the cores were injected with 6 µL of $^{35}SO_4^{2-}$ radioactive tracer at 2-cm intervals down to a 10-cm depth and incubated for 2 hr. Background (control) cores were not incubated, but immediately sectioned in 2-cm increments into 10 mL 20 % ZnAc. After incubation, the cores were sectioned into 10

mL of 20 % ZnAc and vortexed well to fix any free sulfide present and to "kill" further microbial activity. The samples were frozen until further analysis.

In preparation for the distillation method for sulfate reduction rate measurement, samples were returned to room temperature and spun-down at 4,200 x g (5000 rpm) for 10 min. The spun-down sediment was weighed, and 100 μL of the pore water sulfate was counted using a scintillation counter (Beckman LS 3500). The remaining pore water was discarded into the ^{35}S waste container. After the sediment was washed with N_2 purged de-ionized water, one gram of sediment was transferred to a round bottom flask of a distillation apparatus. The distillation apparatus consisted of several gas-tight round-bottom reaction flasks that were each supplied with a gas-bubbling tube, a condenser, and a zinc acetate trap. The unit was continuously purged with N_2 gas.

The acid-volatile sulfide (AVS), which consists mainly of hydrogen sulfide, was volatilized by the addition of 8 mL of 12N hydrochloric acid. The slurry was distilled for 30 min and the reduced AVS was collected in the first trap containing 10 mL of 5 % (w/v) zinc acetate (ZnAc). The chromium-reducible sulfur (CRS), which includes pyrite and elemental sulfur, was produced by adding 15 mL of boiling reduced chromium, Cr^{2+}. The slurry was allowed to boil for 45 min and CRS was collected in a second trap containing 20 mL of 20 % ZnAc. Radiolabeled AVS and CRS were counted using the scintillation counter, and their concentrations were determined using Cline's method (see previous section).

The equation used to calculate sulfate reduction rates for a particular sediment sample is as follows:

$$SRR = [SO_4] * \frac{\text{TRS cpm}}{\text{g sediment distilled}} * \frac{\text{g sediment incubated}}{\text{time incubated}} * \frac{1.06}{\text{porewater cpm}} * \Phi$$

SRR = sulfate reduction rate (nmol/cm^3-day)

$[SO_4]$ = sulfate concentration (nmol/mL)

cpm = radioactive counts per minute for ^{35}S

TRS = total reducible sulfur (AVS + CRS)

1.06 = isotope fractionization factor (Fossing and Jorgenson, 1989)

ρ_b = bulk density (g/cm^3)

ρ_p = particle density (g/cm^3)

ρ_w = density of Skidaway River water (g/cm^3)

Φ = porosity of sediment (cm^3/cm^3)

Fossing and Jorgenson (1989) found standard deviation values ranging from 0.39 % to 2.985 % for sulfate reduction rates ranging from 33 to 83 nmol/cm^3-day. In addition, they found standard deviation values ranging between 2.8 to 6.7 % for AVS concentrations of 6.2 to 19.3 nmol/cm^3. Standard deviations for CRS ranged from 3.8 to 9.7 % for concentrations from 12.4 to 151.9 nmol/cm^3. These standard deviations were applicable to the measurements in this study to assess the validity of the data points.

Extraction of Porewater for Total Mercury Analysis

Total Hg determination in the porewater was determined according to a modified version of EPA Method 1631. Total Hg in the sediment was not analyzed during this period since prior studies established that solid-phase Hg levels were consistent with other studies for contaminated and uncontaminated sediments (Sauer, 2003). Additionally, solid-phase mercury compared to porewater mercury does not substantially contribute to mercury bioavailability for SRB-mediated mercury methylation (Benoit *et al*., 1999). Therefore, studies on mercury speciation were focused on the mobile phase, i.e. dissolved mercury. Prior to analysis, 1 mL of a 0.1 bromate/bromide solution was added to the acidified sample to oxidize all forms of mercury to mercuric ion form. This mixture was combined with 2.5 mL of 6N HCl in a pre-weighed 60-mL Teflon vial and then diluted to 25 mL with tap water. After 30 min, 50 µL of hydroxylamine hydrochloride was added to destroy free halogens; the solution was allowed to stand for an additional five minutes.

To begin analysis, a lime trap was connected to a gold trap. The gold trap, as described by Smith (1993), consists of a gold foil (1cm x 10 cm x 0.25 mm) that is rolled and placed in a quartz tube (1/4 in x 15 cm). The lime trap consists of a quartz tube packed with K_2CO_3, which captures acid vapor in the sample stream and thus prevents acid deposition of the gold trap. The upstream end of the lime trap was then connected to the gas-liquid separator (Tekran). Prepared samples were pumped through a peristaltic pump set at 25 revolutions per minute. This setup simultaneously combined stannous chloride ($SnCl_2$) solution with the prepared samples; the $SnCl_2$ reduced all mercury

species to volatile Hg(0) (quicksilver). After reaction with $SnCl_2$, the solution entered the gas-liquid separator and was purged through the lime trap to the gold trap, where mercury vapor was adsorbed. The loaded gold trap was dried for five minutes by purging argon through it at 250 mL/min. The trap was then heated for three minutes (to approximately 350 °C) to thermally desorb Hg into the CVAF detector. Argon flowed through the trap at 60 mL/min. The cold vapor atomic fluorescence (CVAF) detector (Tekran 2500) detector measured the amount of total mercury in the sample stream, and measurement was charted by the integrator (HP 3394) in peak-area mode.

A standard curve was produced from a 5 μg/L stock standard. Standards of 0.5, 0.25, 0.1 0.05, and 0 ng were made in 60-mL Teflon vials containing 2.5 mL of 6N HCl. The correlation coefficient (r^2) of the standard curve was always greater than 0.99. A continuing calibration standard was run after every 10 samples to verify that the instruments remained calibrated.

In previous studies, a detection limit of 0.019 ng was ascertained, based on three times the standard deviation of 0.05 ng replicates. For a typical 2-mL sample, this translates into a detection limit of 9.70 ng/L.

Quality control was ensured by analyzing four replicates of the 0.25 ng standard solution, or the initial precision and recovery sample (IPR). The average percent recovery and standard deviations of the percent recoveries for the four replicates were calculated and compared to the quality control acceptance criteria outlined in EPA Method 1631.

Effect of Sample Volume on Mercury Analysis

Figure 3.4 presents the results of a total mercury volume experiment. This experiment was conducted to determine the minimum sample volume needed to obtain accurate total mercury data. Higher total mercury concentrations were observed in smaller volume samples, while lower concentrations were observed in higher volume samples. Therefore, the experiment was conducted to determine whether sample volume influenced total mercury concentrations. Sediment was taken from Grove's Creek pristine marsh and from LCP contaminated sediment that was stored in the barn freezer. A sample volume at or below 1 mL produced a total mercury concentration greater than 100 ng/L in Grove's Creek sediment and greater than 2000 mg/L in LCP sediment. The experiment demonstrated that a minimum volume of 2 mL was necessary to obtain feasible results for total mercury analysis. However, the minimum volume could not be obtained easily using sippers. Multiple sipper extractions took too much time and placed added disturbance to the mesocosms. Moreover, we observed significantly high total mercury concentrations (> 100 ng/L) in July 2000 and stipulated that contamination was possible in samples collected by sippers. Therefore, only cores were used to collect samples for total mercury in February 2001 and May 2001.

As described by the mercury volume experiment, sample volume impacted mercury results. Traditionally, total mercury is analyzed using at least 10 mL of sample, which is easily obtained from water column samples or surface waters. Pooling of samples from multiple locations has also been done with sediment porewater samples, but this method may sacrifice location- and depth-specific sampling. In our case, taking more cores or

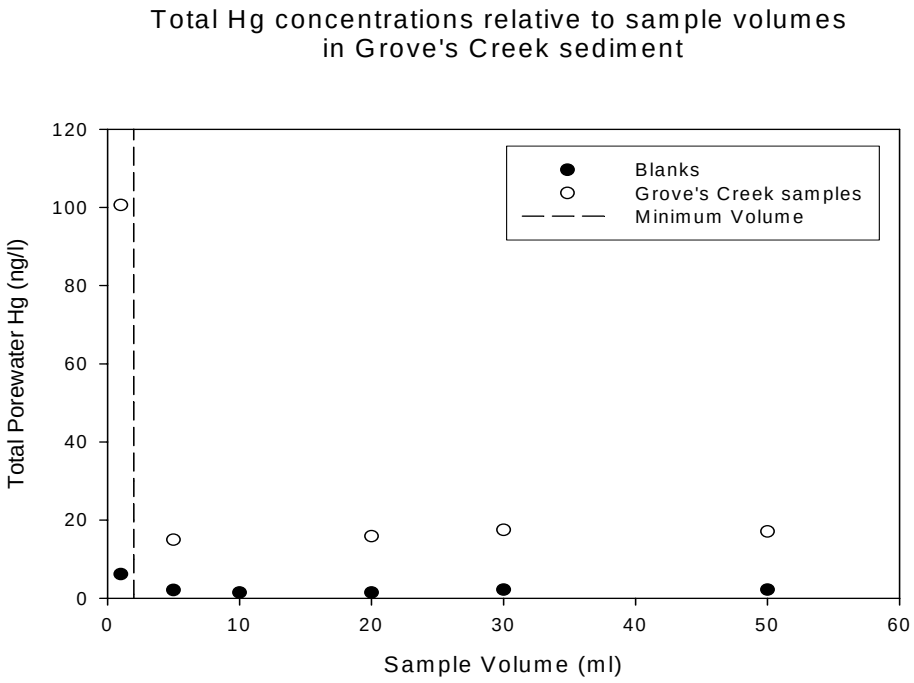

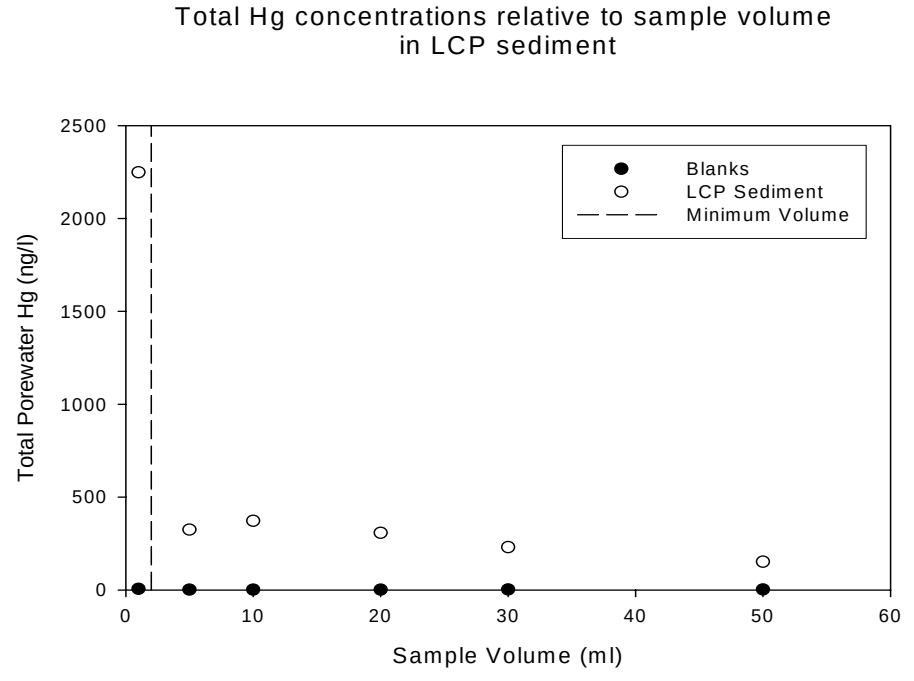

Figure 3.4 Results from the mercury volume experiment. A minimum of 2mL is required for obtaining feasible samples for total mercury analysis.

larger cores would detrimentally disrupt the mesocosms and therefore was not feasible. In addition, since our technique limited our sample volumes to less than 5 mL, a miniscule amount of mercury contamination would greatly skew measurements. If this project had been focused only on mercury analysis and not sulfate biogeochemistry and rate processes, we would have been able to obtain at least 5 mL of sample. In the case of methyl mercury porewater measurements, sample volume was not a concern since contamination was unlikely as long as sample instruments were thoroughly cleaned. The recommendation for future studies is to subscribe to the pooling technique as other researchers have done if feasible.

Extraction of Porewater for Methylmercury Analysis

Methylmercury concentrations in the porewater were determined using a modified version of EPA Method 1631 and following the procedure of Bloom (1989), Horvat *et al*. (1993), and Liang *et al*. (1994). The main difference with this technique from previous techniques is the sample volume; pore water samples were in the 1- 5 mL range and required dilutions with water for analysis. The method was performed by distillation, aqueous phase ethylation, adsorption on a Tenax trap, chromatographic desorption, and CVAF using a Tekron 2500 CVAF detector and HP 3395 integrator (Smith 1993).

Prior to analysis, all Teflon bottles were meticulously cleaned in hot concentrated nitric acid. The bottles were soaked in the nitric acid bath for 3 d upon initial cleaning. Following this procedure, the bottles were rinsed with tap water, and filled with twice-distilled nitric acid. The acid-filled bottles were placed on a hot plate for 3 additional

days. The bottles were then emptied and filled with tap water acidified with 5 mL HCl and stored in tightly sealed ziplock bags.

Distillation was performed using an aluminum heating block and cold-water chiller. In a 30-mL Teflon vial (the distillation vial), several milliliters of pore water were diluted to 10 mL with distilled water. To maintain acidity, 50 µL of 12 N HCl were added. A 60-mL Teflon vial with 7 mL of distilled water served as the collection vial. The distillation vial was placed in the heating block, which was set to a temperature of 145 °C. The collection vial was placed in the chiller and connected to the distillation vial. Distillation continued until approximately 80 % of the 10-mL sample was distilled. Thus, the collection vial was removed from the chiller once it contained 15 mL of distillate (7 ml water + 8 mL distillate). The sample was then diluted to 20 mL with distilled water. Finally, the sample solution was adjusted to a pH of approximately 5.0 by µL -level additions of citrate and 4% KOH. Prepared samples were kept refrigerated in the dark.

Ethylation began with the addition of 60 mL of distilled water and 100 µL of citrate (for acidity) to an ethylation vessel. An aliquot of prepared sample estimated to contain 10- 100 pg of methyl mercury was added to the mixture. Mercury was ethylated by adding 50 µL of ice-cold 1 % sodium tetraethyl borate [$NaB(Et)_4$] and then closing the vessel. A trap consisting of Tenax resin within a quartz tube was connected to the vessel; the set-up was allowed to equilibrate for 15 min. Bubbling of argon (250 mL/min) through the ethylation vessel for 12 min purged the highly volatile ethylated mercury species into the trap. The trap was then dried with argon for seven minutes.

The trap was transferred to the analytical train and allowed to equilibrate for one minute under argon flow (40 mL/min). The trap was then heated for 30 sec to approximately 250 °C for thermal desorption. The sample stream was sent through a U-tube gas chromatograph, where separation of the species took place at 100 °C. A pyrolysis tube located downstream transformed the species to Hg (0) at 850 °C. The resulting mercury vapor was input directly into the CVAF detector, and the measurement was charted by the integrator in peak-area mode.

A standard curve was produced using a 100 µg/L stock standard (1 µg/mL Hg solution). One milliliter of stock standard was diluted to 100 mL with distilled water to a 1000 ng/L working standard. This working standard also included 100 µL of concentrated HCl, which stabilized the standard. Aliquots of working standard in concentrations of 100, 50, 20, 10, and 0 pg were added to the ethylation vessel.

Previous studies have determined a detection limit of 2.28 pg, based on three times the standard deviation of 10 pg replicates. For a typical 1-gram sample, this translates into a detection limit of 2.28 pg/g.

Quality control was ensured by running continuing calibration verification standards (CVS) after every 10 samples, and the result must be within 10 % of the original value in order to continue with analysis. If criteria were not met, the instrument was recalibrated and samples since the last acceptable calibration verification check must be rerun until standards are met.

Enumeration of Sulfate-Reducing Bacteria (SRB)

Sulfate-Reducing Bacteria Pure Cultures

Pure freshwater cultures of *Desulfovibrio desulfuricans*(DSV), *Desulfobulbus propionicus*(DSB), *Desulfococcus multivorans* (DSC), *Desulfobacter curvatus* (DBACTER), and *Desulfobacterium autotrophicum* (DSBM) were obtained from DSMZ (Deutche Sammlung von Mikroorganismen und Zellkulturen GmbH) for the calibration of microbial cell abundance. Each species is representative of five distinct sulfate-reducing bacteria (SRB) phylogenetic groups. Anaerobic enrichment media similar to those of Widdel and Bak (1992) were used to grow and maintain pure cultures (Appendix B). Cultures were initiated in serum vials under strict anaerobic conditions in an anaerobic chamber (Coy Labs, 90% N_2, 10% CO_2 and H_2 mix). Cultures were allowed to grow in the dark for approximately 30 d before transfer to fresh media.

Preservation of Sediment Samples

Sediment cores taken in duplicate for each mesocosm were immediately sectioned into 2-cm increments at the sampling site. The 2-cm increments were homogenized and placed in 50-mL centrifuge tubes. Five grams were transferred to another 50-mL centrifuge tube and preserved in 45 mL of 3.7 % formalin in artificial seawater (ASW). The recipe for ASW is shown in Appendix C.

Whole Cell Extraction

The following protocol was adapted from methods published by Velji and Albright (1985) and Frischer *et al*. (2000). One gram of the preserved sediment was transferred to a 15-mL centrifuge tube. Sodium pyrophosphate (PPi) was then added to the sediment slurry to a final concentration of 0.01 M. A 3-µL addition of concentrated polyoxyethylenesorbitan monoleate (Tween-80, Sigma Chemical) was added to a final concentration of 0.06 %. The samples were vortexed vigorously for 1 min and incubated at room temperature for 30 min. After incubation the slurry was vortexed for 15 sec and centrifuged at 700 x g (2000 rpm) for 2 min. After centrifugation, the supernatant extract was collected and transferred to a fresh tube with a Pasteur pipette. The sediment was washed using 10 mL of Artificial Sea Water, ASW (see Appendix B), vortexed for 1 min and the supernatant was added to the original extract. The sediment was washed with ASW and spun two more times and each time the supernatant was added to the original extract. The solution was then collected by centrifugation at 12,000 x g (Avanti J-25, Beckman) for 10 min at 4°C. After centrifugation, the supernatant was discarded and the pellet was resuspended in 3 mL of sterile ASW. If fine particles were still present, the samples were centrifuged at 200 x g (1000 rpm) for 1 min, and the supernatant was transferred to sterile 5-mL polypropylene tubes. Samples were then stored at 4 ºC until DAPI analysis.

Enumeration of Bacteria using DAPI

Total cell abundance was determined by staining preserved cells with 4'6'-diamidino-2-phenylindole (DAPI) and counted under epifluorescence microscopy, as described by Williams *et al*. (1998). A stock solution of DAPI stain was prepared at 50 µg/mL in dH_2O, filtered through a 0.2 µm GS filter (Millipore), and stored in the dark at 4 ºC.

Serial dilutions of 1:10, 1:100, and 1:1000 were accomplished by adding 10 mM $MgSO_4$ (pH = 6.4) to sample aliquots. The total volume of diluted cells was 1 mL. DAPI stain was added at a volume of 100 µL to samples that were subsequently vortexed for 30 sec prior to incubation at room temperature in the dark for 30 min. After incubation, a 0.2 µm, 25 mm Whatman GF/F filter was placed on top of a vacuum bottle. Approximately 1 mL of dH_2O was added on the filter to secure it on the vacuum bottle. A 0.2 µm black polycarbonate filter was placed on top of the GF/F filter and a glass column was clamped to the vacuum bottle. A vacuum was pulled on the apparatus, and 1 mL of the cell suspension was slowly pipetted on top of the filter. Samples were then washed 3 times with 1 mL of 1 mM $MgSO_4$. The polycarbonate filter containing the cells was mounted on a slide with mounting solution. A small drop of immersion oil was placed between the filter and the cover slip. Total cell counts were accomplished using an epifluorescence microscope (Olympus BX-60) equipped with a 100X UPLANFL-NA 1.3 oil objective and a WIDE UV filter set (U-M536), containing an exciter filter BP 330-285, dichroic mirror DM 400, and barrier filter BA 420. The total concentration of cells was determined using the following equation:

$$\text{cells/mL} = \frac{(\text{Avg. \# cells/field}) * (24{,}269 \text{ fields per view}) * (\text{dilution})}{\text{Volume filtered}}$$

The number of fields per filter is based on the 100X objective with a conversion factor of 5.73 pixels/μm and an image size of 640 X 480 dots per inch. The dilution factor is 1:10, 1:100, or 1:1000.

Quantification of SRB 16S rRNA Using Oligonucleotide Probes

Blotting Membranes for Hybridization

A dilution series determined that 10^6 cells/slot yielded hybridization densities suitable for densitometry (Frischer *et al*., 2000). Therefore, at least 10^6 cells/slot from pure culture and sediment were immobilized to nylon membranes using a slot-blot apparatus (Schliecher & Schell, Keen, N.H.). A known number of cells from pure culture were blotted adjacent to core sample blots to estimate the actual numbers of cells based on hybridization density.

Following blotting, RNA were UV cross-linked for 30 sec at the 120,000 microjoule setting in a UV cross-linker (UV Stratalinker model 1800, Stratagene Cloning Systems). The blots were then baked *in vacuo* at 80 °C for 2 hr to dry the blots. Membranes were stored at -20°C until use.

Radioactive Labeling and Probing with 16S rRNA Probes

Oligonucleotide sequences specific for DSB, DSV, DSC, DSBM, and DBACTER (shown previously in Table 2.1) were synthesized at the University of Georgia Molecular Genetics Facility using an ABI DNA/RNA synthesizer (model 394) and end-labeled based on the procedures of Stahl and Amann (1991), Braun-Howland *et al*. *(*1993), and Frischer *et al*. (1996). The oligonucleotides were end-labeled with 60 μCi of [γ-^{32}P]ATP (6,000 Ci/mmol, Du Pont/NEN) by first diluting 1μL of oligonucleotide in 29 μL of ddH_2O. For each probe to be labeled, 10 mM of Spermidine and 5 μL of 10X

polynucleotide reaction buffer (Promega) were added and mixed with the pipette tip. Behind the acrylic shielding, 1.5 µL of [γ-^{32}P] ATP (NEG-502Z) was carefully added to each tube and immediately placed in the acrylic holder. To this solution, 2 µL of polynucleotide kinase was added and mixed with pipette tip. The labeled probes were then incubated in a water bath for 2 hr at 37 ºC.

The % incorporation of the probes was determined by diluting 2 µL of the oligo reaction mix into 98 µL of EDTA (pH=8.0). Four labeled DE811 filters (Whatman) were spotted with 3 µL of the diluted mixture for each probe and briefly dried under an infrared lamp. Two filters were placed in scintillation vials containing 5 mL of scintillation fluid (this is the Total). The other 2 filters were washed in 100 mL of 0.5 M $NaPO_4$ (pH=6.8, Appendix D) at room temperature for 5 min each. Following the washes, the filters were dried under infrared lamp and placed in scintillation vials containing 5 mL of scintillation fluid (this is the Wash). The vials were incubated for 30 min at room temperature and then counted in a scintillation counter (Beckman LS 3500). The Total counts per minute and Wash counts per minute were averaged to calculate the % incorporation:

$$\% \text{ Incorporation} = (\text{cpm Wash}/\text{cpm Total}) * 100$$

20-60 % incorporation was expected if oligonucleotides were labeled properly.

Membrane blots were wetted with 6X SSPE. 6X SSPE was prepared by mixing 15 mL 20X SSPE (see Appendix D) and 35 mL dH_2O and poured into a weigh boat. Blots

were placed inside hybridization bottles and then pre-hybridized in PerfectHyb Plus solution (Sigma) and placed in 50 mL or 100 mL hybridization tubes. The tubes were placed in a rotating incubator (Robbins Scientific, Model 2000) warmed to the hybridization temperature (55 ºC) for 15 min. Labeled probes were also heated to 55 ºC until use. After incubation, the whole amount of each ^{32}P-labeled probe was added to each bottle behind shielding. The bottles were then placed in the incubators at 55 ºC over night. Following hybridization, blots are washed in wash buffer (Appendix D) and incubated at the hybridization temperature for 20 min. After washing, the hot fluid is poured into a glass waste bottle. The blots are washed 2 more times and the fluid is added to the glass waste bottle. The blots are removed from the hybridization bottles and dried briefly under an infrared lamp, attached to filter paper, and placed in film disks to incubate for at least 24 hr at -80°C. Hybridization is detected by autoradiography using the Quantity One version 4.1.1 software package and a GS-710 Calibrated Imaging Densitometer system (Bio-Rad Laboratories, Hercules, CA).

CHAPTER IV
DATA RESULTS

Sampling Schedule

Table 4.1 presents the BERM sampling schedule from June 2000 through May 2001. Porewater chemistry cores and sippers were obtained for sulfate and sulfide analysis. Extraction of porewater for mercury cores and sippers consisted of both total Hg and methyl Hg measurements. *Spartina* heights were determined by measuring the height of the tallest shoot in both vegetated mesocosms. In general, sampling events followed the seasonal growth cycle of *Spartina*: the July 2000 event represented *Spartina* during peak vegetative growth; the February 2001 event represented *Spartina* minimal growth after reproduction; and the May 2001 event represented *Spartina* just before vegetative growth.

Physical Characteristics of the BERM

Sediment Density and Porosity

Tables 4.2, 4.3, and 4.4 compare the physical characteristics of the BERM sediment in the three mesocosms for each sampling period. Values for saturated bulk density, porosity, and particle density are averaged between duplicate cores. The flow of water, which is impacted by the physical characteristics of the sediment, moves through the sediment and transports oxygen and sulfate to the lower depths of the sediment.

Table 4.1 BERM Sampling Schedule.

	POREWATER				SOLID PHASE	MESOCOSM PARAMETERS				
Sampling Date	Chemistry Cores (centrate)[1]	Hg Cores (centrate)[2]	Chemistry Sippers[3]	Hg Sippers[4]	SRR Cores	Temperature	Salinity	Mesocosm Volume	*Spartina* Height	Sediment Density/ Porosity
6/22/00						X	X			
6/26/00						X	X			
6/27/00						X	X			
7/26/00	X		X	X	X	X		X		X
10/5/00								X	X	
12/11/00									X	
12/13/00						X	X			
12/14/00						X	X			
1/25/01						X	X	X	X	
1/26/01						X	X			
2/7/01	X	X	X	X	X	X		X		X
4/17/01						X				
5/2/01	X	X	X	X	X	X	X	X		X

[1]Chemistry Cores – Centrate analyzed for sulfate and sulfide.
[2]Hg Cores – Centrate analyzed for total Hg and Methylmercury.
[3]Chemistry Sippers – Sipper sample analyzed for sulfate and sulfide
[4]Hg Sippers – Sipper sample analyzed for total Hg and Methylmercury.

Table 4.2 Physical characteristics of BERM sediment in July 2000.

Pristine Vegetated			
Depth Interval (cm)	Saturated Bulk Density (g/cm^3)	Porosity	Particle Density (g/cm^3)
0-2	1.353	0.654	1.947
2-4	1.426	0.656	2.156
4-6	1.388	0.613	1.965
6-8	1.484	0.571	2.110
8-10	1.701	0.607	2.681
Contaminated Vegetated			
Depth Interval (cm)	Saturated Bulk Density (g/cm^3)	Porosity	Particle Density (g/cm^3)
0-2	1.200	0.752	1.734
2-4	1.128	0.716	1.417
4-6	1.160	0.779	1.612
6-8	1.207	0.775	1.829
8-10	1.155	0.772	1.638
Contaminated Unvegetated			
Depth Interval (cm)	Saturated Bulk Density (g/cm^3)	Porosity	Particle Density (g/cm^3)
0-2	1.142	0.760	1.505
2-4	1.187	0.776	1.718
4-6	1.226	0.778	1.921
6-8	1.254	0.782	2.022
8-10	1.178	0.770	1.662

Table 4.3 Physical characteristics of BERM sediment in February 2001.

Pristine Vegetated			
Depth Interval (cm)	Saturated Bulk Density (g/cm^3)	Porosity	Particle Density (g/cm^3)
0-2	1.314	0.621	1.784
2-4	1.281	0.544	1.674
4-6	1.298	0.573	1.758
6-8	1.281	0.685	1.835
8-10	1.361	0.633	1.996
Contaminated Vegetated			
Depth Interval (cm)	Saturated Bulk Density (g/cm^3)	Porosity	Particle Density (g/cm^3)
0-2	1.134	0.717	1.483
2-4	1.059	0.651	1.355
4-6	1.159	0.756	1.562
6-8	1.184	0.779	1.712
8-10	1.153	0.666	1.393
Contaminated Unvegetated			
Depth Interval (cm)	Saturated Bulk Density (g/cm^3)	Porosity	Particle Density (g/cm^3)
0-2	1.188	0.749	1.652
2-4	1.209	0.770	1.794
4-6	1.219	0.777	1.879
6-8	1.170	0.781	1.688
8-10	1.089	0.735	1.359

Table 4.4 Physical characteristics of BERM sediment in May 2001.

Pristine Vegetated			
Depth Interval (cm)	Saturated Bulk Density (g/cm^3)	Porosity	Particle Density (g/cm^3)
0-2	1.216	0.638	1.541
2-4	1.321	0.697	1.976
4-6	1.262	0.695	1.780
6-8	1.412	0.783	2.706
8-10	1.042	0.633	2.059
Contaminated Vegetated			
Depth Interval (cm)	Saturated Bulk Density (g/cm^3)	Porosity	Particle Density (g/cm^3)
0-2	1.089	0.810	1.836
2-4	1.069	0.687	1.175
4-6	1.025	0.694	1.038
6-8	1.127	0.744	1.725
8-10	1.105	0.789	1.400
Contaminated Unvegetated			
Depth Interval (cm)	Saturated Bulk Density (g/cm^3)	Porosity	Particle Density (g/cm^3)
0-2	1.312	0.707	2.094
2-4	1.336	0.700	2.026
4-6	1.245	0.676	1.699
6-8	1.222	0.716	1.707
8-10	1.162	0.668	1.425

Table 4.5 Summary of sediment characteristics.

	Average Bulk Density (g/cm^3) *n=30*[1]	*Average Porosity* *n=30*	*Average Particle Density (g/cm^3)* *n=30*
Pristine	1.340 (± 0.138)[2]	0.640 (± 0.058)	1.998 (± 0.317)
Contaminated Vegetated	1.130 (± 0.051)	0.739 (± 0.047)	1.527 (± 0.226)
Contaminated Unvegetated	1.209 (± 0.061)	0.743 (± 0.038)	1.743 (± 0.210)

[1]*n* = Number of samples.

[2]Value in parentheses represents standard deviation of *n* samples.

Therefore, sediment characteristics directly influence sulfate-reducing bacteria activity and chemical oxidation in the sediment. Since pristine sediment and contaminated sediment were collected in different geographical locations, sediment characteristics were compared to determine whether geochemical and microbial profiles could be directly compared. Table 4.5 shows a summary of the BERM characteristics of the sediment. Values were obtained by averaging data from all of the cores for each mesocosm (n=30). The standard deviations are shown in parentheses.

The contaminated sediment from the LCP site had a higher porosity than the uncontaminated sediment from Grove's Creek marsh. In addition, contaminated

sediment had a lower saturated bulk density than the pristine sediment. In 1999 and spring 2000, the average porosities for pristine, contaminated vegetated, and contaminated unvegetated mesocosms were 0.665, 0.819, and 0.838, respectively. Bulk densities were 1.456, 1.214, and 1.253 g/cm^3, respectively. Therefore, porosities in all mesocosms have slightly decreased since then, while bulk densities have increased. Possible explanations for this include compaction of the soil and filling of the voids by bacterial growth. No significant trend in physical characteristics versus depth were observed.

Underdrain Effluent Volume

Effluent volumes were measured during October 2000, January 2001, and May 2001. The average underdrain effluent volumes for the pristine, contaminated vegetated, and contaminated unvegetated mesocosms are shown in Table 4.6. The values in parenthesis are effluent volumes expressed as percentages of pore volume. The pore volume was calculated by multiplying the sediment volume by the average sediment porosity. Effluent volumes in the unvegetated mesocosm were generally higher than the vegetated mesocosms in October and January; however, the effluent volume in this mesocosm was much lower in May. This may have been caused by clogging in the pipe from the unvegetated mesocosm or water percolating out of the unvegetated sediment was simply slower at the time of measurement.

Table 4.6 Underdrainage effluent volumes.

	Pristine Vegetated	Contaminated Vegetated	Contaminated Unvegetated
10/5/00	182 L (6 %)[1]	204.8 L (7 %)	273 L (9 %)
1/25/01	150.2 L (5 %)	168.4 L (6 %)	273 L (9 %)
5/2/01	168.4 L (6 %)	204.8 L (7 %)	13.7 L (0.5 %)

[1]Effluent samples were collected over a single tidal cycle expressed in liters and as percentages of pore volume (in parenthesis).

Temperature

Temperature readings for 0-, 5-, and 10-cm depths in each mesocosm were measured in December 1999, February 2000, March 2000, and July 2000 (Figure 4.1). Temperatures only decreased by 2 -3 °C with depth in each mesocosm during December, March, and July sampling events. Since temperature differences were not significant, average temperature measurements were taken at the 5-cm depth below the sediment surface in subsequent sampling events (February and May 2001). Depth profiles between mesocosms were nearly identical, except for that of March 2000 in the unvegetated mesocosm. Without plants casting a cooling shadow on the sediment surface, the contaminated unvegetated mesocosm had the warmest temperatures. Another anomaly occurred in all mesocosms during the February event. Instead of a decrease in temperature with depth, sediments were warmer with depth. The warming effect suggests that the sediment surface acted as an insulator, preventing extreme temperatures in the subsurface.

Weather conditions during the July 2000 and February 2001 samplings were partly cloudy, and air temperatures at the time of sampling in July and February were of 26 °C

and 15 °C, respectively. The May 2001 sampling had very sunny weather conditions with an air temperature of 21°C. Figure 4.2 presents the plot of air temperature and mesocosm soil temperature over seasonal cycles. Air temperatures were collected from the Savannah international airport from the WTOC-TV web site (http://www.savannah-weather.com/weather/archive.htm).

Salinity

Salinity in the surface water in each mesocosm and at the fuel dock (approximately 600 feet from the BERM facility) was obtained using a refractometer. Measurements were taken over a seasonal period and recorded. Salinity measurements in the mesocosms differed from those of the fuel dock, but all measurements followed a similar trend throughout the season (Figure 4.3). Salinity is not temperature dependent and therefore does not show a seasonal trend. Daily fluctuations in salinity were not significant; salinity varied by 1-2 ppt during each tidal cycle in the mesocosms and the fuel dock. Comparatively, offshore salinity readings taken by the South Atlantic Bight Synoptic Offshore Observational Network (SABSOON), average approximately 34 ppt and can range below 31 to over 36 ppt. However, the readings generally vary only 1-2 ppt during a 24 hr period (See http://www.skio.peachnet.edu/projects/sabsoon_web/tower.html). Therefore, salinity at the fuel dock and in the mesocosms were generally lower than salinity offshore, but the small degree of fluctuation within each tidal cycle indicates substantial mixing both offshore and inshore.

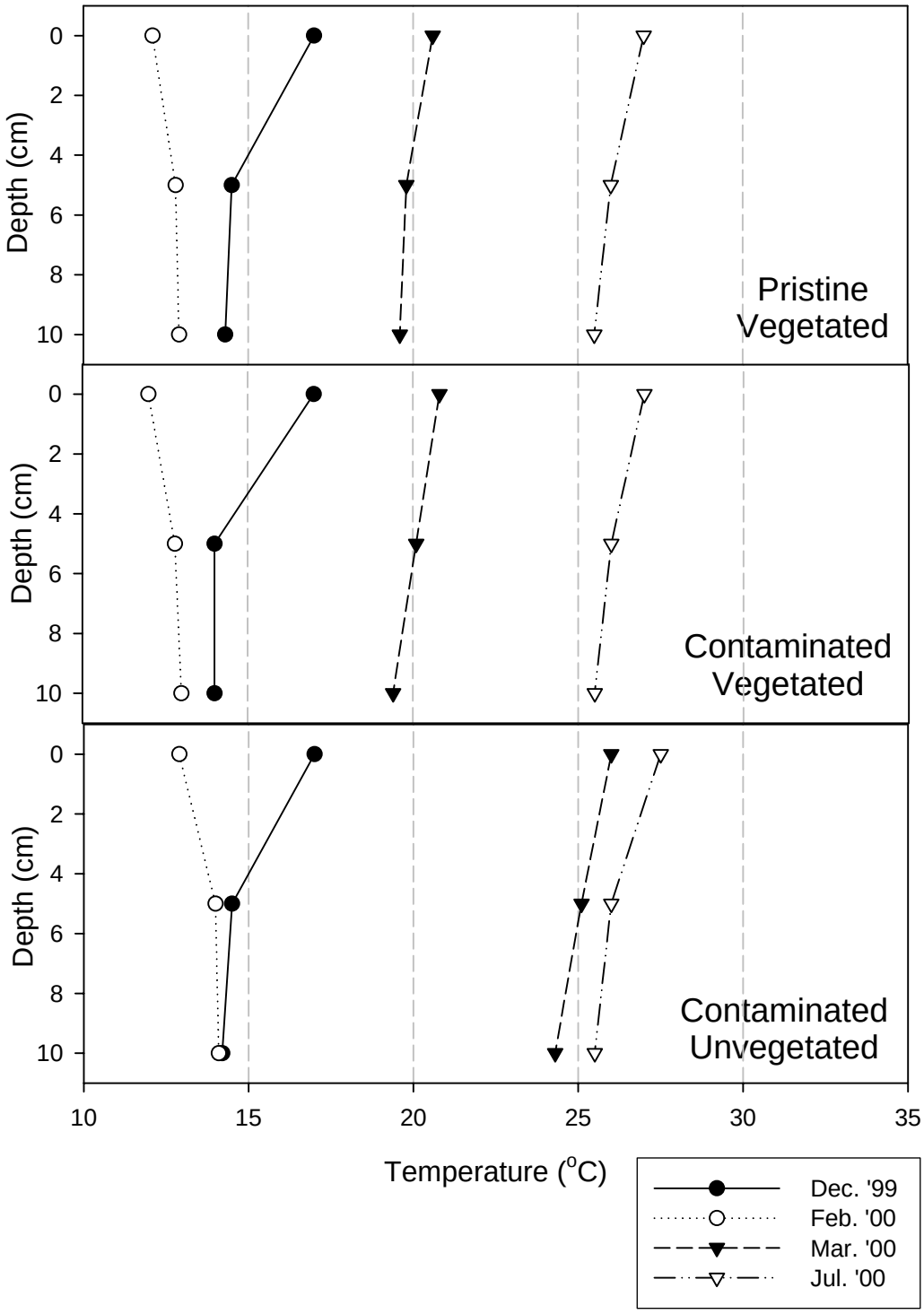

Figure 4.1 Depth profiles of temperature readings in BERM.

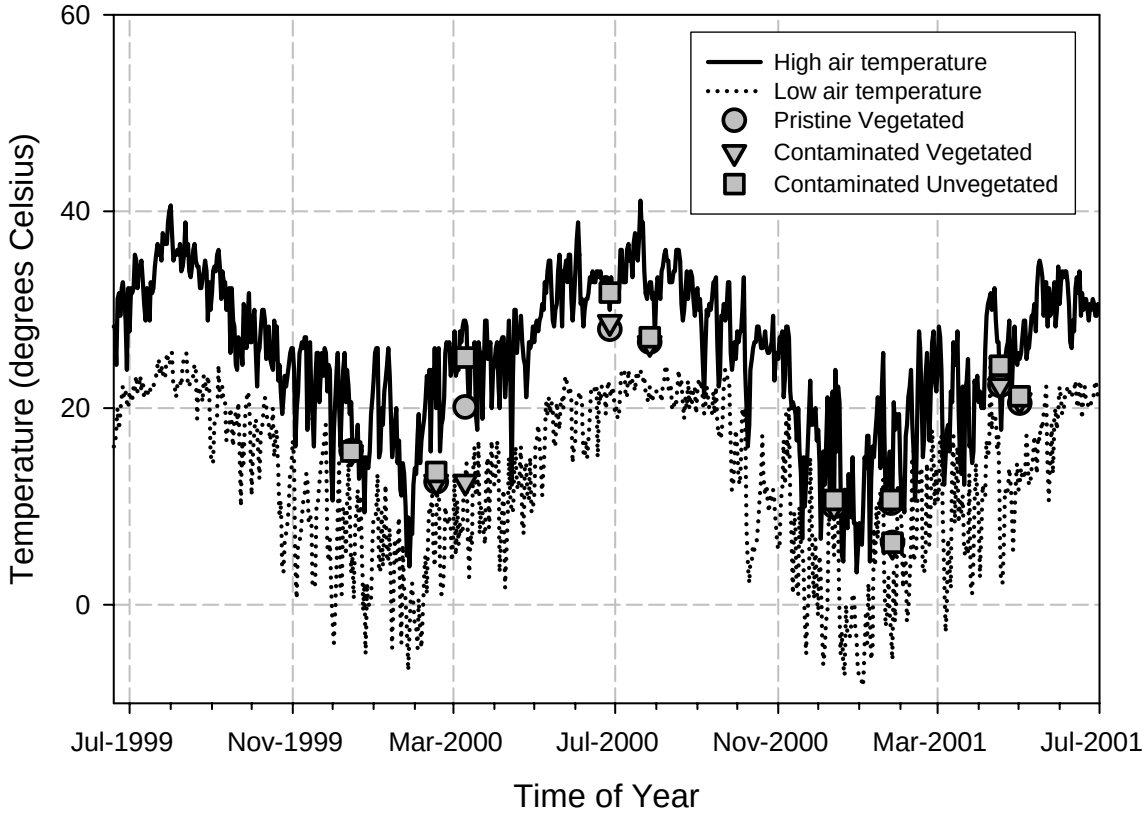

Figure 4.2 Seasonal variations in air and BERM sediment temperature readings.

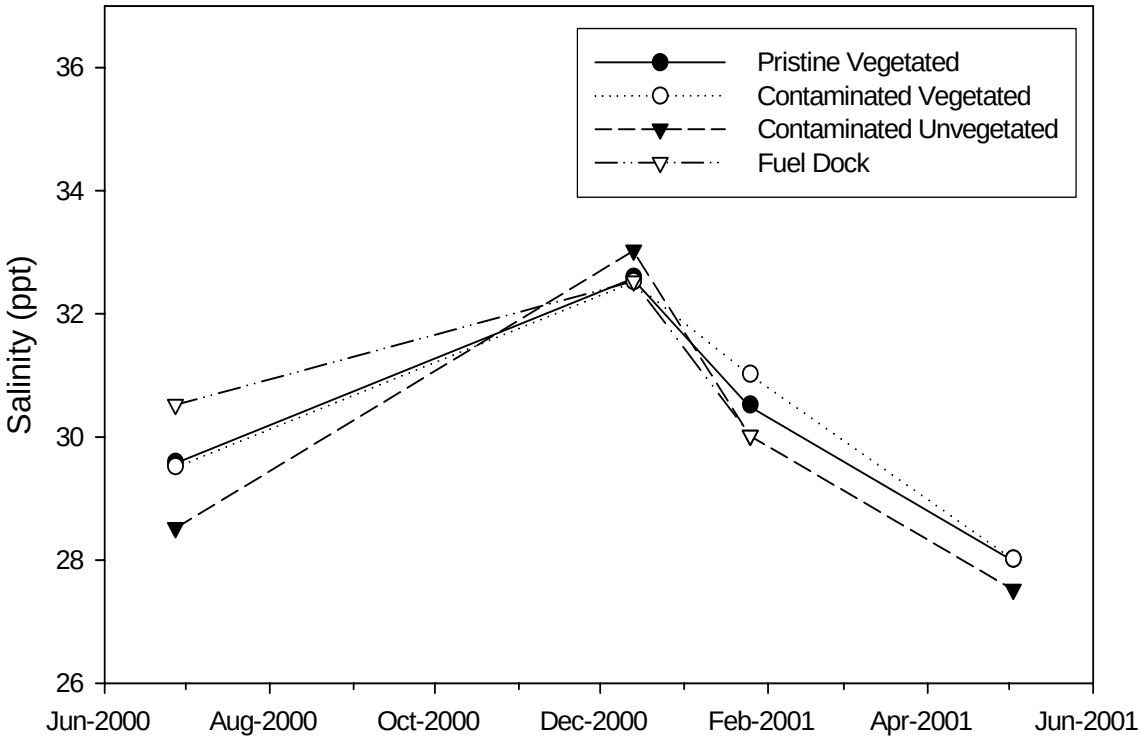

Figure 4.3 Salinity in BERM surface water.

Spartina Height Measurements

The height of the tallest shoot was measured for each vegetated mesocosm from October 2000 to June 2001 to compare growth between the contaminated and pristine mesocosms. *Spartina* height differences between pristine and contaminated mesocosms were not significant (Figure 4.4). Therefore, mercury contamination did not appear to stunt vegetative growth.

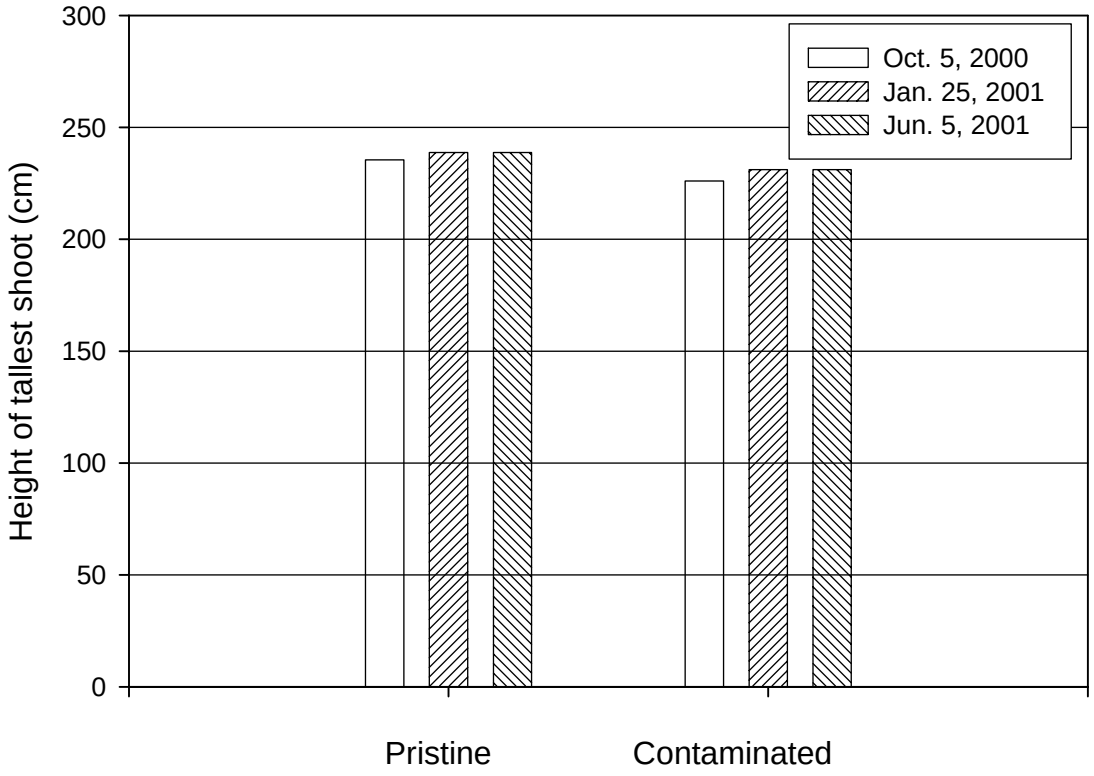

Figure 4.4 *Spartina alterniflora* height measurements (Mean differences between pristine and contaminated sediment were not significant within 95% confidence.

Porewater Geochemistry

Porewater Sulfate

Figure 4.5 shows the porewater sulfate data from Grove's Creek. Grove's Creek is a shallow stream that is located approximately 2.09 km from the Skidaway Institute of Oceanography. The sampling site was adjacent to the creek and harbored dense *Spartina alterniflora* marsh grass. Sampling took place in December 2000 during low tide. Small core barrels (15-cm length, 2-cm i.d) and large core barrels (41-cm length, 4.7-cm i.d.) were used for sampling intact sediment to determine whether porewater sulfate profiles were affected by sediment volume. Large core barrels could not be used for sampling in the BERM since they would cause too much destruction to the sediment. However, an attempt was made to determine whether smaller sediment volume would be sufficient for sampling. Figure 4.5 shows little difference between small core and large core sulfate profiles. Therefore, small core barrels were sufficient for sampling the BERM system in this study.

Figure 4.6 compares the sulfate profile from Grove's Creek in December 2000 with that of the BERM pristine vegetated sediment from February 2001. Sulfate did not vary significantly with depth in the Grove's Creek sediment. In the BERM pristine mesocosm, sulfate did vary with depth and concentrations were higher compared to those in the Grove's Creek sediment. More frequent freshwater influx into Grove's Creek may dilute surface level sulfate concentrations, causing lower sulfate levels throughout the sediment.

Sulfate profiles from the vegetated and unvegetated mesocosms at each sampling period are presented in Figures 4.7 through 4.9. Data for the pristine vegetated mesocosm and the contaminated vegetated mesocosm were combined into one graph for vegetated sediment (upper plot). Data for pristine vegetated sediment (M1) is indicated by white symbols, while data for contaminated vegetated sediment (M2) is indicated by black symbols. Contaminated unvegetated sediment (M3) is presented in the lower plot in each figure. Sulfate profiles in the unvegetated sediment decreased with depth during summer and spring. However, in the vegetated mesocosms, sulfate depletion with depth was not as significant during warmer months when plants were in the active growth stages. In winter, the sulfate profiles in both vegetated and unvegetated mesocosms were more homogenous throughout the sediment and sulfate depletion was less prominent with depth.

Sulfate depletion with depth is commonly observed in anoxic salt marsh sediments (Howes *et al*., 1984; Howarth and Giblin, 1983; Kostka and Luther, 1995). Sulfate concentrations near the surface tend to be consistent with those of the overlying water and decrease with depth. Data from June 1999 and January 2000 obtained by Sauer (2003) and data shown in Figures 4-7 through 4-9 show that sulfate depletion is less significant with depth during colder months. Concentration gradients with depth are also lower in vegetated sediment compared to unvegetated sediment, particularly in summer and spring months.

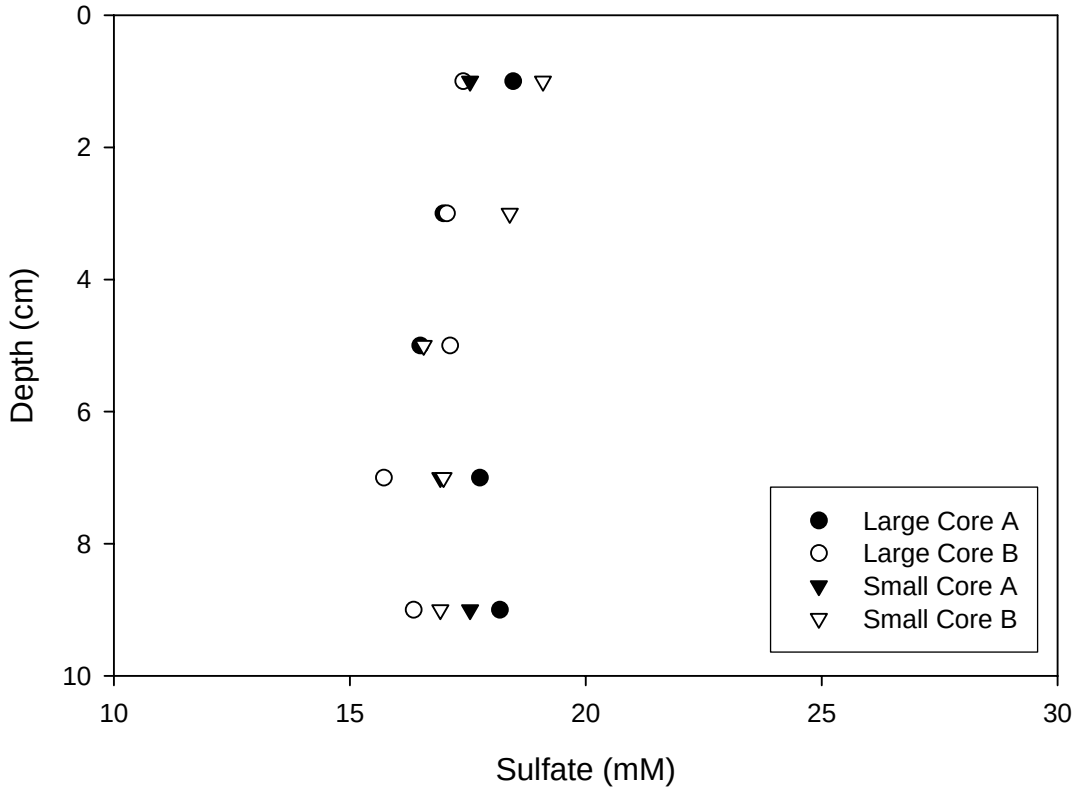

Figure 4.5 Porewater sulfate from Grove's Creek sediment in December 2000. Data from small and large cores are not statistically significant (P>0.05).

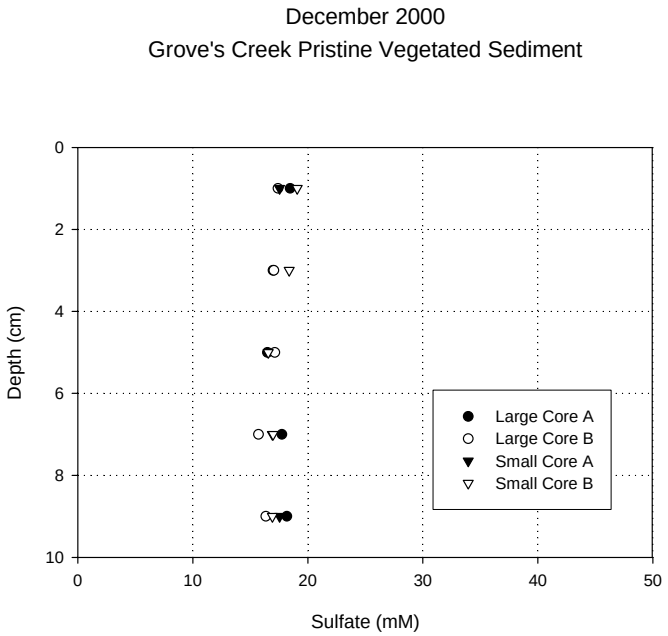

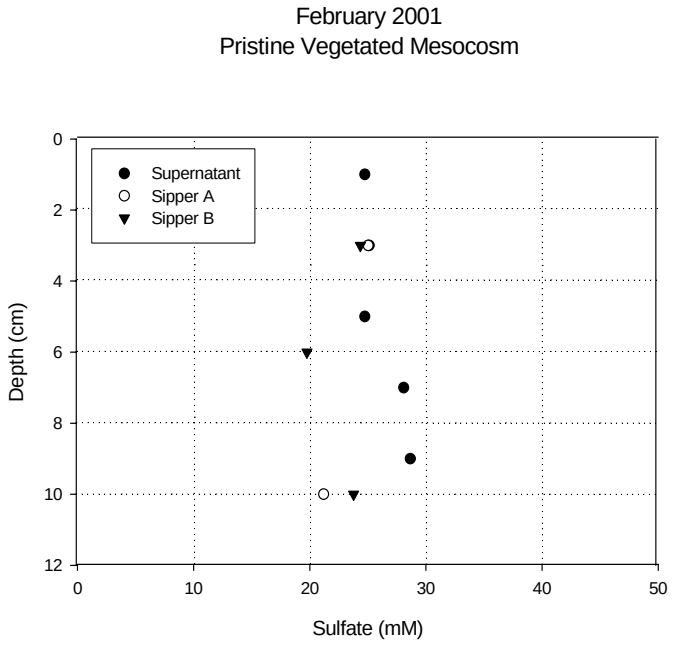

Figure 4.6 Comparison of sulfate profiles between Grove's Creek and BERM pristine vegetated sediment.

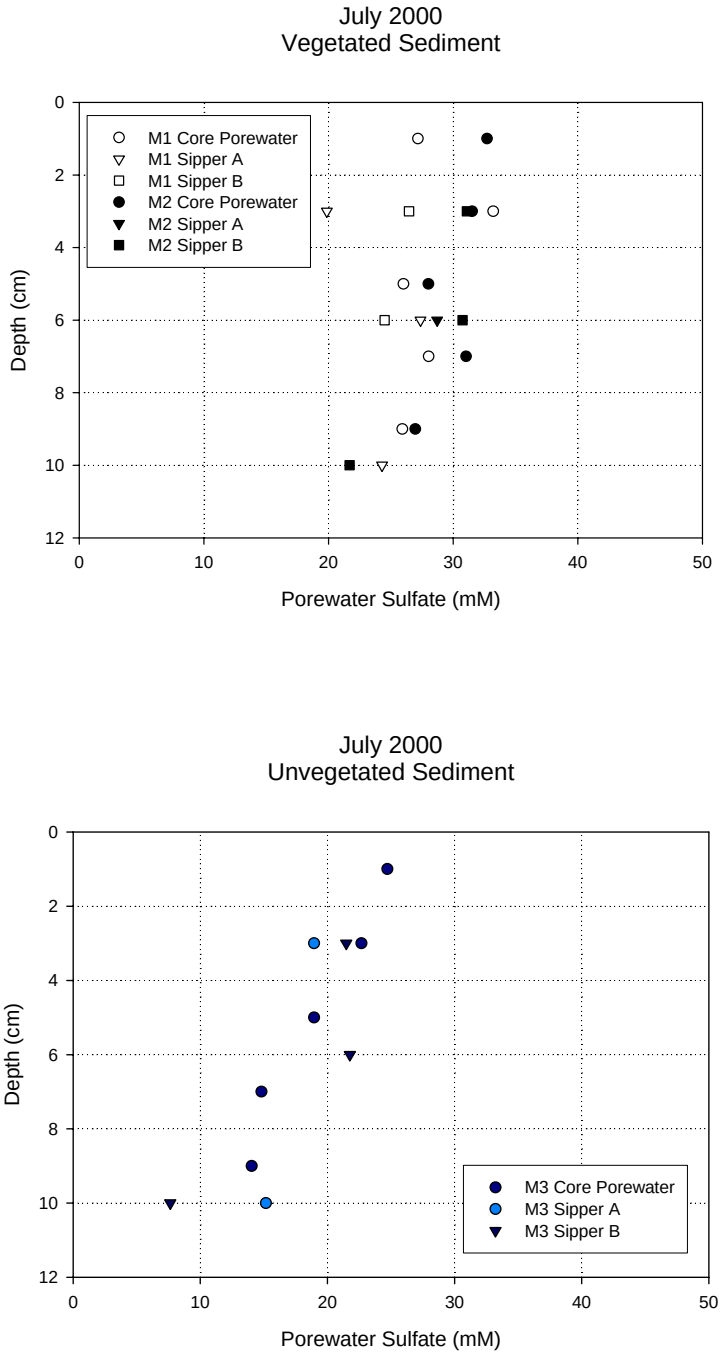

Figure 4.7 Porewater sulfate profiles for vegetated and unvegetated mesocosms from July 2000 sampling. M1is pristine vegetated mesocosm. M2 is contaminated vegetated mesocosm. M3 is contaminated unvegetated mesocosm.

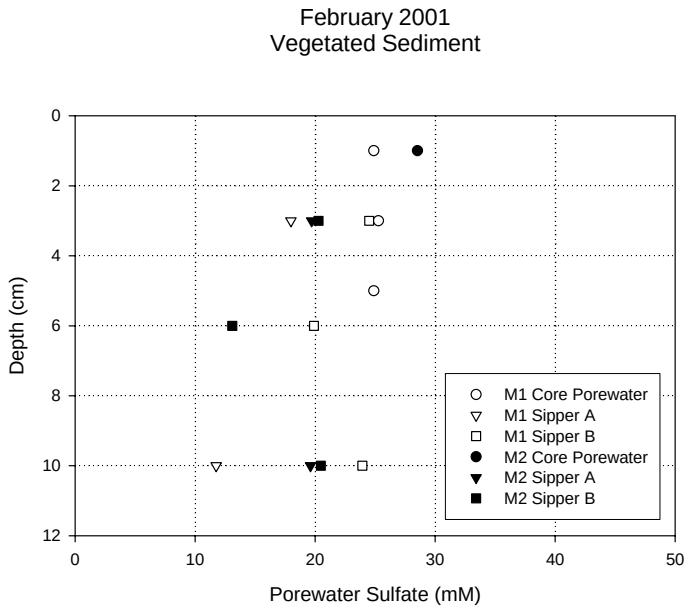

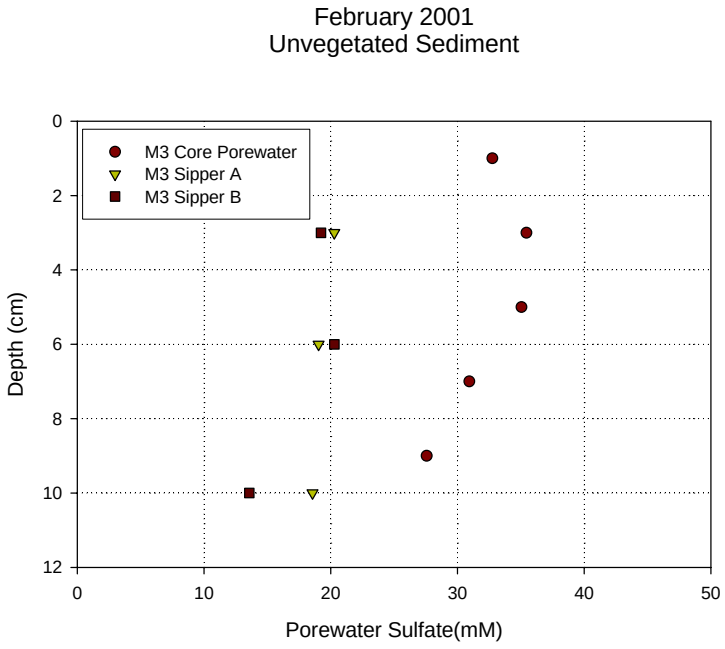

Figure 4.8 Porewater sulfate profiles for vegetated and unvegetated mesocosms from February 2001 sampling. M1is pristine vegetated mesocosm. M2 is contaminated vegetated mesocosm. M3 is contaminated unvegetated mesocosm.

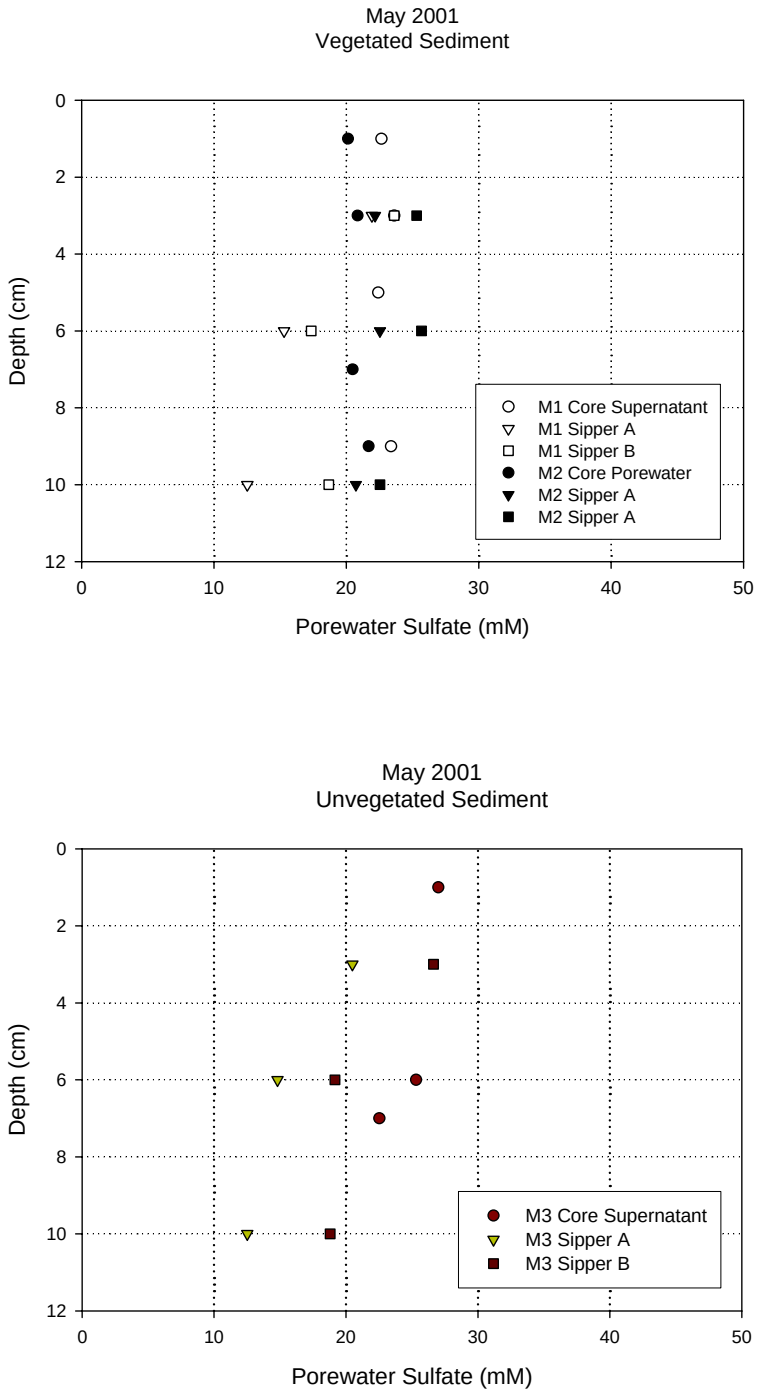

Figure 4.9 Porewater sulfate profiles for vegetated and unvegetated mesocosms from May 2001 sampling. M1is pristine vegetated mesocosm. M2 is contaminated vegetated mesocosm. M3 is contaminated unvegetated mesocosm.

Porewater Sulfide

Figures 4.10 through 4.12 show the sulfide profiles for the vegetated and unvegetated mesocosms at each sampling period. Sulfide in vegetated sediment during July remained below 10 μM at all depths. However, in the unvegetated sediment, sulfide increased to 74 μM in the lower depths of the sediment. In February, sulfide concentrations were variable throughout the sediment depths. Sulfide concentrations increased slightly with depth in the unvegetated sediment. Sulfide samples in May remained below 10 μM in both vegetated and nonvegetated mesocosms. In general, sulfide concentrations remained low in the vegetated sediment during plant growth in the summer and spring and increased during plant senescence in the winter. Apparently, an increase in plant activity stimulates sulfate re-oxidation even at lower depths of the sediment.

It is believed that the roots of *Spartina* participate in gas transfer and excrete oxygen to lower depths. In addition, overlying water containing dissolved oxygen also contribute to oxygen intrusion into surface sediments. The oxygen then has the opportunity to react with the sulfide produced from sulfate reduction to regenerate sulfate; a process called sulfide oxidation. Therefore, sulfate accumulates in the top 0-2 cm of the sediment and even in the lower depths in the vegetated mesocosms. During the winter, *Spartina* is senesced and activity is lower than in the summer months. Hence, gas transfer is decreased in the subsurface and sulfate-reducing bacteria can then actively reduce sulfate to sulfide, preventing sulfate accumulation.

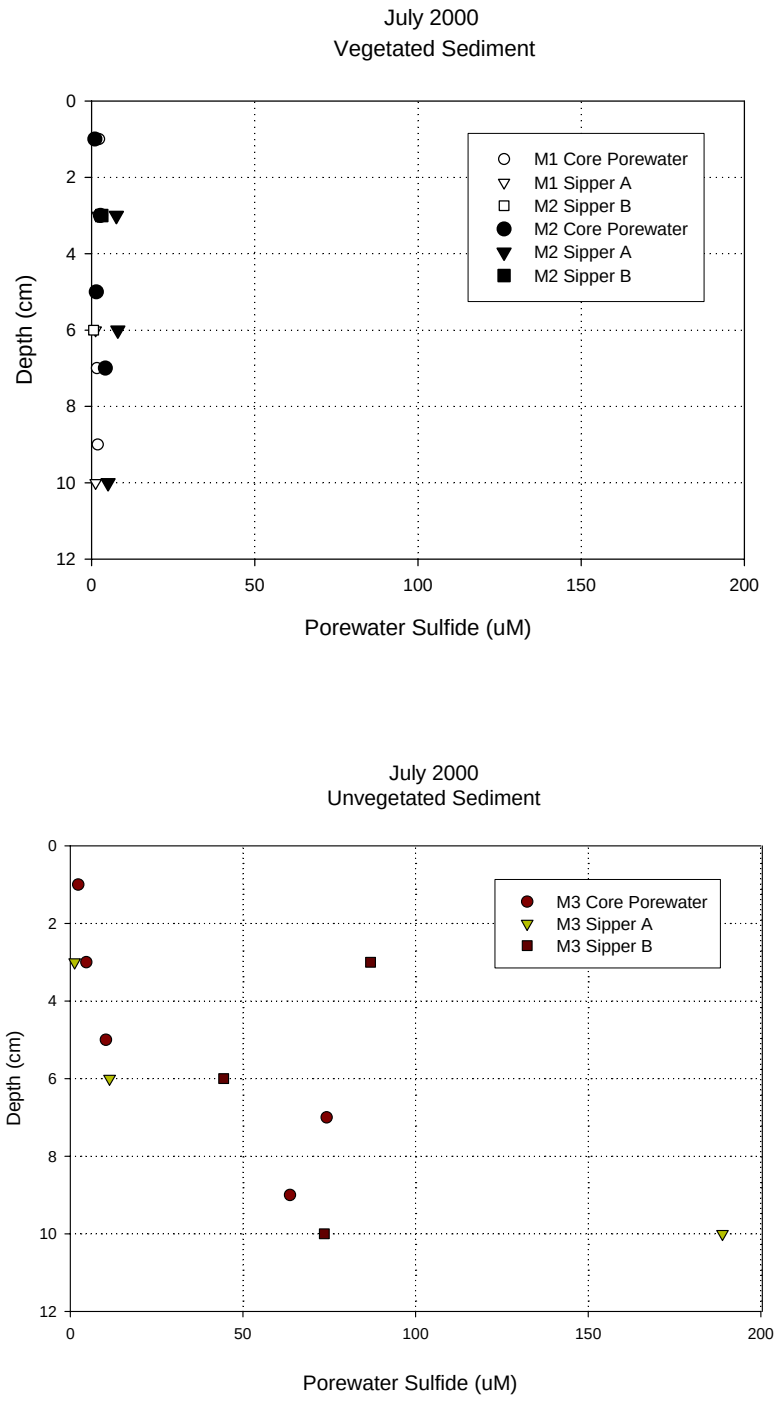

Figure 4.10 Porewater sulfide profiles for vegetated and unvegetated mesocosms from July 2000 sampling. M1 is pristine vegetated mesocosm. M2 is contaminated vegetated mesocosm. M3 is contaminated unvegetated mesocosm.

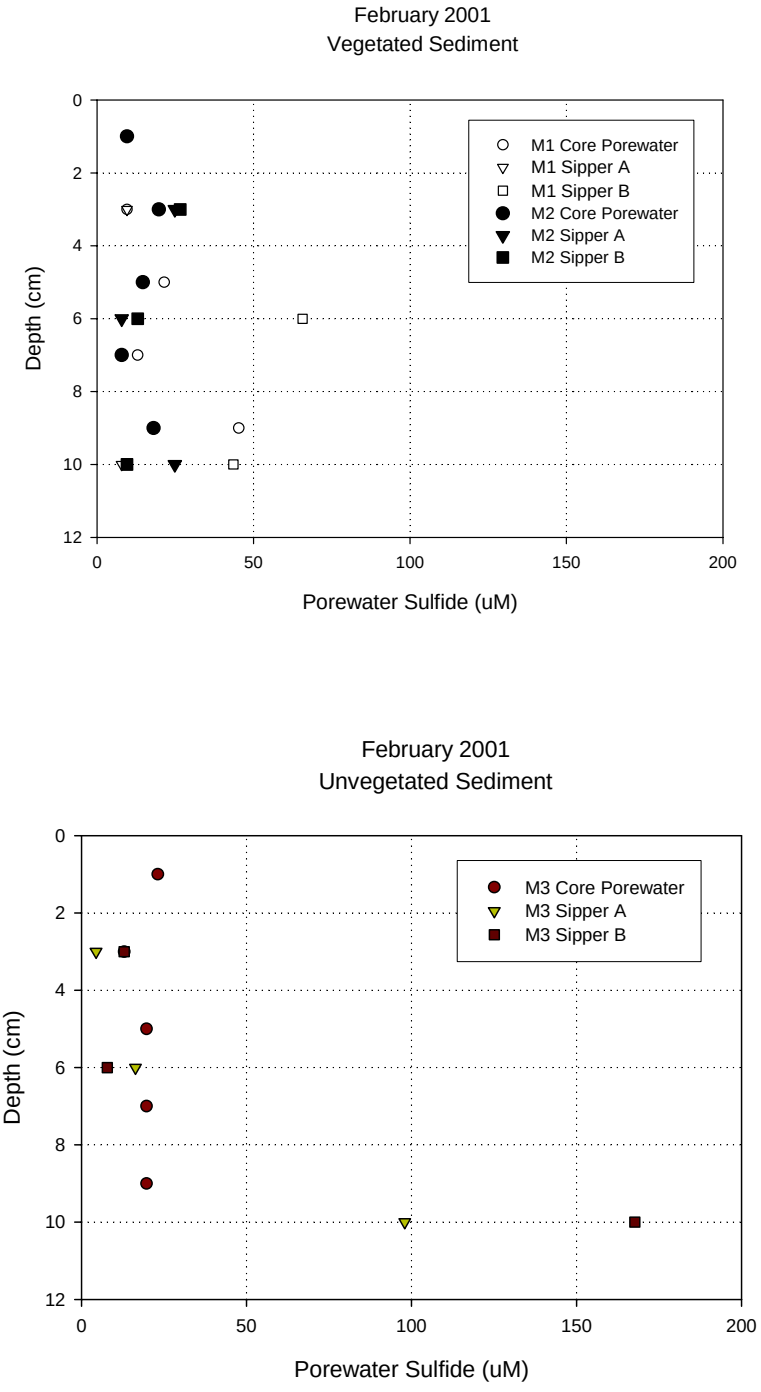

Figure 4.11 Porewater sulfide profiles for vegetated and unvegetated mesocosms from February 2001 sampling. M1 is pristine vegetated mesocosm. M2 is contaminated vegetated mesocosm. M3 is contaminated unvegetated mesocosm.

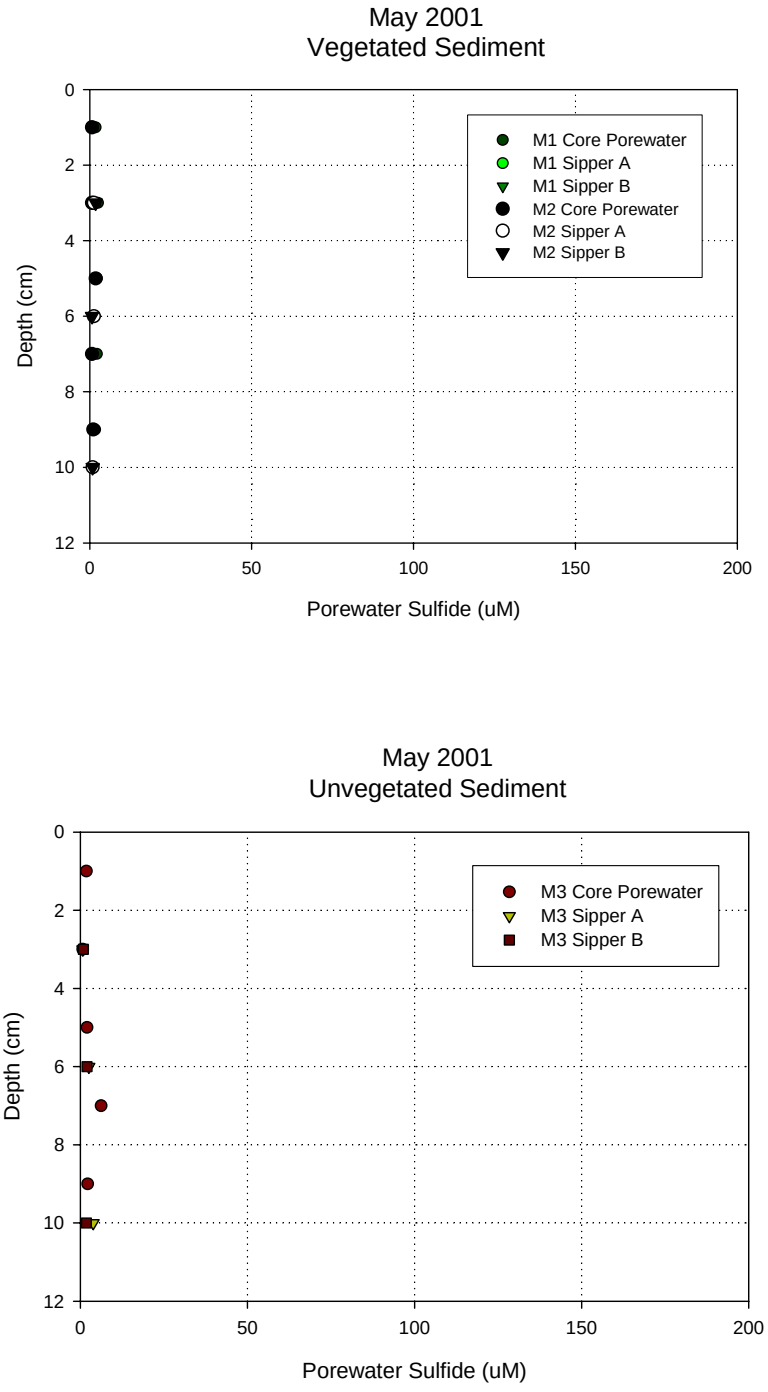

Figure 4.12 Porewater sulfide profiles for vegetated and unvegetated mesocosms from May 2001 sampling. M1 is pristine vegetated mesocosm. M2 is contaminated vegetated mesocosm. M3 is contaminated unvegetated mesocosm.

Sulfate Reduction Rates

Depth profiles of average sulfate reduction rates (SRR) for each sampling event are shown in Figures 4.13 through 4.15. Data from duplicate cores and average of duplicate cores from the pristine vegetated (M1), contaminated vegetated (M2), and uncontaminated vegetated (M3) mesocosms are provided in each figure. Maximum rates exceeding 3,000 nmol/cm^3-d at 1-cm-depth were observed in vegetated sediments (M1 and M2) in July 2000 when plants were most active. In contrast, minimum rates below 2,000 nmol/cm^3-d in all mesocosms occurred in February 2001. SRR data collected by Sauer (2003) also showed higher rates in summer months, but maximum rates remained below 2,000 nmol/cm^3-d. The increase in SRR from 1999 to 2000 could be due to increased plant activity and subsequent increased microbial activity. *Spartina* height measurements taken in July 1999 averaged 141 cm in pristine sediment. In October 2000, the average height increased to 235 cm.

Depth profiles generally decreased with depth in July 2000 and February 2001, predominately in vegetated sediments. For example, in July, average SRR in contaminated unvegetated sediment went from 730 nmol/cm^3-d at the surface to 128 nmol/cm^3-d at the 10-cm-depth, a change of 602 nmol/cm^3-d over 9 cm. In comparison, in pristine unvegetated sediment during July, a change of 1.8 nmol/cm^3-d over 9-cm was observed. Depth profiles in May 2001 were homogenous throughout the sediment, when plants were in the beginning stages of reproductive growth.

Figure 4.16 presents the temporal changes in sulfate reduction rates for each mesocosm. During July 2000, vegetative growth peaked and sulfate reduction rates in

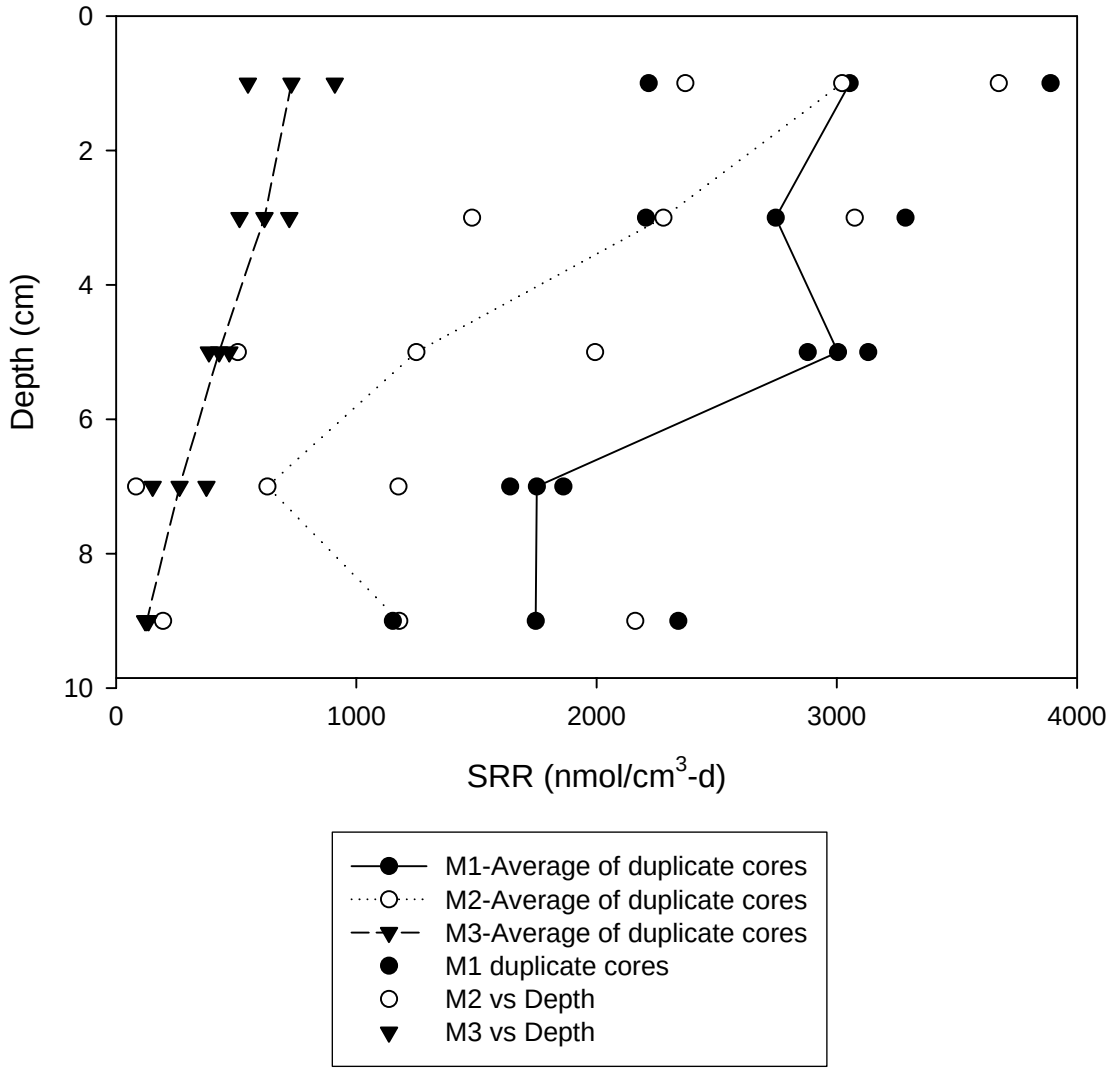

Figure 4.13 SRR-depth profiles for July 2000 sampling.

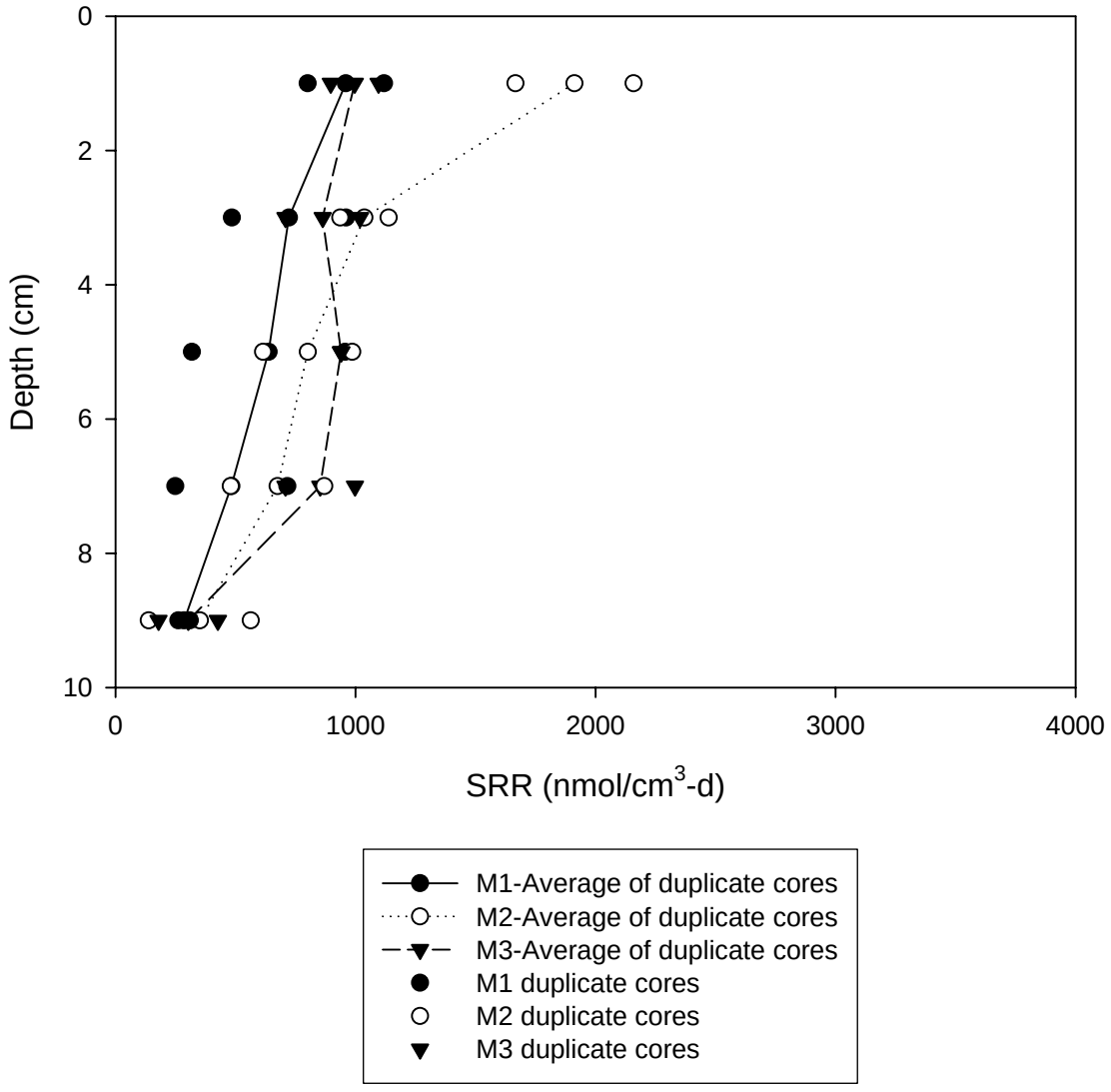

Figure 4.14 SRR-depth profiles for February 2001 sampling.

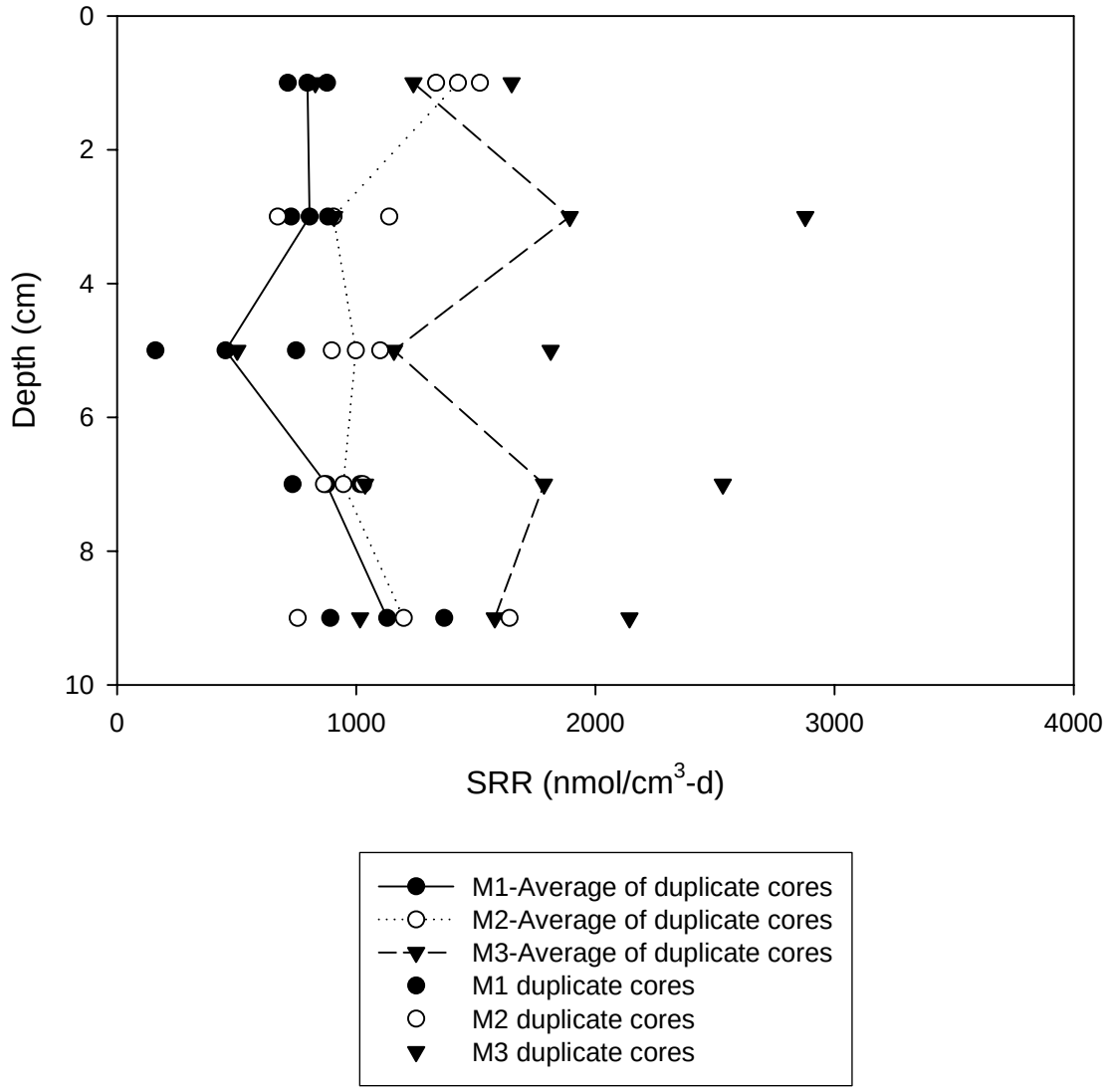

Figure 4.15 SRR-depth profiles for May 2001 sampling.

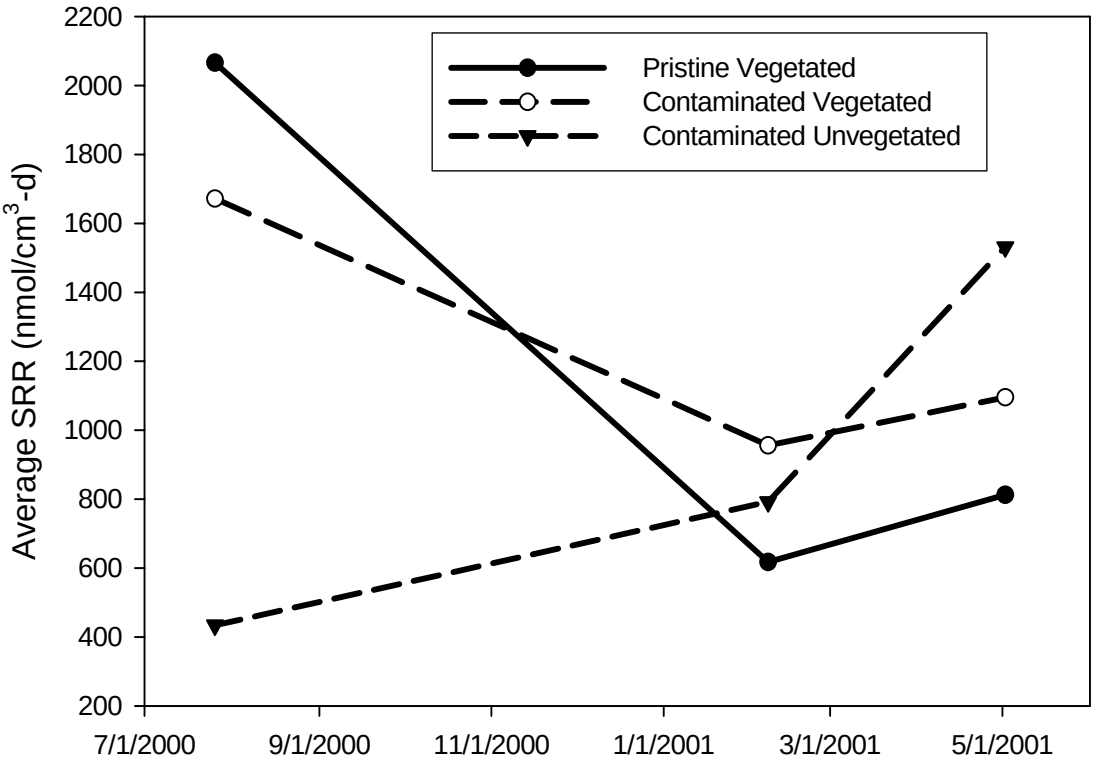

Figure 4.16 Seasonal variation of SRR in BERM mesocosms.

the vegetated sediment were quite high. However, the unvegetated mesocosm did not show maximum sulfate reduction rates during summer months. The absence of plant activities could explain the decreased rates in July 2000. During February when plants were not actively growing, rates were at their lowest, all remaining below 1,000 nmol/cm^3-d. In May 2001, SRR increased slightly, with the unvegetated SRR surpassing the vegetated SRR. During the last sampling event, *Spartina* plants were still senesced, which may explain why the increase in SRR in vegetated sediment from February to May was not significant compared to that in unvegetated sediment. Additionally, the SRR increase in the unvegetated mesocosm could be attributed to the abundant formation of algal mats during this time period.

Sulfide Oxidation Rates

Results from this study indicate that sulfate reduction rates are much higher than the diffusive flux of sulfate entering the sediment. Surface porewater sulfate actually exceeds that of the overlying waters so that the diffusive flux is out of the sediments. Therefore, excess sulfate at the sediment surface must come from another source. Several reports suggest that sulfide oxidation may be significant in surface sediments (Chanton *et al*., 1987; Berner and Westrich, 1985). The downward flow of water through intertidal marsh sediment transport dissolved oxygen to the belowground sediment. Additionally, active marsh plants, such as *Spartina alterniflora*, participate in gas exchange in the root zone and release dissolved oxygen in root exudates. In the presence of oxygen, sulfide has the opportunity to oxidize to sulfate. Therefore, two dynamic

processes are taking place in the sediment. Anaerobic sulfate-reducing bacteria consume sulfate, and aerobic (oxidizing) conditions re-oxidize sulfide back to sulfate.

The mesocosms in this study showed consistently higher concentrations of porewater sulfate in the surface (top 2 cm) sediments than in the overlying water in all three mesocosms. Therefore, it is hypothesized that exposure to air at the sediment surface during low tide encourages sulfide oxidation and increases sulfate in surface sediments to levels that exceed that of the seawater supply. However, in vegetated sediments, sulfate levels were high at the surface and lower depths due to the homogenous distribution of the plant roots.

Previously reputed studies (Jorgensen, 1977; Lord and Church, 1983; Giblin and Howarth, 1984; Thandrup *et al*., 1994) have looked at the relationships between sulfate in porewaters, sulfate reduction rates, and percolation rates of water through sediment. Their results showed that sulfide re-oxidation was significant in surface sediments. For example, Jorgensen (1977) calculated a budget of the sulfur cycle in a Danish fjord based on in situ sulfate reduction rates and oxygen uptake rates, as well as sulfur compounds. He determined that only 10 % of reduced sulfide was precipitated by metal ions, while the rest was re-oxidized at the surface. Enrichment of sulfate occurred in sediments and could not be accounted for by sulfate reduction alone.

Sulfate re-oxidation rates in marsh sediment are calculated using a material balance approach. The mass balance is dependent on three components on a lift-to-lift (2-cm increments of core sediment) basis: sulfate concentrations in the porewater (obtained per lift from a single core per mesocosm), sulfate reduction rates (determined

per lift from duplicate cores per mesocosm), and underdrain volumes (measured for each mesocosm during low-tide period).

For the surface (0-2 cm) lift, S_{sw} represents the sulfate concentration in overlying seawater from the influent. S_i represents the sulfate concentration in porewater in the surface lift and is indicative of sulfate transported downward to the next lift. For subsequent (2-10 cm) lifts, S_{i-1} represents the sulfate concentration in porewater transported out of the overlying lift and S_i represents the sulfate concentration of the current lift. S_o represents the sulfate concentration transported out of the overlying lift when porewater is exhausted (explained below).

The mass balance terms were assigned times of reaction. The advection of sulfate was dependent on the movement of water through a lift of sediment – once water drained from a lift entirely, porewater exhaustion occurred. The term t* accounts for porewater exhaustion and was calculated from pore velocity. Below a certain depth, exhaustion does not occur and t* reaches t_2. The term t_2 is the length of time in which the sediment surface is free of overlying water during one tidal cycle (equals 6 hr). Lifts affected by porewater exhaustion (the vadose zone) were treated differently than lifts not affected (the saturated zone).

Water flushed through each mesocosm differently due to variations in sediment origins and physical properties as well as the presence or lack of vegetation. The rate at which water flowed through the sediment was expressed as face velocity. Average volumes of water collected after a single tidal cycle pristine vegetated, contaminated vegetated, and contaminated unvegetated mesocosms during fall and winter events were

166, 187, and 272 L, respectively. Correspondingly, face velocities were 0.257, 0.290, and 0.387 L/cm^2-hr. Converted to pore velocity, these values were 0.402, 0.390, and 0.520 cm/hr. Differences in these rates may have resulted from the stabilization effect of *Spartina* vegetation and sponge-like behavior of root material. Water flowed more readily in unvegetated sediment. More rapid flow affected chemical transport and mass balance of the system by more quickly exhausting the porewater in surface sediment lifts. Thus, t* is shortest for LCP-unvegetated.

Once porewater was exhausted ($t^* < t_{2)}$, mass balance was re-evaluated since advection no longer existed (as mentioned above). Face velocity (v_f) and porosity (Φ) were known, so t* was calculated a priori by $t^* = 2\ \Phi / v_f$ (based on a lift of length = 2 cm).

The input of sulfate into a lift plus newly generated sulfate from re-oxidation equals the output of sulfate out of the lift plus the newly reduced sulfate:

$$S_{i-1}*v_f*\pi*t_1 + SOR*2\pi*T = S_i*v_f*\ \pi*(t_1+t^*) + SRR*\ 2\pi*T$$

The terms for this mass balance equation are defined as follows:

Sediment lift, i = a subsample of a whole sediment core with radius = 1 cm, length = 2 cm

Face velocity, v_f = velocity of water base on a change of volume over a period of time, normalized to cross-sectional area, i.e. volume of flow per unit cross-sectional area per unit time; comparable to Darcy velocity (L/cm^2-hr)

t_1 = length of time in which the sediment surface is flooded during one tidal cycle; equals 6.75 hr.

T = length of time of one complete cycle, equals 12.75 hr.

t* = time it takes for a sediment lift to drain at a downward pore velocity after the flood period is complete; varies for each mesocosm

t_2 = length of time in which sediment is free of overlying water during one tidal cycle ; equals 6 hr; $t_2 = T-t_1$

S_{sw} = sulfate concentration in influent or overlying seawater (mM)

S_i = porewater sulfate concentration of lift i (mM)

S_{i-1} = porewater sulfate concentration of lift directly overlying lift i (mM)

SOR = sulfide oxidation rates ($nmol/cm^3$-d)

SRR = sulfate reduction rates ($nmol/cm^3$-d)

Rearranged and simplified, the mass balance yields the following equation for lifts affected by porewater exhaustion (vadose zone):

$$SOR = SRR + (v_f * t_1 / 2\ T)\ (S_i - S_o) + S_i\ \Phi/T$$

The following equation is used for remaining lifts not affected by porewater exhaustion:

$$SOR = SRR + (v_f /2)\ (S_2 - S_1)$$

Sulfide oxidation rates were higher in surface sediments in all mesocosms (Figure 4.17). A slight peak occurred at the 6-8 cm and at the 8-10 cm depths in vegetated sediment due to scattering of data and because sulfate concentrations did not deplete significantly in lower depths. Figure 4.18 compares estimated sulfate oxidation rates (SOR) and sulfate reduction rates (SRR) for each mesocosm during each sampling period. SOR were much greater in magnitude than SRR at surface sediments. In some cases, SOR were greater than SRR by a factor of 10 to 30 in surface sediments. The amount of oxygen supplied to drive SOR can be resolved, but what is supplying the sulfide for SOR if it is not sulfate reduction? This model assumes that all porewater sulfate is converted to sulfide and the prediction is based on a face velocity and volume of water moving through the sediment. Note in the above equations that SOR equals SRR *plus* the concentration of porewater sulfate times a face velocity term, which may greatly magnify the SOR calculation. Therefore, SOR predictions may be somewhat exaggerated.

Surface sediments receive the greatest input of oxygen because oxygen is entering the surface sediment from both the atmosphere and from inflowing water, chemical oxidation and to a smaller extent, *Spartina* root exudates and bioirrigation. Sauer (2003) estimates that only 31% of oxygen is diffused from inflowing water into the vadose zone. Another 30% is attributed to chemical oxidation and *Spartina* and algal input. However, additional pore volume from air could contribute to the input of oxygen into the subsurface. A decrease in partial pressure of oxygen below ambient 21 % could induce a diffusive gradient, enhancing transport of oxygen into the sediment.

This approach does have inherent uncertainties, mainly with the way in which sulfate concentrations are used. First, SRR, SOR, and sulfate concentrations were not obtained independent of one another. Recall that porewater sulfate is an input parameter in the calculations of SRR and SOR. Also, SRR is an input parameter in the calculation of SOR. Hence, an underestimation or overestimation of sulfate concentrations would carry through to all SRR and SOR calculations. Second, any solid-phase sulfate that may go into solution is unaccounted for if it is taken up by other sequestering compounds. Porewater sulfate, not total sulfate in sediment, was measured and applied in the equations. Hence, the presence of other constituents, such as gypsum ($CaSO_4$), would underestimate sulfate concentrations.

Total Mercury in the Porewater

Figure 4.19 shows data collected for total mercury in the porewater. Data were averaged for each mesocosm per sampling event. The total porewater mercury includes both organic and inorganic mercury. Total mercury concentrations ranged between 40 and 170 ng/L. Standard error bars indicate deviations within data used to compute the mean values plotted on the bar graph.

As discussed in Chapter 3, a total mercury volume experiment demonstrated that a minimum volume of 2 mL was necessary to obtain feasible results for total mercury analysis. However, because the minimum volume could not be obtained easily using sippers, cores were used to acquire samples in February and May sampling events. Only

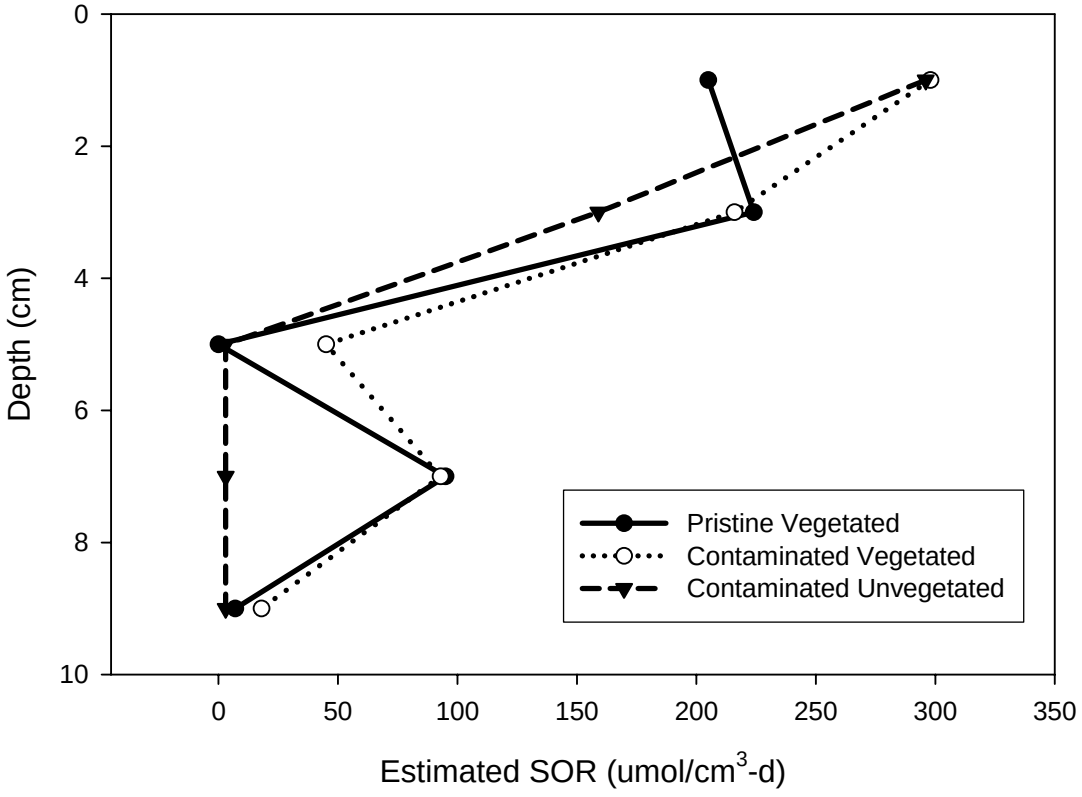

Figure 4.17 Estimated sulfide oxidation rates (SOR) in mesocosm in pristine vegetated, contaminated vegetated, and contaminated unvegetated mesocosms.

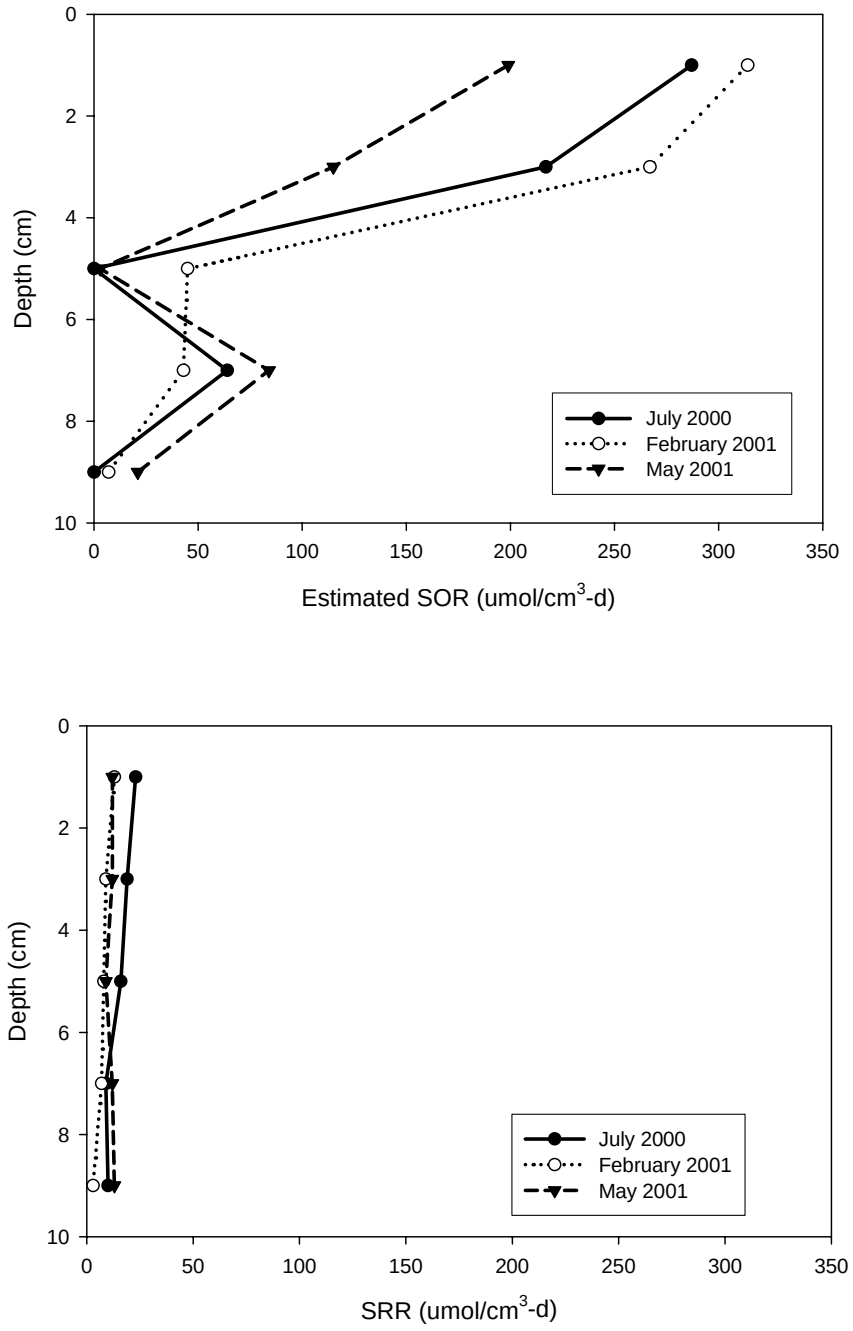

Figure 4.18 Comparison of estimated sulfide oxidation rates (SOR) and sulfate reduction rates (SRR) over a seasonal cycle.

one data point was plotted for pristine sediment in July 2000 because the other data points were either 3 times higher in magnitude or was lost during analysis.

Methylmercury in the Porewater

Figure 4.20 shows data collected for methyl mercury in the porewater. Data were averaged for each mesocosm per sampling event. Methylmercury concentrations ranged between 1 and 48 ng/L. Standard error bars indicate deviations within data used to compute the mean values plotted on the bar graph. No trend in methylmercury concentrations was observed in the pristine sediment. MeHg in the contaminated sediments were higher during the summer and spring than in winter and is attributed to increased microbial activity. However, on average, methyl Hg concentrations were low (less than 30 ng/L) in the contaminated sediment, while total Hg concentrations were fairly high. Therefore, demethylation may be significant in this marsh system.

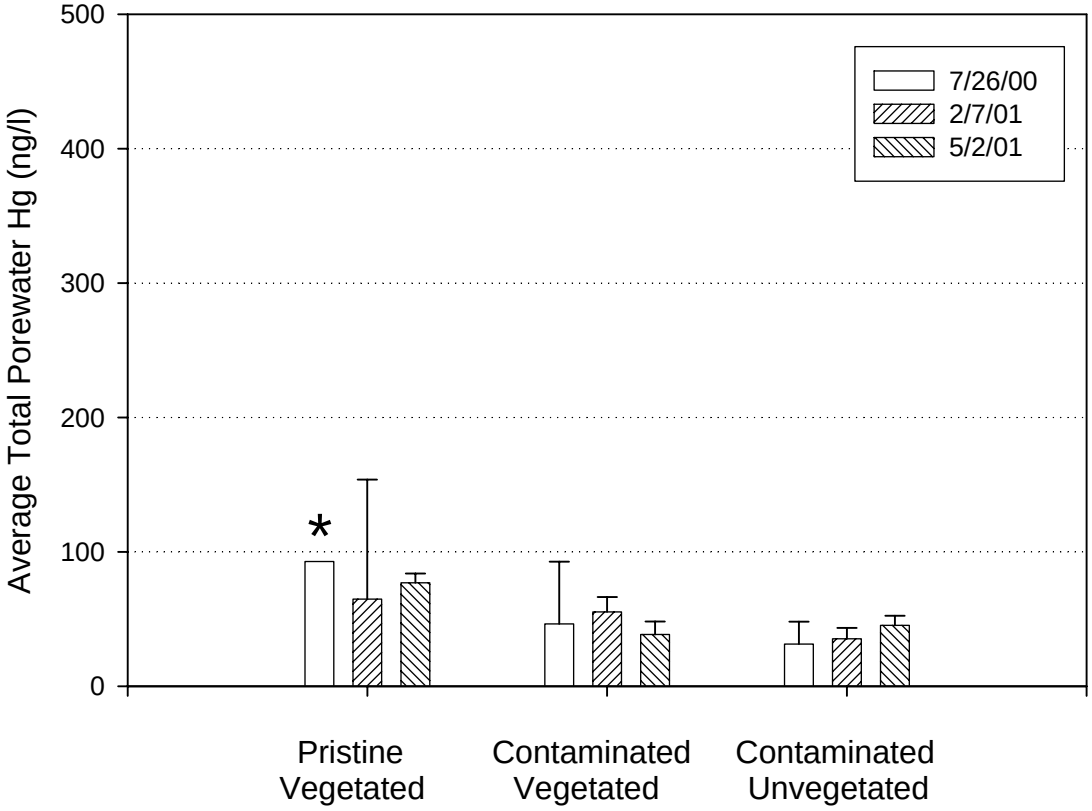

Figure 4.19 Total mercury in BERM mesocosms at each sampling event. Error bars indicate standard deviations of three samples in each mesocosm. Pristine sediment in July 2000 does not have an error bar since only one data point was used. Data compared between mesocosms were not significant within 95 % confidence. ***** Sample collected from sipper only and only one sample data point used.

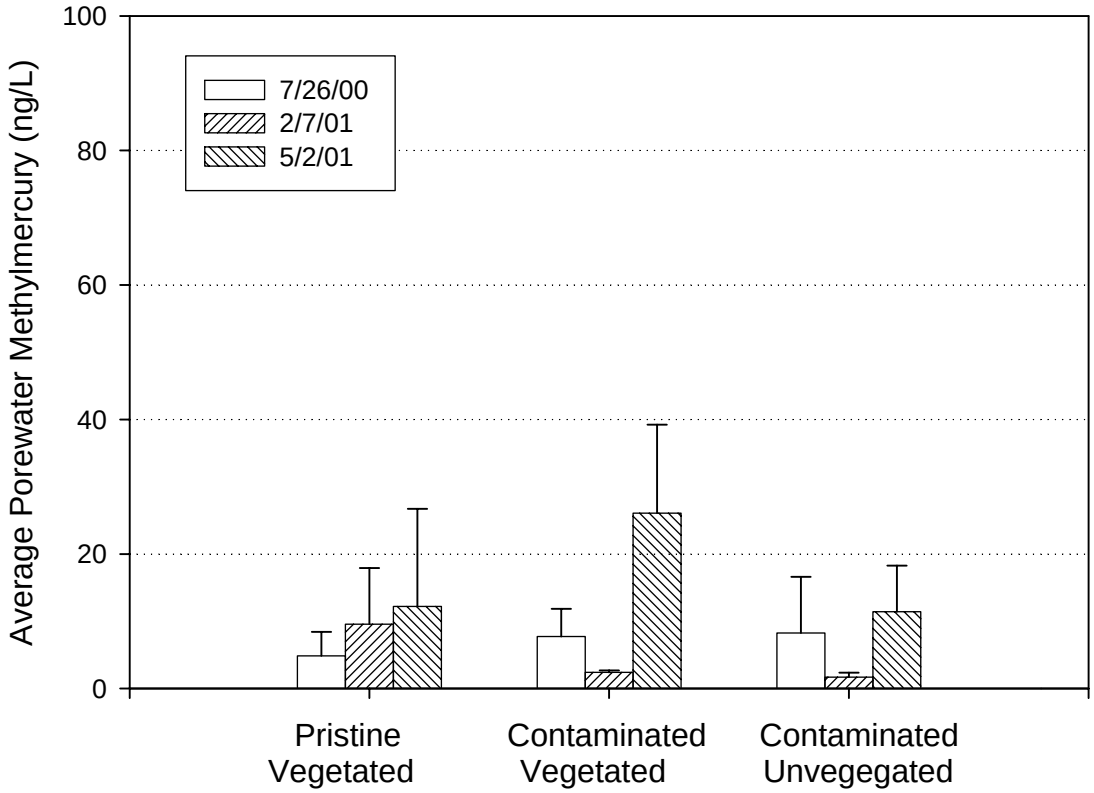

Figure 4.20 Methylmercury in BERM mesocosms at each sampling event. Bars indicate standard deviations of three samples in each mesocosm. P <0.5 between mesocosms was reported.

Microbial Community Structure Analysis

Relative Distribution of Sulfate-Reducing Bacteria in the Sediment

Figures 4.21 through 4.23 show the seasonal distribution of the community of sulfate-reducing bacteria (SRB) in the pristine, contaminated vegetated, and contaminated unvegetated sediment. Relative distributions were determined by normalizing the optical density values to the highest value for each probe and then normalizing the specific probes to the optical densities of the UNIV probe. Finally, the normalized optical densities of the specific probes were normalized again to the highest values obtained to generate ratios of 1 or less. During July 2000 and May 2001, the community was stratified and all species followed similar trends, except for the contaminated unvegetated mesocosm in July where *Desulfobacter* sp. deviated from the community trend. During February, the SRB community was diversified and more variable throughout the sediment in all mesocosms.

Direct quantification of SRB cells was determined using pure culture data. Pure culture cells were quantified using DAPI fluorescence and served as positive controls for oligonucleotide probing. Seasonal changes in the SRB community structure were observed and presented in Figures 4.24 through 4.26. *Desulfobacter* dominated the SRB community in winter and spring.

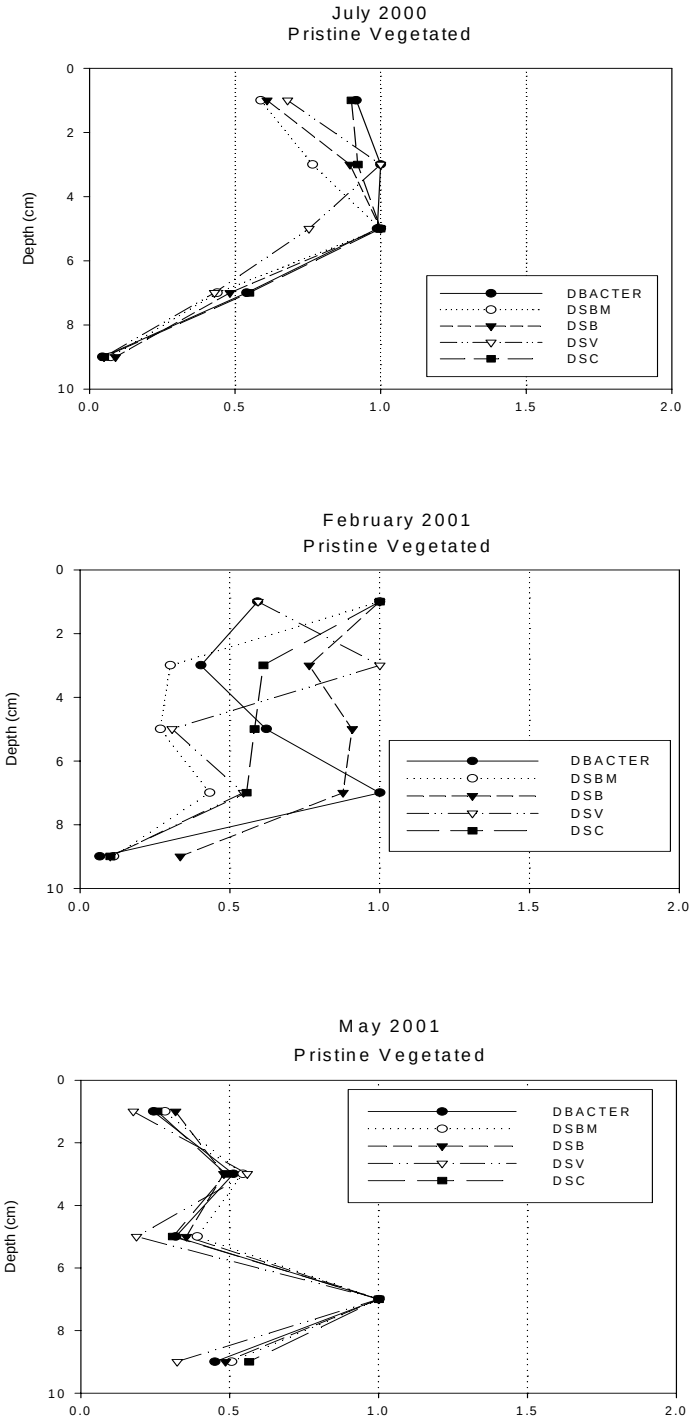

Figure 4.21 Relative distribution of SRB in pristine vegetated sediment.

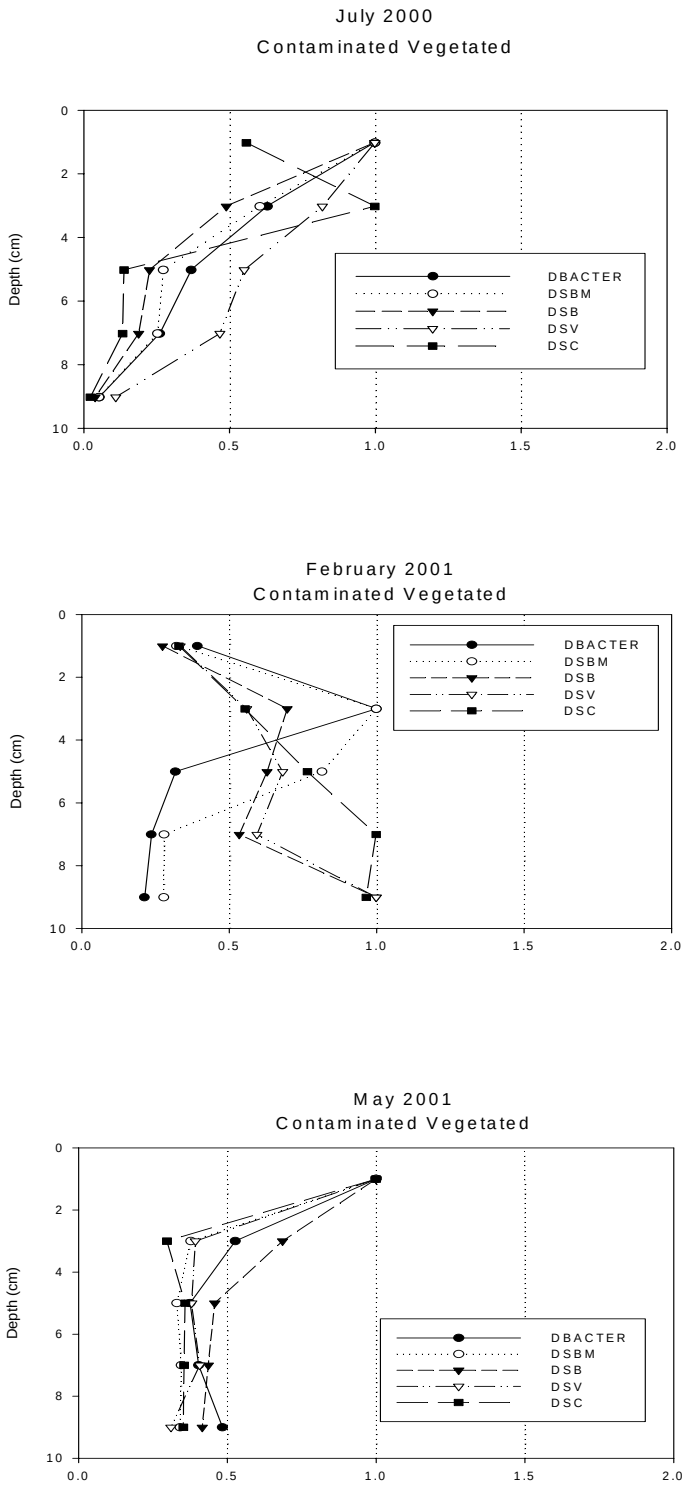

Figure 4.22 Relative distribution of SRB in contaminated vegetated sediment.

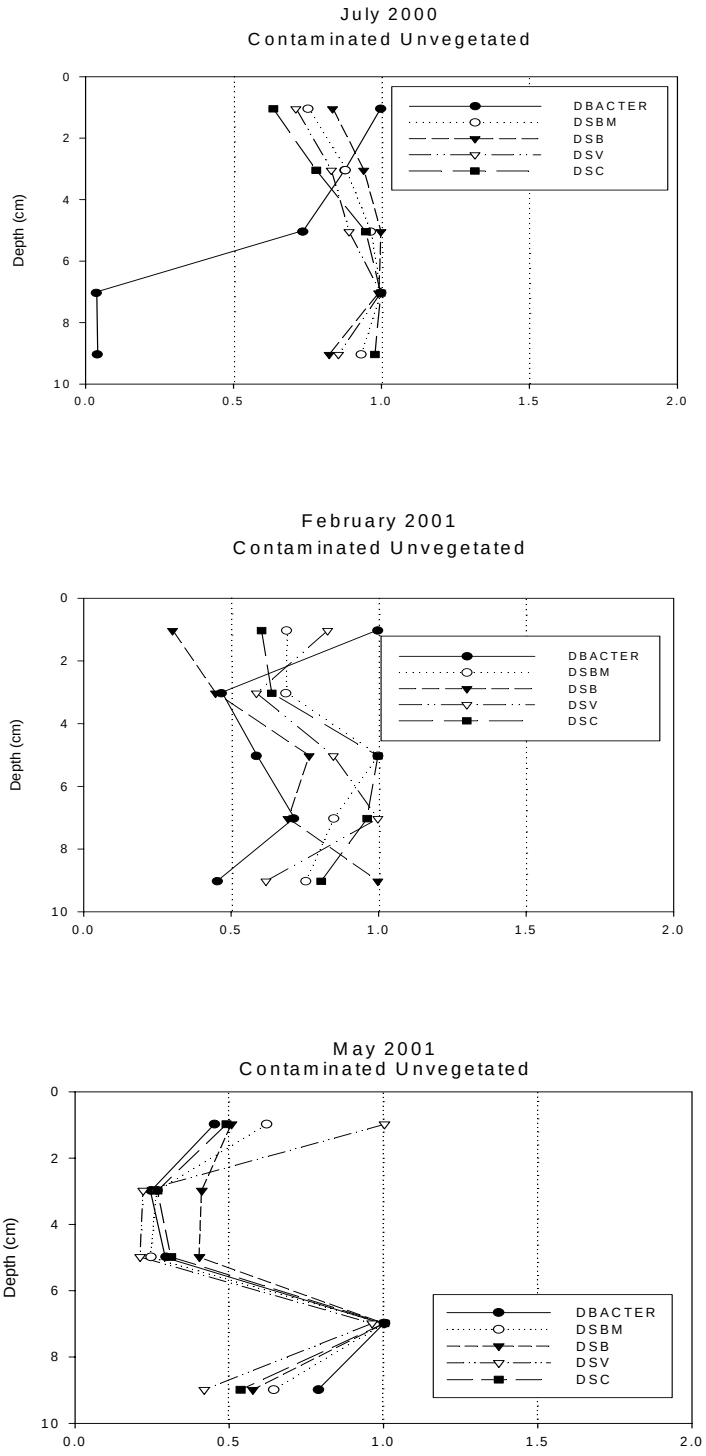

Figure 4.23 Relative distribution of SRB in contaminated unvegetated sediment.

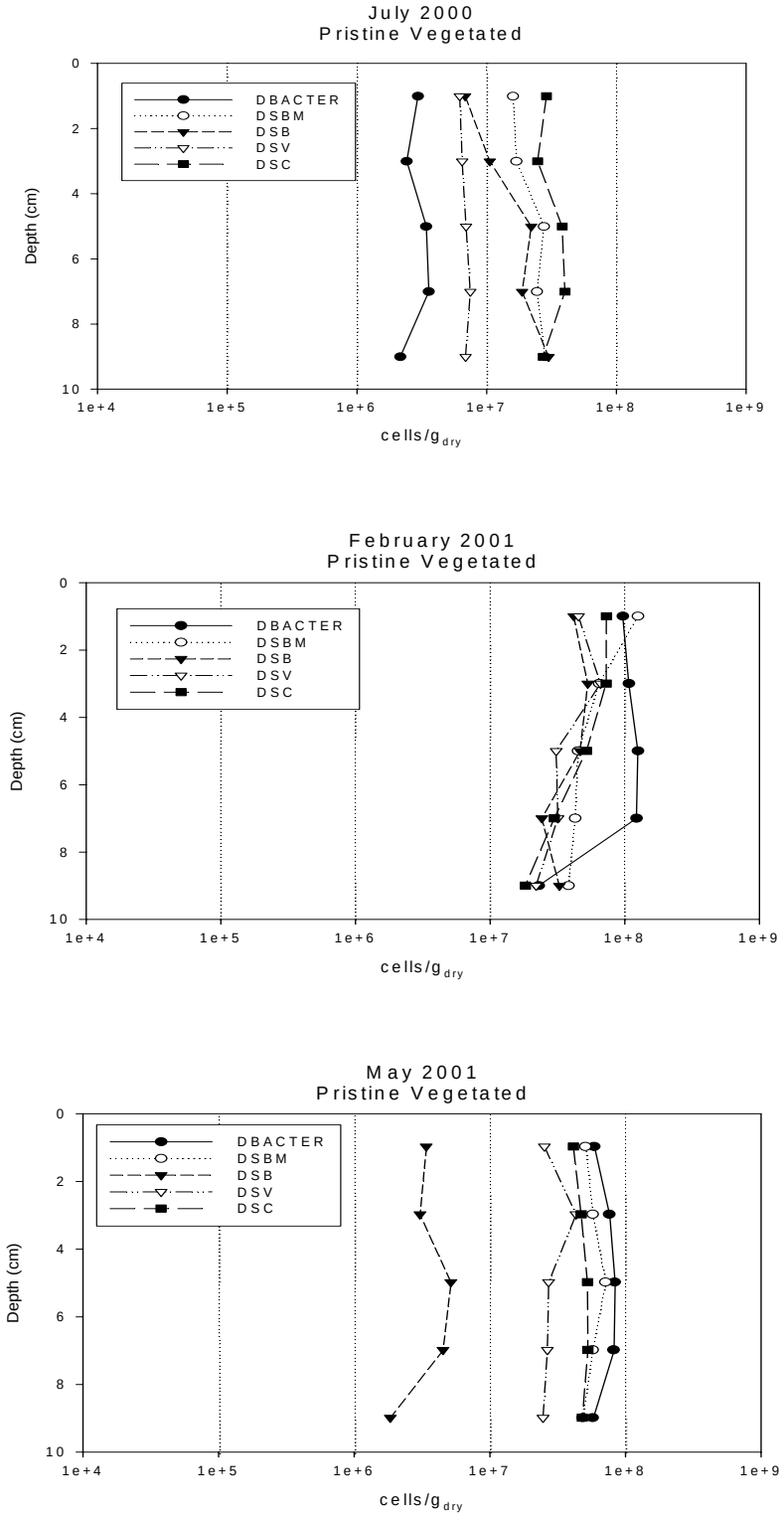

Figure 4.24 Distribution of SRB community structure in pristine vegetated mesocosm.

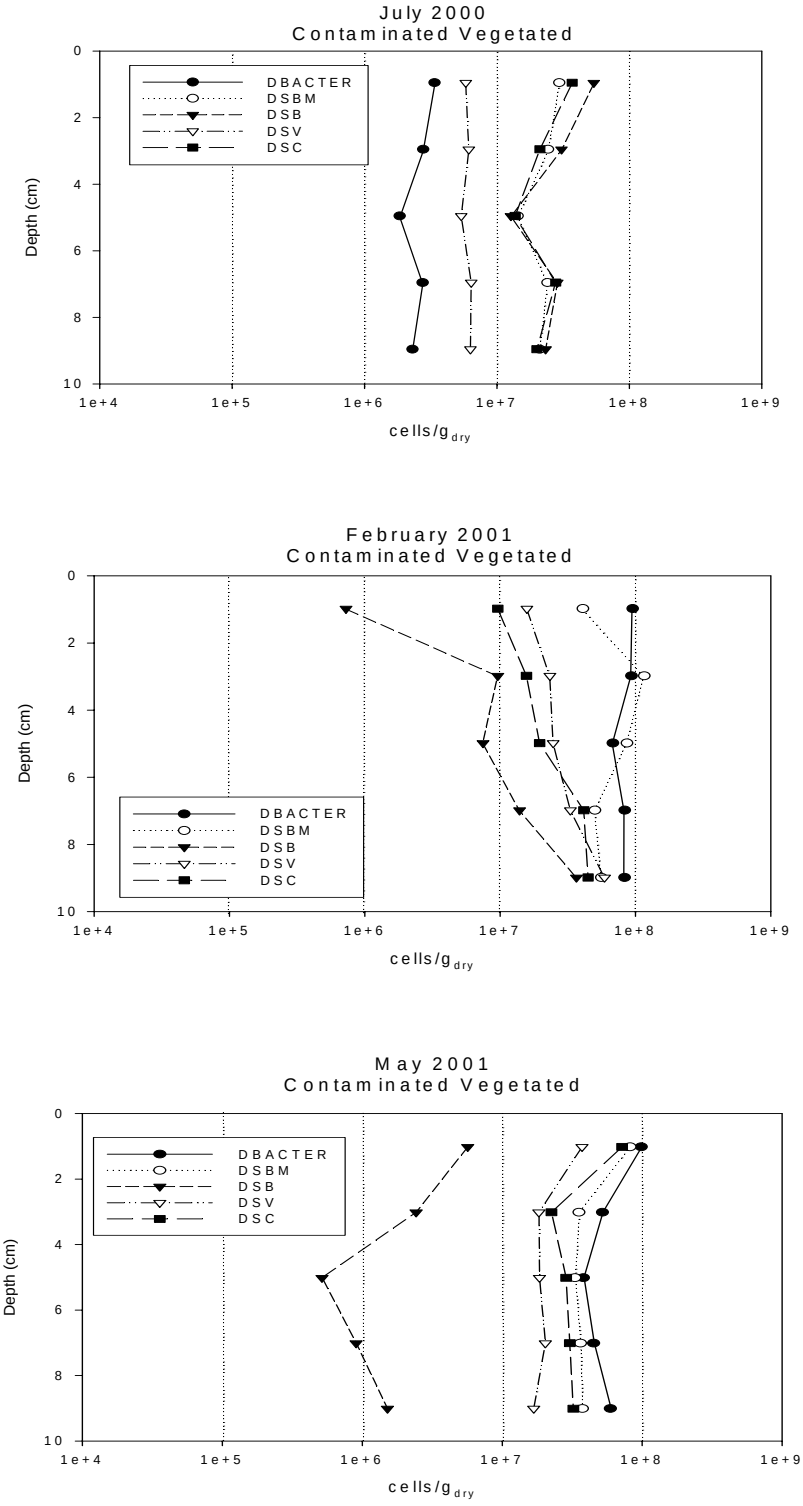

Figure 4.25 Distribution of SRB community structure in contaminated vegetated mesocosm.

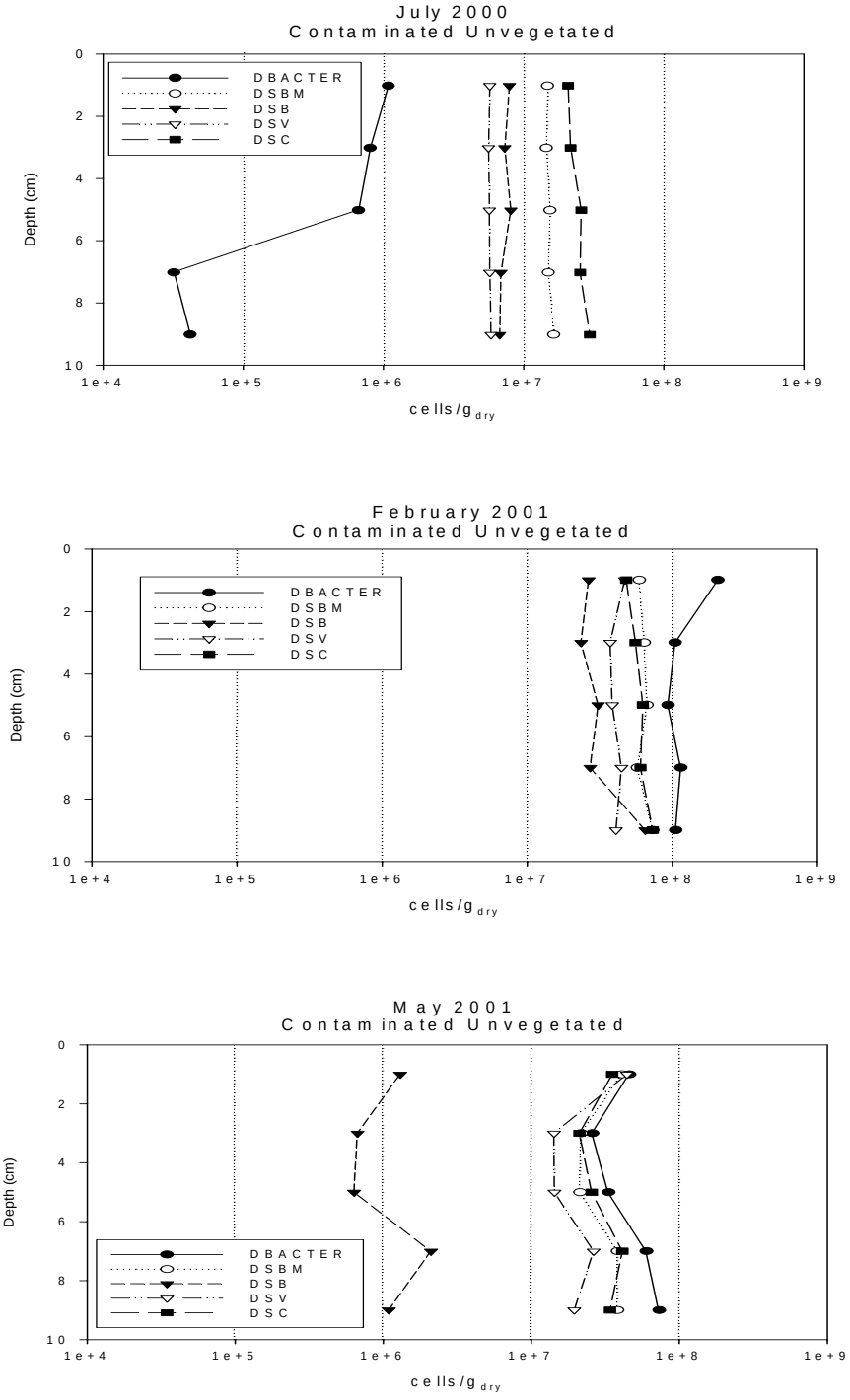

Figure 4.26 Distribution of SRB community structure in contaminated unvegetated mesocosm.

CHAPTER V
APPLICATION OF RESULTS TO PREDICT MERCURY METHYLATION RATES

Recent studies by King *et al*. (1999, 2000, and 2001) observed that sulfate-reducing bacteria (SRB) phylogenetic groups in pure culture methylate mercury at different rates when mercury methylation rates (MMR) were normalized to sulfate reduction rates (SRR). Additionally, it was observed that members of the family *Desulfobacteriaceae* had higher rates of mercury methylation than the *Desulfovibrionaceae* family when MMR was normalized to SRR. This chapter will apply the novel concepts introduced by King *et al*. to this study and investigate differences in MMR between different phylogenetic groups in a simulated salt marsh system.

Calculations of SRR for Individual Phylogenetic Groups

SRR was calculated for each phylogenetic group based on average SRR and 16S rRNA quantification data. Since sulfate reduction is dependent on SRB metabolism, the rate of respiration by individual groups must be taken into account. For each phylogenetic group, the fraction, Z_i, was calculated:

$$Z_i = \frac{X_i}{X_{Total}}$$

Z_i is equal to the ratio of active cells of a phylogenetic group per gram of sediment (X_i) to the total number of active cells in the population per gram of sediment (X_{Total}) and represents the metabolic contribution each phylogenetic group makes to total SRR

activity. The term *i* corresponds to the phylogenetic group *Desulfobacter* (DBACTER), *Desulfobacterium* (DSBM), *Desulfobulbus* (DSB), *Desulfovibrio* (DSV), or *Desulfococcus* (DSC). This equation does hold some uncertainty as it assumes that all cell specific rates are equal. Figure 5.1 reports Z_i averaged over three mesocosms for each phylogenetic group during each sampling event. Figure 5.2 compares average Z_i between the three mesocosms.

Desulfobacterium and *Desulfobacter* comprised the majority of the SRB rRNA in February 2001 and May 2001 ranging between 24 to 36 percent, but *Desulfococcus* dominated in July 2000, comprising 38 percent of the SRB rRNA. The reason why *Desulfococcus* outcompeted *Desulfobacterium* and *Desulfobacter* in July may be explained by carbon metabolism. *Desulfobacterium* and *Desulfobacter*, which are capable of complete acetate oxidation, dominate when acetate is the sole source of carbon in the sediment (King *et al*., 2000). Members of the group *Desulfococcus* also use acetate as an electron donor, but also a number of other electron donors, including lactate, ethanol, C_1 to C_{14} fatty acids, secondary alcohols, and proprionate with complete oxidation to CO_2 (Widdel and Bak, 1992). Such nutritional versatility could be highly advantageous in this complex environment. Therefore, it is possible that during the July sampling event, plants exuded a wide variety of organic nutrients that *Desulfococcus* and other groups were able to utilize and consequently out-compete *Desulfobacterium* and

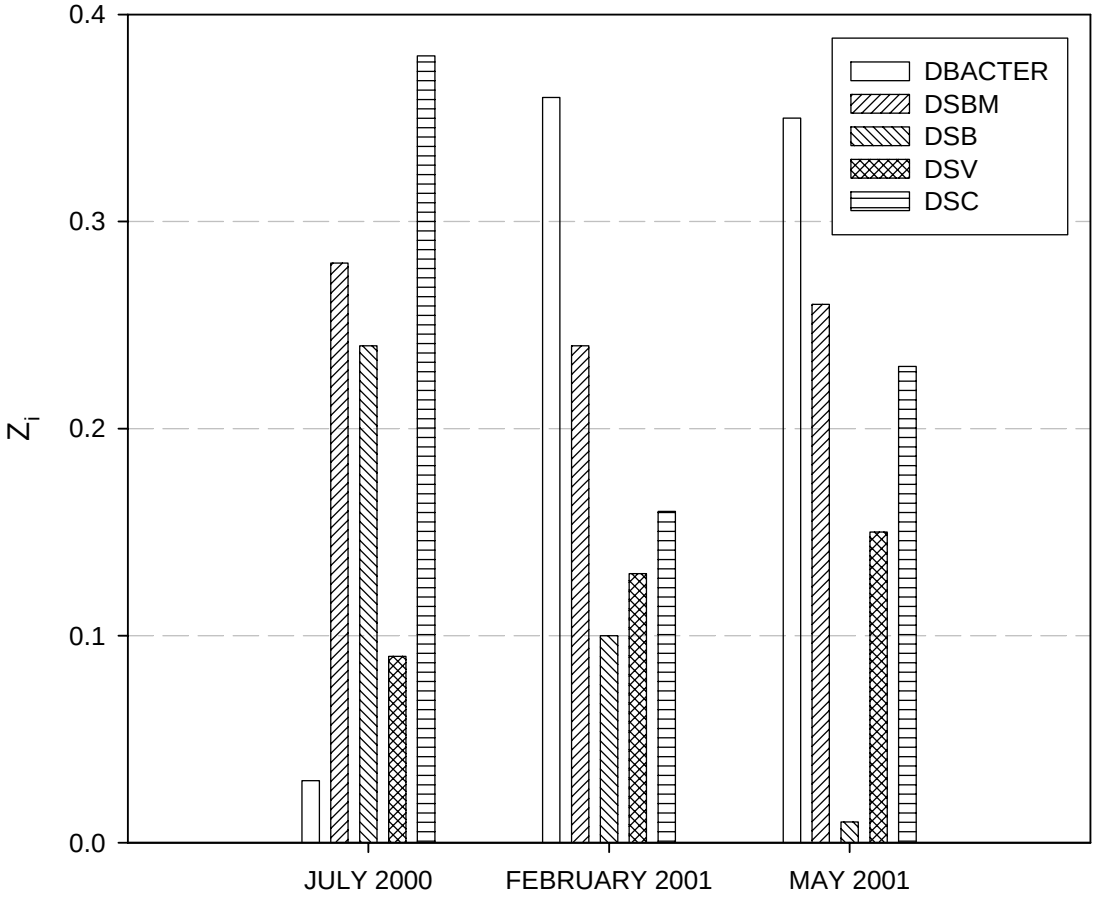

Figure 5.1 Calculated Z_i for each phylogenetic group averaged for each sampling event.

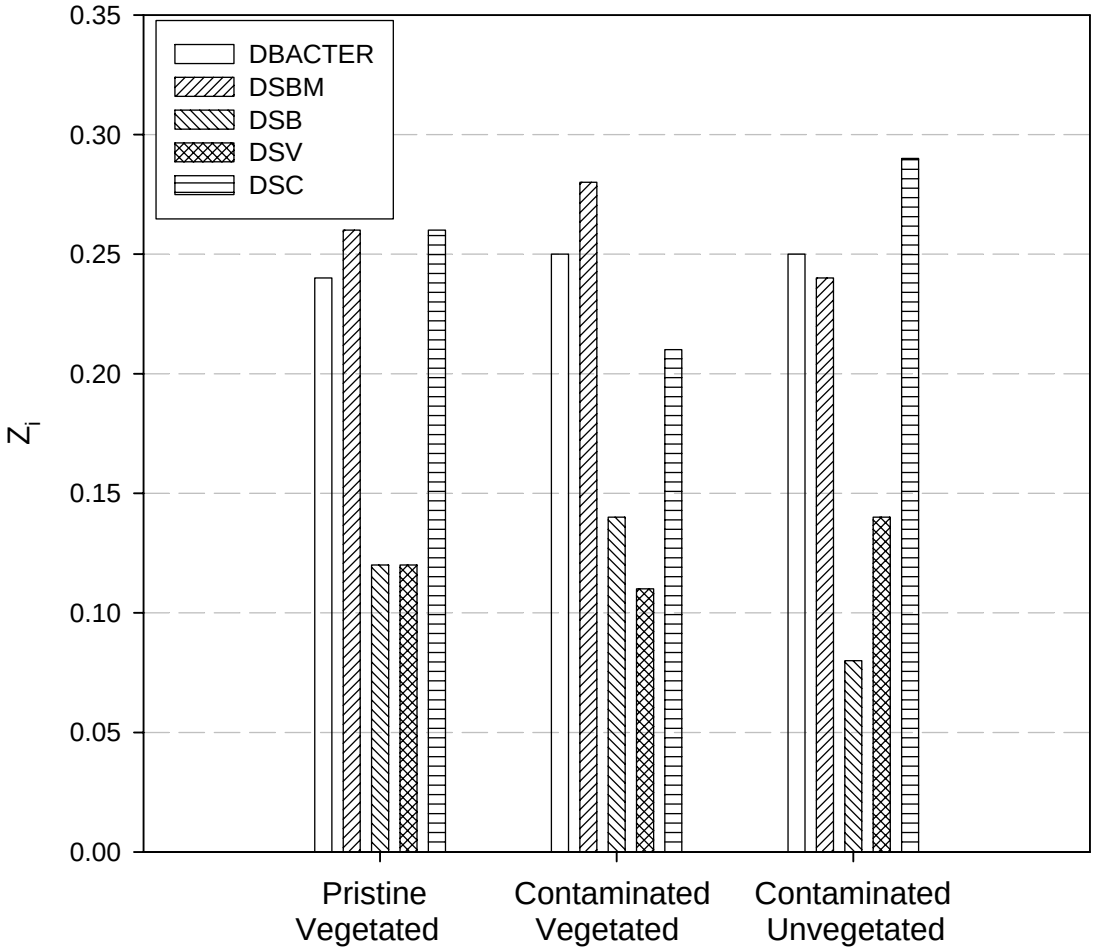

Figure 5.2 Calculated Z_i for each phylogenetic group averaged for each mesocosm.

Desulfobacter members. Rooney-Varga et al. (1997) observed that *Desulfococcus* members and two other closely related species played a dominant role in the salt marsh sediment and their relative abundances corresponded with *Spartina* growth stages. A complete characterization of the compounds present in plant exudates and redox conditions would provide a more definite explanation for this inconsistency.

Hines *et al*. (1999) found that members of the family *Desulfobacteriaceae*, which include the *Desulfobacterium, Desulfobacter, and Desulfococcus* groups, accounted for the majority of the SRB rRNA throughout the year, but increased significantly during active vegetative growth by *Spartina alterniflora*. Although these three groups generally dominated the community throughout the season in our study, they did not increase significantly during July or May when plants were most active or decrease significantly in the winter when plants were least active. The lack of clear seasonal trends in SRB abundance is surprising given the strong seasonal variation in SRR. However, it is possible that certain members of SRB are able to endure long periods of cold and remain dormant in the marsh as suggested by Hines *et al*. (1999).

Differences in community structure between mesocosms were not significant. However, as observed in Figure 5.2, it was apparent that *Desulfobacter* (DBACTER), *Desulfobacterium* (DSBM), and *Desulfococcus* (DSC) were higher in number relative to the total SRB than members of *Desulfobulbus* (DSB) and *Desulfovibrio* (DSV) in all mesocosms. Therefore, these observations indicate that DBACTER, DSBM, and DSC dominate the SRB community, whether plants are present or not.

The unvegetated mesocosm may not have been as different from the vegetated mesocosms as originally anticipated. As suggested by loss-on-ignition data, contaminated sediment contained twice as much organic carbon available for microbial respiration than pristine sediment (Sauer 2003). Therefore, contaminated sediment is either receiving input of carbon from an unknown source or the sediment already contains an abundant carbon supply. Marsh sediment is already organically rich in nutrients that can sustain microbes throughout the year. Additionally, algal mats were present in the unvegetated sediments, which may have also helped sustain SRB populations.

It has been shown that *Spartina* supplies oxygen and organic carbon simultaneously to the sediment (Hines *et al*., 1999). Carbon input would stimulate sulfate reduction but oxygen exudation would limit the growth of anaerobic SRB members. Hence, SRB activity may be dampened by the oxidative processes taking place in vegetated sediment. Additionally, oxygen input by *Spartina* would also stimulate sulfide oxidation processes, as evidenced by the lower sulfide levels and higher sulfate levels in vegetated sediment during active plant growth.

Just as metabolic activity varies among phylogenetic groups, SRR varies among phylogenetic groups both in pure culture and in natural sediment (King *et al*. 2000 and 2001). Therefore, individual SRR values can be calculated from the fraction of 16S rRNA of each individual group (Z_i) and observed activity of sulfate-reduction relative to all phylogenetic groups. The following equation illustrates the calculation of SRR for each individual phylogenetic group:

$$SRR_i = [Z_i] * [SRR]$$

Figures 5.3 and 5.4 compare SRR on a per cell basis for each phylogenetic group between sampling events and between mesocosms, respectively.

SRR activity attributed to individual SRB groups did not differ greatly between summer, winter, and spring (Figure 5.3). Similarly, differences in SRR_i were not significant between vegetated and unvegetated mesocosms (Figure 5.4). However, observed SRR that was measured for the total SRB population did follow changes in plant growth and was affected by the presence or absence of vegetation as presented in the above-mentioned figures. DSBM was the largest contributor to sulfate reduction relative to the other SRB groups throughout the year in all three mesocosms. Therefore, although individual contributions of each SRB phylogenetic group did not appear to be impacted by plant growth or lack thereof, the sum of all contributions more clearly demonstrates that these differences are apparent. In other words, the other non-dominating SRB groups made contributions that affected the community as a whole.

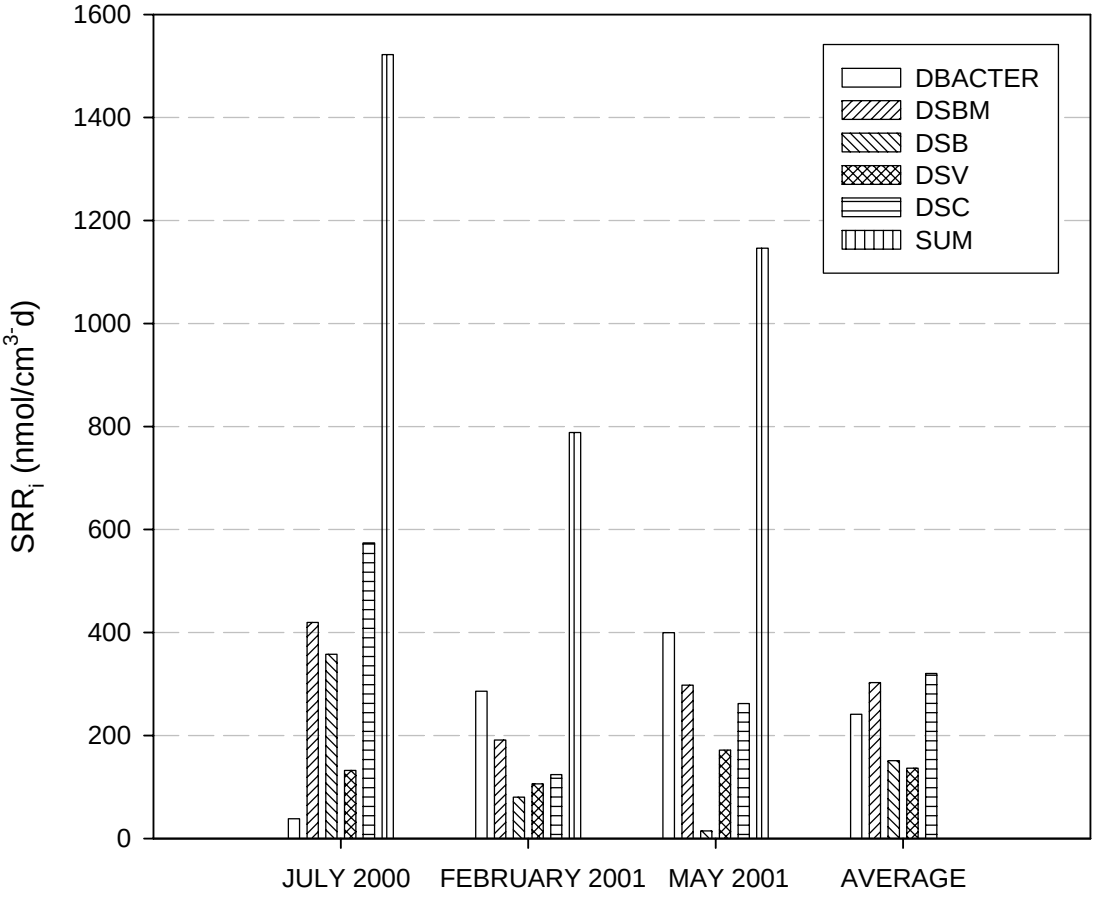

Figure 5.3 Calculated SRR_i (nmol/cm^3-d) for individual SRB phylogenetic groups during each sampling event.

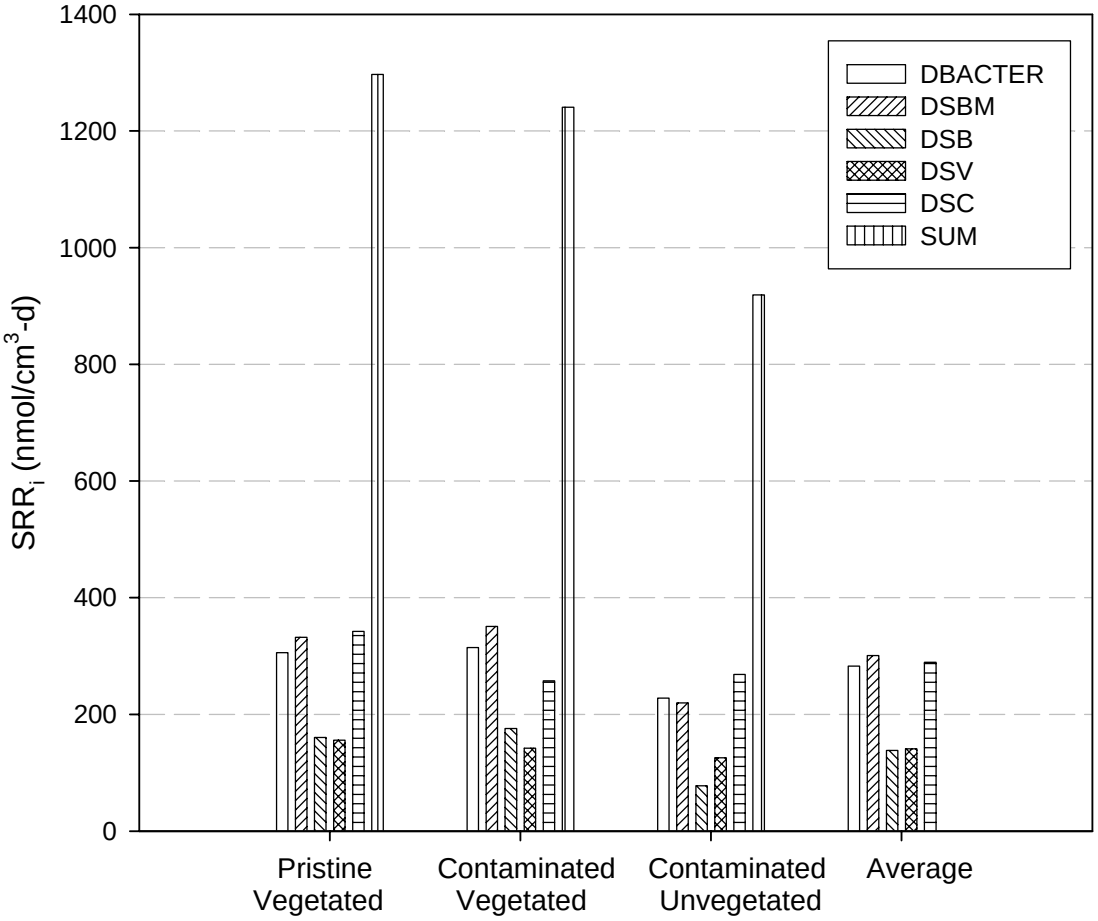

Figure 5.4 Calculated SRR_i (nmol/cm^3-d) for individual SRB phylogenetic groups averaged over three sampling events for each mesocosm.

Calculations of MMR Based on Observed SRR and Pure Culture f*

MMR for each individual phylogenetic group is dependent on the individual SRR (SRR_i) and the function f*. The f* values were defined in pure culture as described by King *et al*. (1999, 2000, 2001) and represent the maximum quantity of methylmercury produced per sulfate reduced by that specified phylogenetic group. Table 5.1 presents average f* values as determined by King *et al*. (1999, 2000, 2001). The series shows that methylmercury production is dominated by *Desulfobacterium*, followed by *Desulfococcus*.

Table 5.1 f* values determined by King *et al*. (1999, 2000, 2001).

	f* term (nmol/nmol)
DBACTER	4.1×10^{-6}
DSBM	2.58×10^{-5}
DSB	2.9×10^{-7}
DSV	1.4×10^{-6}
DSC	4.6×10^{-6}

The following equation defines MMR for each individual phylogenetic group as a function of SRR_i and f*:

$$MMR_i = f_i^*(SRR_i)$$

Figure 5.5 presents the calculated MMR for each phylogenetic group in each sampling event and Figure 5.6 presents calculated MMR for each mesocosm.

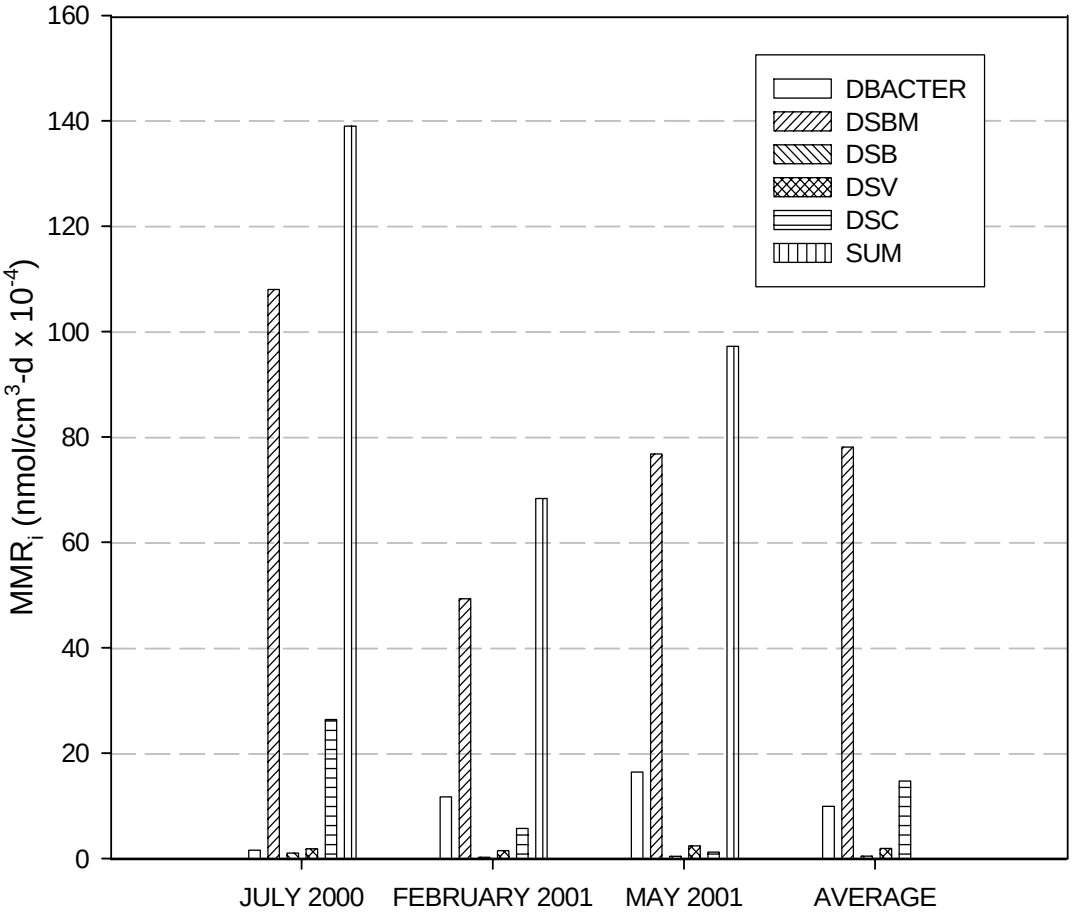

Figure 5.5 Estimated MMR (nmol/cm^3-d) for individual phylogenetic groups for each sampling event.

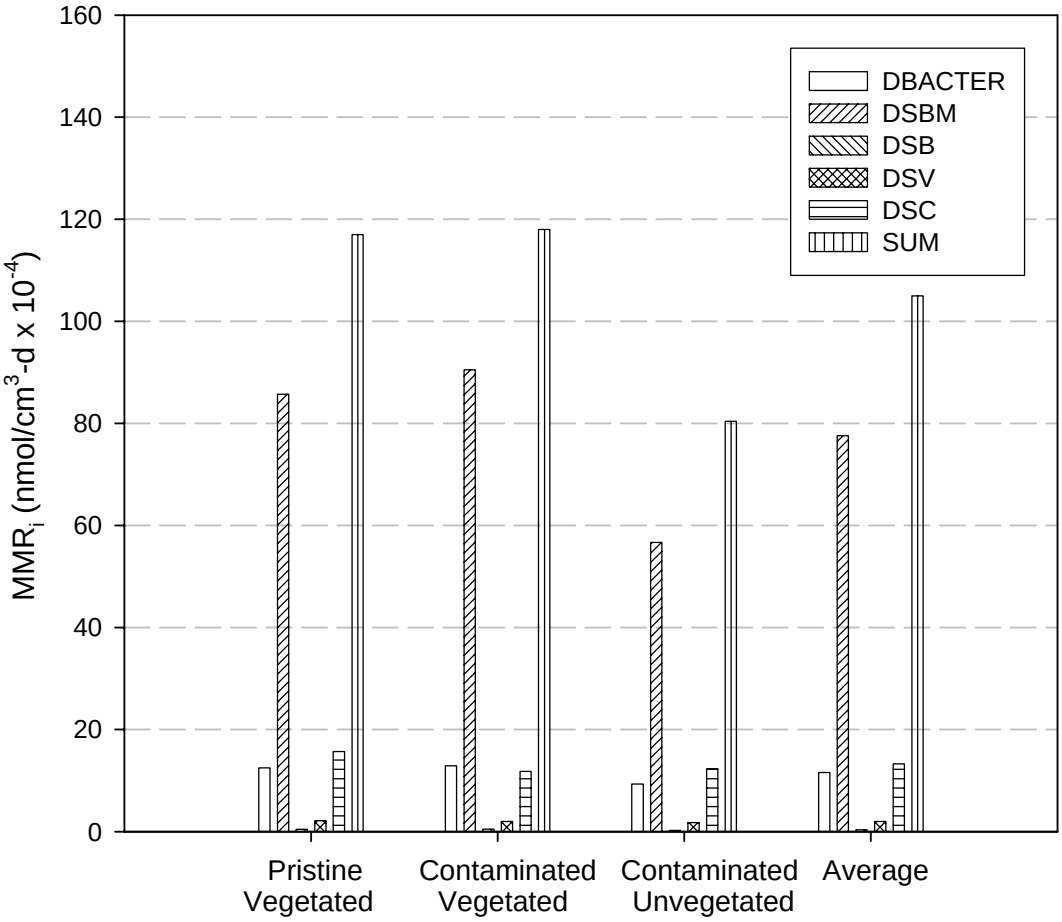

Figure 5.6 Estimated MMR (nmol/cm^{3}-d) for individual phylogenetic groups for each mesocosm.

Similar to what was observed with SRR_i, MMR did not vary temporally or between mesocosms for individual SRB groups. However, the incidence of methylmercury production normalized to SRR for all sampling periods and mesocosms is as follows: *Desulfobacterium* > *Desulfococcus* > *Desulfobacter* > *Desulfovibrio* > *Desulfobulbus* *Desulfobacterium* had the highest mercury methylation rates among the SRB groups during all sampling events. It has been suggested that acetate utilizers, like members of the group *Desulfobacterium* have an advantage over lactate utilizers, like members of the group *Desulfovibrio.* King *et al*. (2000) suggest that differences in mercury methylation between phylogenetic groups are linked to carbon metabolism. They observed that SRB groups that use acetate as the sole carbon source methylate mercury at higher rates compared to other groups.

Total mercury and methyl mercury concentrations measured in porewater similarly lacked temporal differences between contaminated and uncontaminated mesocosms (Chapter 4). Average total mercury in July 2000 was 56.8 ng/L, 51.8 ng/L in February 2001, and 53.6 ng/L in May 2001. Average methyl mercury levels in July, February, and May were 6.93 ng/L, 4.53 ng/L, and 16.55 ng/L, respectively. Therefore, predicted MMR for individual phylogenetic groups corresponded with total Hg and MeHg trends.

As shown in Figure 5.6, total MMR activity was higher in the vegetated sediment compared to unvegetated sediment. However, this did not correspond to MeHg concentrations measured in porewater. Higher MMR would expectedly produce higher levels of MeHg, but this was not the case. Average MeHg was 8.86 ng/L in pristine sediment, 12.06 ng/L in contaminated vegetated sediment, and 7.10 ng/L in contaminated

unvegetated sediment. This suggests that the plant roots are bringing oxygen into the sediments stimulating demethylation and thus preventing MeHg accumulation in the vegetated sediment.

In summary, differences between phylogenetic groups in terms of cell number and sulfate reduction, and mercury methylation capability are not significantly apparent. However, determination of SRR on a per cell basis was solely based on microbial cell quantification. Even if all groups are alive and active, there is no sure way of estimating which group is actually reducing sulfate without studying one SRB group at a time and inhibiting all others. Additionally, each SRB group may be using other sources of energy besides sulfate. For example, members of the *Desulfobulbus* spp. are stimulated by oxygen to disproportionate S^0 generated from the oxidation of reduced S in the subsurface (Lovely *et al*., 1994). In fact, *Desulfobulbus* increased in June when *Desulfobacter* decreased. Therefore, community dynamics are very complex, which complicates the task of finding correlations between cell quantification and process rate measurements.

As seen in the estimated MMR calculations, predicted MMR are heavily influenced by f* values determined in pure culture. Since mercury bioavailability in pure culture is quite different from that in the marsh, there may be some discrepancies between estimated and measured MMR. However, *in situ* quantification of SRB cells and MMR calculations are in agreement that members of the *Desulfobacteraceae* family dominate over other families of the SRB community in terms sulfate-reduction and mercury methylation.

CHAPTER VI
CONCLUSIONS AND RECOMMENDATIONS FOR FUTURE STUDIES

This thesis has ascertained the principal biological and chemical drivers that control mercury methylation and the impacts of seasonal variability on these processes. The ultimate goal of this project was to elucidate plant and microbial controls on mercury methylation in contaminated salt marsh sediments. Our results indicate that plant and microbial interactions play a significant role in mercury methylation. This thesis has provided data that shows how seasonal variations in *Spartina alterniflora* growth and senescence affect the community structure of mercury-methylating bacteria in the sediment. The following summarizes these findings.

Geochemical Stratification

Vertical redox stratification of natural salt marsh sediments are primarily controlled by external forces, such as sunlight, hydrodynamic energy, and oxygen diffusion. Biotic processes, including microbial and plant interactions also stimulate and are stimulated by their redox environment. As sulfate-reducing bacteria use a whole array of energy sources, redox stratification zones are differentiated by the type and availability of electron acceptors and donors, as well as organic and inorganic inputs to the sediment. Plants exude carbon nutrients that stimulate microbial proliferation and activity. Therefore, changes in the sediment resulting from plant activities would characteristically be accompanied by changes in microbial structure (Hines *et al*., 1999).

Spatial variations in sulfate and sulfide in the sediment followed changes in plant growth activity and physiology as observed in other studies (Hansen, 1993; Howarth and Giblin, 1993, Hines *et al*., 1999). In vegetated sediments, sulfate concentrations at the upper 2-cm of the sediment were not significantly different from those at the lower depths; therefore, sulfate concentrations did not correlate with depth in the vegetated sediment. Sulfide concentrations were generally low (< 2 mM) in all sediments and in some cases increased with depth. Established studies by Kostka and Luther (1995) and King (1988) observed that dissolved sulfide concentrations increase with depth in saltmarsh sediments. Dissolved sulfide is quickly trapped in sediment by precipitation with metal ions, such as iron. Up to 90 percent of the sulfide produced, reaches the oxic surface layers of the sediment, where it is oxidized back to sulfate via intermediate oxidation steps (Jorgensen, 1977). Therefore, sulfide oxidation was significant in the sediment under study. During the summer months, plants were actively exchanging carbon dioxide and oxygen as well as nutrients for vegetative growth. Hence, the plants kept sulfate concentrations high at the upper 2-cm of the sediment by providing oxygen for sulfide oxidation. In the winter, plants were senesced and less active (less gas exchange), so sulfide oxidation was not as prevalent and sulfate was depleted more quickly with depth in the vegetated sediment. In contrast, sulfide remained at low concentrations in the vegetated mesocosms due to gas transfer, which encouraged re-oxidation of sulfate. In the unvegetated mesocosm, sulfide accumulated because plants were not present to stimulate gas transfer.

The presence of snails and fiddler crabs also impacted sulfate chemistry and sulfate reduction. Although macrofauna were purposely left out of the mesocosms at the beginning of this study in 1998, the presence of burrows and snails observed in 1999-2001 indicates that their eggs were carried in by the influent seawater or brought in by wind or birds. Burrows and snails were observed in the pristine and contaminated mesocosms, but not in the unvegetated mesocosm. Therefore, macrofauna apparently use *Spartina* detritus as a food source. Fiddler crabs and snails could be responsible for the increased sulfate at lower depths in the vegetated sediment by bioirrigation. These organisms transport organic matter and oxygen to lower depths and thus replenish sulfate.

Vertical stratification of the SRB community was not apparent in the marsh sediment. Stratification was observed in relative abundance data, but direct cell quantification revealed no definite maxima at the 0-2 cm sediment depth where highest SRR were observed. In fact, SRB abundances were within the same order of magnitude throughout the 10-cm column of sediment. In a study by Hines *et al*. (1999), highest relative abundances were observed in the 6-8 cm depth, and lowest abundances were observed at the surficial 0-2 cm depth, which did not correspond to the depth profiles of SRR. They argue that living *Spartina* roots occur at deeper depths, and therefore may influence SRB at those depths. More surprisingly, *Spartina* root mass in Georgia salt marshes has been found to descend to 50 cm-depths (Schubauer and Hopkinson, 1984). Hence, depth penetration of *Spartina* roots could impact SRB community stratification and spatial variability in the salt marsh.

Seasonal Variability in Process Rate Measurements

The factors that control sulfate and sulfide cycling also control sulfate reduction and sulfide oxidation. Sulfate reduction rates (SRRs) were higher in summer months during plant vegetative growth and lower in winter when plants were senescing and in spring when plants were in the reproductive stage. During the summer, SRR in vegetated sediment was higher than in the other two mesocosms, but in winter and spring these differences were less significant.

Sulfate reduction rates generally decrease with depth in salt marsh sediments (Hines *et al*., 1999, King *et al*., 1999). The same trends were observed in this study. However, sulfate reduction is heavily influenced by organic matter inputs and these inputs may result in higher sulfate reduction rates in the bottom sediments (Howarth and Teal, 1979). July 2000 profiles showed high rates of sulfate reduction in vegetated sediment as a result of high plant growth and activity. Additionally, the pronounced presence of algal mats during the summer months may have also contributed dissolved organic carbon (DOC) that may fuel these sediment processes. Contrastingly, in February 2001, sulfate reduction rates were lower at all depths and the trend was not as prominent due to plant senescence and decreased activity. In May 2001, sulfate reduction rates did not decrease significantly with depth as expected. The mild spring conditions delayed vegetative growth and activities. As a result, sulfate and sulfide concentrations and sulfate reduction rates were lower than that of July. Additionally, sulfate is not limiting to sulfate reduction in the rhizosphere of both vegetated mesocosms. If sulfate reduction rates were dependent on sulfate concentrations in the sediment, we would expect to see decreasing

sulfate reduction rates with decreasing sulfate concentrations. Therefore, organic matter inputs by *Spartina alterniflora* serve as potential energy for the sulfate-reducing microbial community.

Differences in sulfate reduction rates between vegetated and unvegetated mesocosms were significant during active plant growth. Average SRR data for the contaminated unvegetated mesocosm in July showed lower rates of sulfate reduction compared to those of the vegetated sediment. This was attributed to the decreased organic matter input from vegetation into the sediment. In February, sulfate reductions rates between unvegetated and vegetated sediment were not significantly different. Since plants were not as active during the winter, we saw lower rates in all mesocosms. In May, due to mild spring conditions, SRR in the vegetated mesocosms increased slightly but increased substantially in the unvegetated mesocosm.

During the last sampling event, *Spartina* plants were still senesced, which may explain why the increase in SRR in vegetated sediment from February to May was not significant compared to that in unvegetated sediment. Lower Spartina activity did not result in fewer SRB cells, but sulfate reduction activity was diminished. Another reason for the sudden SRR increase in the unvegetated mesocosm could be partially attributed to the abundant formation of algal mats during this time period. Although algal mats were constantly removed from the unvegetated mesocosm, they would immediately grow back within a day. The seasonal timing of algal production may not be the same as higher plants; hence, benthic algae may sustain SRBs even in cooler months and in non-Spartina populated environments.

Based on the model used to estimate Sulfide Oxidation Rates (SOR) in Sauer (2003), SORs appear to be significant in the vegetated sediment. SORs are up to 30 times greater than SRR in some cases, especially in the top few centimeters of the sediment, possibly due to increased oxygenation in surface sediment. Even at lower depths, sulfide oxidation was prevalent because sulfate did not decrease with depth. Since predicted SORs are based on SRR, the depth profile is also very similar – they both decrease with depth.

The SORs calculated from the model appear to be exaggerated in the top few centimeters in the sediment because these rates cannot be realistically sustained. This exaggeration may be explained by the following assumptions. First, SRR, SOR, and sulfate concentrations were not obtained independent of one another. Recall that porewater sulfate is an input parameter in the calculations of SRR and SOR. Also, SRR is an input parameter in the calculation of SOR. Hence, an underestimation or overestimation of sulfate concentrations would carry through to all SRR and SOR calculations. Second, any solid-phase sulfate that may go into solution is unaccounted for if it is taken up by other sequestering compounds. Porewater sulfate, not total sulfate in sediment, was measured and applied in the equations. Hence, the presence of other constituents, such as gypsum ($CaSO_4$), would underestimate sulfate concentrations.

Oxygen entering the system through *Spartina* roots could potentially be impacting mercury speciation in the sediment. Certain species of SRB are known to participate in oxidative demethylation in anoxic sediments (Pak and Bartha, 1998 and Oremland *et al*., 1991). Pak and Bartha observed that methylation and demethylation correlate positively

with organic matter and dissolved sulfate in lake sediments. The significance of demethylation will be discussed further in the following sections.

Total Mercury, Methylmercury, and Estimated MMR

Porewater concentrations of MeHg and total Hg were not considerably different between vegetated and unvegetated sediments or between contaminated and uncontaminated sediments. Additionally, no temporal trends in methylmercury and total mercury concentrations from July 2000 through May 2001 were observed. Similarly, mercury data from June 1999 through March 2000 in Sauer's study (2003) did not show significant differences between mesocosms. In general, we observed very low concentrations of porewater methyl Hg (less than 30 ng/L) in the all mesocosms and total porewater mercury levels ranging from 40 to170 ng/L. The low levels of MeHg and lack of dissimilarity between all three mesocosm systems could be attributed to (i) the enhancement of demethylation of in situ methylmercury in parallel with MeHg production (demethylation is keeping up with methylation); (ii) a low level of methylation due to the phylogenetic composition of the microbial communities; and (iii) environmental factors that limit mercuric ion [Hg(II)] bioavailability. Therefore, the similar levels of total available mercury in the sediment porewaters indicate a similar potential for methylation in the three mesocosms, independent of "contamination" conditions.

Mercury demethylation occurs either through an organomercurial lyase pathway (Robinson and Tuovinen, 1984; Nakamura *et al*. 1990) or through an oxidative process

(Oremland *et al*., 1991). The former process represents a true detoxification response by bacteria, while the latter is thought to reflect the metabolism of a small organic molecule by heterotrophic (organic utilizing) bacteria. Sulfate-reducing bacteria and methanogens have been known to demethylate mercury in anoxic environments (Pak and Bartha, 1998). Additionally, Marvin-Depasquale and Oremland (1998) reported that MeHg degradation occurs at *in situ* concentrations, suggesting that mercury methylation and demethylation are tightly coupled. Therefore, demethylation may be just as significant as methylation in the mesocosm sediments.

As described previously, the phylogenetic composition of the SRB community was similar in all three mesocosms. If SRB are in fact the primary drivers of mercury methylation and demethylation, this may explain why mercury levels did not vary between mesocosms. Moreover, the balance between methylation and demethylation may be a way for the microbes to keep mercury concentrations "in-check".

Mercury speciation is another principal driver for mercury methylation. Elemental mercury has a high vapor pressure, a low solubility, does not combine with inorganic or organic ligands, and therefore is not available for methylation. The mercurous ion (Hg[I]) combines with inorganic compounds only and cannot be methylated. The mercuric ion (Hg[II]) combines with both inorganic and organic ligands, and can be methylated.

Methylation is influenced by environmental variables that affect both the availability of mercuric ions for methylation and the growth of the methylating microbial populations. At lower pH, methylation rates increase because the increase in number of protons liberates divalent Hg from complexes, making them available for methylation

(Andersson *et al*., 1990; Miskimmin *et al*., 1992; Stein *et al*., 1996). However, the pH levels measured in mesocosm porewaters ranged from 6 to 7 (Sauer, 2003); hence, mercury methylation may have been limited by neutral pH conditions. Secondly, the presence of sulfides can also complex with mercuric ion, making it unavailable for methylation. Benoit *et al.* (1999) demonstrated that dissolved sulfide varies inversely with methylmercury production. Average sulfide concentrations in the mesocosms were comparably high compared to literature values and appear consistent with low levels of methylmercury production.

Distribution of Sulfate-Reducing Bacteria

Spartina activities presumably impact the sulfate-reducing bacteria activity and community structure in salt marsh sediments. During July and May when plants were active and growing, the SRB community was stratified and all species followed similar trends, except for the contaminated unvegetated mesocosm in July where *Desulfobacter* sp. deviated from the community trend. During February when plants were senesced, the SRB community was diversified and more variable throughout the sediment in all mesocosms.

Members of the *Desulfobacteriaceae* family dominated the SRB community. *Desulfobacter* accounted for 35% of the population, *Desulfobacterium* accounted for 26% of the population, and *Desulfococcus* accounted for 23% of the population. *Desulfovibrio* and *Desulfobulbus* together only accounted for 16 % of the population. Hines *et al*. (1999) found that members of the *Desulfobacteriaceae* family dominated

other SRB groups in marsh sediment and King *et al*. (2000, 2001) observed that these members methylated greater amounts of mercury relative to sulfate reduced compared to other SRB groups. Similarly, in our study, *Desulfobacter* dominated other SRB groups in winter and spring. During the summer, *Desulfococcus* outcompeted *Desulfobacterium* and *Desulfobacter* members due to its nutritional versatility. However, during the mild winter and spring, *Desulfobacter* and *Desulfobacterium* may possess traits that allow them to persist and survive longer than other populations under colder conditions. *Desulfobacterium* cell numbers remained consistently high throughout the year, which suggests that this group may be more adaptable to a variety of temperatures and conditions.

SRB profiles did not correlate temporally with sulfate reduction rates (SRR). SRR were higher in summer in vegetated sediment when plants were active than winter when plants were senesced. However, the number of SRB cells per gram dry weight did not vary significantly throughout the year. Similar findings were observed by Hines *et al*. (1999). They observed that SRB in bulk sediment continued to dominate the bacterial biomass throughout the year, despite the fluctuations in SRR and proposed that SRB were able to survive long periods of cold better than other bacteria in the marsh.

Implications for Mercury Methylation and Demethylation

Estimated mercury methylation rates for individual phylogenetic groups did not vary temporally or show differences between mesocosms. As observed by King et al. (2000), *Desulfobacterium*, on average, appears to methylate mercury at higher rates relative to SRR than other SRB groups. As discussed previously, the incidence of

methylmercury production normalized to SRR for all mesocosms and sampling periods was as follows:

Desulfobacterium > *Desulfococcus* > *Desulfobacter* > *Desulfovibrio* > *Desulfobulbus*

The difference in mercury methylation rates may be linked to carbon metabolism. Acetate-utilizers have the biggest advantage over non-acetate utilizers.

Although demethylating bacteria, such as nitrate- and metal-reducing species and some species of SRB, were not quantified in this study, they may be just as vigorous as the mercury methylating SRB, as indicated by the low methylmercury levels. Therefore, demethylators may be keeping up with methylators.

Relationship between Sulfate Reduction Rates and Mercury Methylation Rates

Past investigations on mercury methylation have shown that there is a positive correlation between porewater mercury levels and sulfate reduction rates. However, the relationship seems to be much more complex than previously thought. Figure 6.1 compares integrated SRR with porewater methylmercury. Integrated SRRs were determined by multiplying average SRR per lift by its representative 2-cm depth and summed together down to a depth of 10cm. The figure combines data from Sauer's study (2003) with data from this study. Sauer's study showed a correlation between MeHg and sulfate reduction and suggested that vegetation limits the availability of the contaminant. However, the data shown in Figure 6.1 does not show a strong correlation. What the figure does present is that the porewater MeHg concentrations in all mesocosms were low and were not significantly different between mesocosms. Therefore, demethylation

seems to be significant in all three mesocosms and independent of vegetation effects. As discussed previously, environmental factors and other mercury transformation processes, such as volatilization and precipitation, may also limit the availability of mercuric ions for methylation.

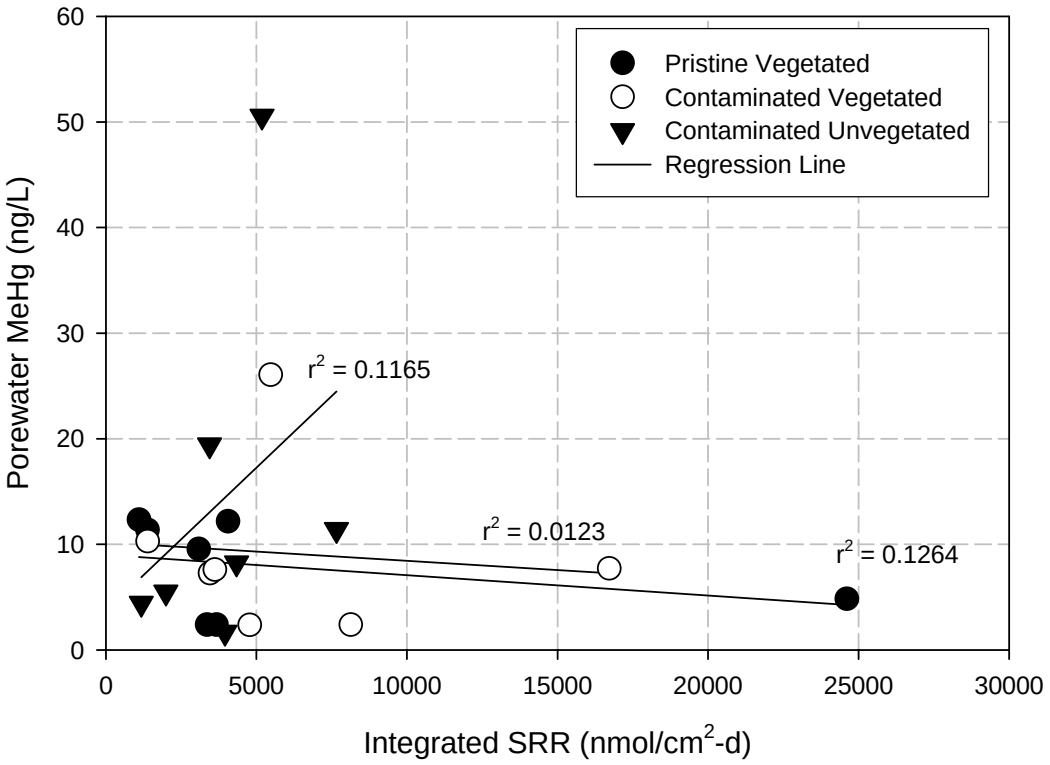

Figure 6.1 Relationship between SRR and porewater MeHg.

In summary, the following conclusions were realized from this study:

- A minimum volume of 2 mL was necessary to obtain feasible results for total mercury analysis. Pooling of samples from multiple locations, if feasible, is recommended.

- Porosities in all mesocosms have slightly decreased since 1999, while bulk densities have increased. Possible explanations for this include compaction of the soil and filling of the voids by bacterial growth. No significant trend in physical characteristics versus depth were observed.
- Salinity levels measured in the mesocosms ranged from 27 to 33 ppt. Since microbial methylation is inversely related to salinity in salt marsh sediments, methylation may have been limited by high salinity levels.
- *Spartina* height differences between pristine and contaminated mesocosms were not significant. Therefore, mercury contamination did not appear to stunt vegetative growth.
- Sulfate concentrations were not correlated with depth in the vegetated sediment, but decreased with depth in the unvegetated sediment.
- Sulfide oxidation appeared to be significant in the upper 2-cm of the sediment as evidenced by higher sulfate concentrations.
- Sulfate reduction rates (SRRs) generally decreased with depth and showed positive correlation with plant growth and temperature.
- Porewater concentrations of MeHg and total Hg were not considerably different between vegetated and unvegetated sediments or between contaminated and uncontaminated sediments.
- Vertical stratification of the SRB community was not apparent in the marsh sediment. SRB abundances were within the same order of magnitude throughout

the 10-cm column of sediment and did not correlate temporally with sulfate reduction rates.

- Demethylation may be keeping up with methylation since methylmercury levels remained low in all mesocosms.

Environmental Engineering Applications and Recommendations

This thesis has presented data that shows that mercury methylation is controlled by plant and microbial activities. A simulated marsh system was used to analyze the relationships between mercury bioavailability, sulfate reductions rates, and SRB speciation *in situ*. It was apparent that demethylation might be significant in this marsh system and suggests that for contaminated sites with low-level mercury levels and a natural population of demethylating bacteria, natural attenuation may be a viable remediation technology. On other sites where more aggressive remediation is desired, the preventative alternative would be to decrease bacterial synthesis of methylmercury by the addition of sulfide complexing agents or metal chelators, which bind to soluble mercury and render them unavailable for mercury methylation. An alternative remediation strategy would be to limit the growth of SRB phylogenetic groups that have a higher potential to methylate mercury relative to SRR. Phytoremediation is a relatively new technology that has been implemented to sequester metals and decrease the mobility of the contaminants in the subsurface. However, caution must be taken when plants are used as a remedial alternative because plants may simply volatilize the pollutants into the

atmosphere or transform pollutants into a more toxic form. In this study, plants stimulated SRB activity, which resulted in increased mercury methylation.

A growing amount of evidence has indicated that some SRB phylogenetic groups have higher rates of mercury methylation relative to SRR. Members of the acetate utilizing family *Desulfobactericeae* were observed to produce methylmercury at more rapid rates than members of the non-acetate utilizing family *Desulfovibrionaceae*. However, the biochemical mechanisms by which these groups methylate mercury are unclear. Therefore, additional studies are needed concerning the cellular processes that control mercury methylation.

The importance of plant-microbial interactions and the impact of these interactions on mercury methylation has been demonstrated. Some studies suggest that certain plants are capable of accumulating mercury in its aboveground shoots (Lasat, 2002; Meagher *et al*., 2002). The bioavailability of mercury to plants is influenced by microbial activities. Microbes are known to alter chemical properties of the rhizospheric soil with subsequent effects on the mobility of metal contaminants. For example, SRB alter mercury bioavailability by producing sulfide chelating agents which bind to mercury, reducing mercury's bioavailability in the sediment. SRB are also responsible for the catalytic transformation of ionic mercury (Hg^{2+}) to highly toxic methylmercury. On the other hand, plants also impact metal bioavailability. For example, *Spartina alterniflora* plants exude organic compounds that stimulate SRB activity and subsequently increase mercury methylation. This thesis has provided data showing *Spartina* growth corresponded to an

increase in sulfate-reduction activity and mercury methylation activity. Therefore, understanding the complex relationship between plants and microbes could lead to potentially viable solutions to clean up soil contaminated with metal contaminants, but only if future research in remediation technologies is developed with this multidisciplinary approach.

APPENDIX A

Map of Skidaway Island and the location of the Skidaway Institute of Oceanography

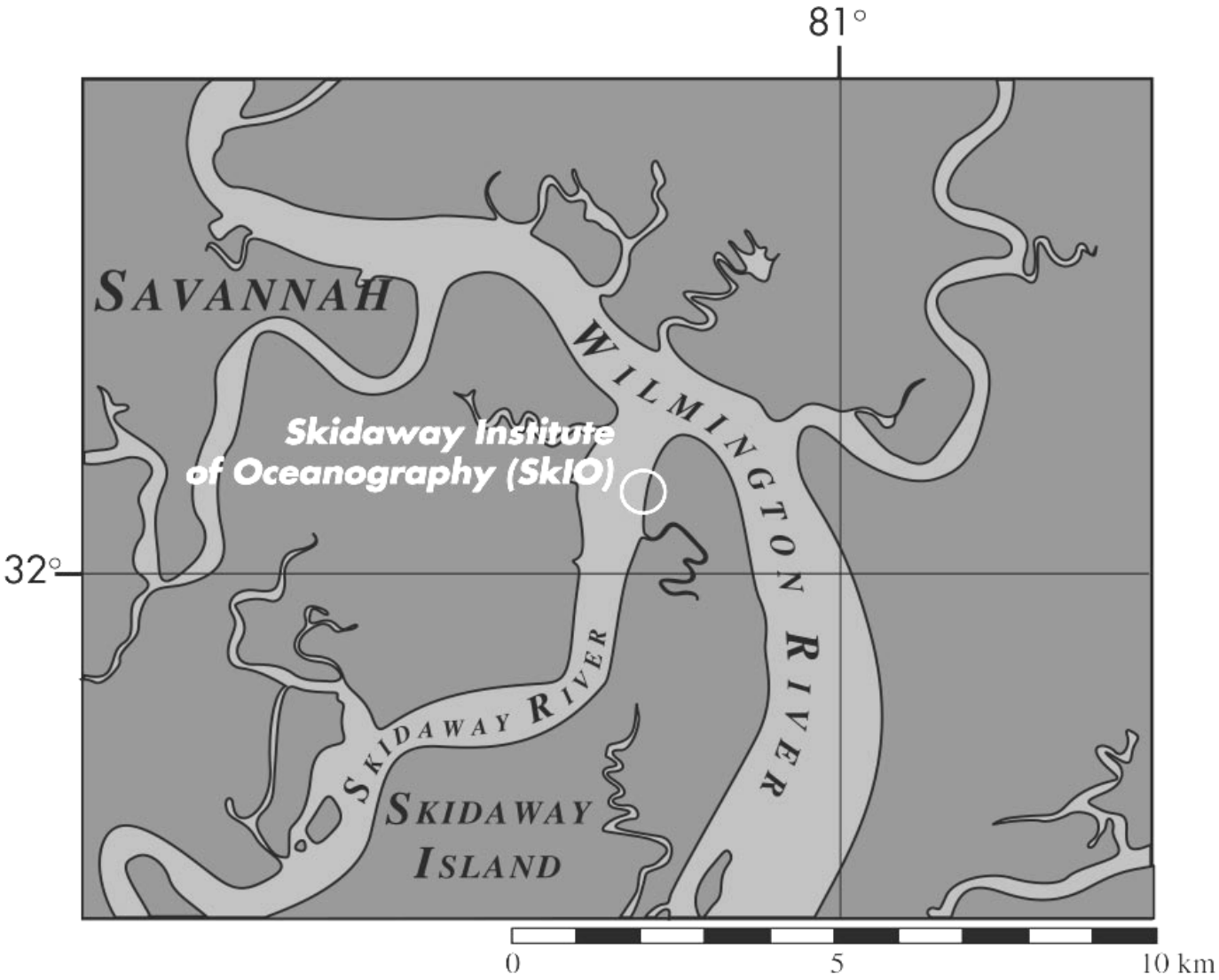

APPENDIX B

Growth Media for Sulfate-Reducing Bacteria Cultures

Component 1

NaCl	1.0 g
$CaCl_2$	0.1g
$NaSO_4$	4.0 g
dH_2O	550 mL

Component 2

$MgCl_2$	0.4 g
dH_2O	50 mL

Component 3

NH_4Cl	0.25 g
dH_2O	50 mL

Component 4

Sodium Lactate	1.5 mL of 6.8 M solution
Yeast Extract	0.1 g
dH_2O	200 mL

Component 5

Na Acetate	5.0 mL of 2.0 M solution
dH_2O	50 mL

Component 6

NaHCO3	2.5 g
dH_2O	50 mL

Component 7

Na Citrate	1.5 g
dH_2O	50 mL

Individual Additions added to 1 L of pure culture media:

Extract these solutions and then add a filter and new needle before dispensing.

Reazurin	100 µL of 0.3 % w/v
Trace Element Solution	1.0 mL
Selenite/Tungstate Solution	1.0 mL
Vitamin Solution	1.0 mL
Na_2S	7.5 mL of 0.20 M
Thiosulfate Solution	3.0 mL of 1.0 M
Reductant Solution	1 mL

APPENDIX C

Artificial Sea Water (ASW)

Component 1	NaCl	22.2 g
	MgSO4	9.8 g
	dH_2O	900 mL
Component 2	KCl	5.5 g
	$NaHCO_3$	1.6 g
	dH_2O	100 mL
Component 3	KBr	0.8 g
	$SrCl_2$	0.34 g
	dH_2O	100 mL
Component 4	Na Silicate	0.4 g
	dH_2O	100 mL
Component 5	NaF	0.24 g
	dH_2O	100 mL
Component 6	NH_4NO_3	0.16 g
	dH_2O	100 mL
Component 7	Na_2HPO_4	0.8 g
	dH_2O	100 mL
Component 8	$CaCl_2 \cdot 2H_2O$	23.8 g
	dH_2O	100 mL
Component 9	EDTA	300 mg
	$FeCl_2 \cdot 6H_2O$	38.4 mg
	$MnCl_2 \cdot 7H_2O$	43.2 mg
	$CoCl_2 \cdot 6H_2O$	0.2 mg
	ZnCl	3.15 mg
	$CuCl_2$	0.025 mg
	H_3BO_3	24.2 mg
	dH_2O	100 mL

APPENDIX D

Components Needed for the Identification of 16S rRNA

Monobasic NaH_2PO_4
137.99 g/l

Dibasic Na_2HPO_4
268.07 g/l
Heat to dissolve

For 0.5M $NaPO_4$ pH 6.8
Dibasic 231.5 mL Na_2HPO_4
Monobasic 268.5 mL NaH_2PO_4
Combine in 1 L bottle, bring up to 900 mL with dH2O. pH if necessary to 6.8 with either NaOH or HCl.

20X SSPE (1 liter)
Dissolve in 800 mL dH_2O
175.3 g NaCl
27.6 g $NaH_2PO{\cdot}H_2O$
7.4 g EDTA
Adjust pH to 7.4 with NaOH
Adjust volume to 1 liter and autoclave

Wash Buffer (1 liter)
300 mL 20X SSPE
5 mL 20 % SDS (add last or else it clumps)
695 mL H_2O

REFERENCES

Aller, R. C., and P. D. Rude. 1988. Complete oxidation of solid phase sulfide by manganese and bacteria in anoxic marine sediments. Geochim. Cosmochim. Acta. **52:**751-765.

Amann, R. I., W. Ludwig, and K.-H. Schleifer. 1995. Phylogenetic identification and *in situ* detection of individual microbial cells without cultivation. Microb. Rev. **59:**143-169.

Amyot, M., J. Lalonde, L. Poissant, and D. Lean. 1999. Mercury in Lake Ontario and the St. Lawrence River. Great Lakes Research Review: Lake Ontario and St. Lawrence River Ecosystem. **4:**1-4.

Andersson, I., H. Parkman, and A. Jernelov. 1990. The role of sediments as sink or source for environmental contaminants: a case study of mercury and chlorinated organic compounds. Limnologica. **20:**347-359.

Bak, F., and N. Pfennig. 1991. Chemolithotrophic growth of *Desulfovibrio sulfodimutans* sp. nov. by disproportionation of inorganic sulfur compounds. Arch. Microbiol. **147:**184-189.

Barkay, T., R. R. Turner, A. Vanderbrook, and C. Liebert. 1991. The relationships of Hg (II) volatilization from a freshwater pond to the abundance of mer genes in the gene pool of the indigenous microbial community. Microb. Ecol. **21:**151-161.

Barrow, N. J., and V. C. Cox. 1992. The effects of pH and chloride concentration on mercury sorption. I. By geothite. J. Soil. Sci. **43:**295-304.

Bartlett, K. B., D. S. Bartlett, R. C. Harris, and D. I. Sebacher. 1987. Methane emissions along a salt marsh salinity gradient. Biogeochemistry. **4:**183-202.

Barton, L. L. (ed.). 1995. Sulfate-Reducing Bacteria, vol. 8. Plenum Press, New York.

Benoit, J. M., C. C. Gilmour, R. P. Mason, and A. Heyes. 1999. Sulfide controls and bioavailibility to methylating bacteria in sediment pore waters. Environ. Sci. Technol. **33:**951-957.

Benoit, J. M., C. C. Gilmour, and R. P. Mason. 2001. Aspects of Bioavailibility of Mercury for Methylation in Pure Cultures of *Desulfobulbus propionicus*. Appl. Environ. Microbiol. **67:**51-58.

Berman, M., T. Chase, and R. Bartha. 1990. Carbon flow in mercury biomethylation by *Desulfovibrio desulfuricans*. Appl. Environ. Microbiol. **56:**298-300.

Berner, R. A. 1982. Early Diagenesis. Princeton University Press, Princeton.

Berner, R. A., and J. T. Westrich. 1985. Bioturbation and the early diagenesis of carbon and sulfur. Am. J. Sci. **285:**193-206.

Bizily, S. P., C. L. Rugh, A. O. Summers, and R. B. Meagher. 1999. Phytoremediation of methylmercury pollution: *mer*B expression in *Arabidopsis thaliana* confers resistance to organomercurials. Proc. Natl. Acad. Sci. USA. **96:**6808-6813.

Bloom, N. S. 1992. On the chemical form of mercury in edible fish and marine invertebrate tissue. Can. J. Fish. Aquat. Sci. **49:**1010-1017.

Bloom, N. S., G. Gill, S. Cappellino, C. Dobbs, L. McShea, C. Driscoll, R. Mason, and J. Rudd. 1999. Speciation and cycling of mercury in Lavaca, Bay, Texas, sediments. Environ. Sci. Technol. **33:**7-13.

Blum, J. E., and R. Bartha. 1980. Effects of salinity on methylation of mercury. Bull. Environ. Contam. Toxicol. **25:**404-408.

Bodek, I., W. J. Lyman, Z. F. Reehel, D. H. Rosenblatt, B. I. Walton, and R. A. Conway. 1988. Environmental Inorganic Chemistry: Properties, Processes, and Estimation Methods. Pergamon Press, New York.

Boulegue, J., C. J. Lord, and T. M. Church. 1982. Sulfur speciation and associated trace metals (Fe, Cu) in the pore waters of Great Marsh, Delaware. Geochim. Cosmochim. Acta. **46:**453-464.

Braun-Howland, E. B., P. A. Vescio, and S. A. Nierzwicki-Bauer. 1993. Use of a simplified cell blot technique and 16S rRNA-directed probes for identification of common environmental isolates. Applied. Environ. Microbiol. **59:**3219-3224.

Capone, D. G., D. D. Reese, and R. P. Kiene. 1983. Effects of metals on methanogenesis, sulfate reduction, carbon dioxide evolution, and microbial biomass in anoxic salt marsh sediments. Appl. Environ. Microbiol. **45:**1586-1591.

Carlson, P. R., Jr., and J. Forrest. 1982. Uptake of dissolved sulfide by *Spartina alterniflora*: Evidence from natural sulfur isotope abundance ratios. Science. **216:**633-635.

Chanton, J. P., C. S. Martens, and M. B. Goldhaber. 1987. Biogeochemical cycling in an organic-rich coastal marine basin. 7. Sulfur mass balance, oxygen uptake and sulfide retention. Geochim. Cosmochim. Acta. **51:**1187-1199.

Choi, S., and R. Bartha. 1994. Environmental factors affecting mercury Methylation in estuarine sediments. Bull. Environ. Contam. Toxicol. **53:**805-812.

Choi, S., T. Chase, and R. Bartha. 1994. Metabolic pathways leading to mercury methylation in *Desulfovibrio desulfuricans* LS. Appl. Environ. Microbiol. **60:**4072-4077.

Choi, S., T. Chase, and R. Bartha. 1994. Enzymatic catalysis of mercury methylation by *Desulfovibrio desulfuricans* LS. Appl. Environ. Microbiol. **60:**1342-1346.

Cline, J. D. 1969. Spectrophotometric determination of hydrogen sulfide in natural waters. Limnol. Oceanogr. **14:**454-458.

Compeau, G., and R. Bartha. 1984. Methylation and demethylation of mercury under controlled redox, pH, and salinity conditions. Appl. Environ. Microbiol. **48:**1203-1207.

Compeau, G., and R. Bartha. 1985. Sulfate reducing bacteria: principal methylators of mercury in anoxic estuarine sediments. Appl. Environ. Microbiol. **50:**498-502.

Craig, P. J., and P. A. Moreton. 1984. The role of sulphide in the formation of dimethyl mercury in river and estuary sediments. Mar. Poll. Bull. **15:**406-408.

Dacey, J. W., and B. L. Howes. 1984. Water uptake by roots controls water table movement and sediment oxidation in short *Spartina* marsh. Science. **224:**487-489.

DeLaune, R. D., and W. H. Patrick. 1980. Nitrogen and phosphorus cycling in a Gulf Coast salt marsh. *In* V. S. Kennedy (ed.), Estuarine Perspectives. Academic Press, New York.

DeLong, E. F., G. S. Wickman, and N. R. Pace. 1989. Phylogenetic strains: ribosomal RNA-based probes for identification of single cells. Science. **243:**1360-1363.

Devereux, R., M. Delaney, F. Widdel, and D. A. Stahl. 1989. Natural relationships among the sulfate-reducing bacteria. J. Bacteriol. **171:**6689-6695.

Devereux, R., S. H. He, C. Doyle, S. Orkland, D. A. Stahl, J. LeGall, and W. B. Whitman. 1990. Diversity and origin of *Desulfovibrio* species: phylogenetic definition of a family. J. Bacteriol. **172:**3609-3619.

Devereux, R., M. D. Kane, J. Winfrey, and D. A. Stahl. 1992. Genus- and group-specific hybridization probes for determinative and environmental studies of sulfate-reducing bacteria. Syst. Appl. Microbiol. **15:**601-609.

Devereux, R., and D. A. Stahl. 1993. Phylogeny of sulfate-reducing bacteria and a perspective for analyzing their natural communities, p. 131-160. *In* J. M. Odom and R. Singleton (ed.), The Sulfate-Reducing Bacteria: contemporary perspectives. Springer-Verlag, New York.

Devereux, R., M. E. Hines, and D. A. Stahl. 1995. S cycling: characterization of natural communities of sulfate-reducing bacteria by 16S rRNA sequence comparisons. Microb. Ecol. **32:**283-293.

Devereux, R., M. Winfrey, J. Winfrey, and D. A. Stahl. 1996. Depth profile of sulfate-reducing bacterial ribosomal RNA and mercury methylation in an estuarine sediment. Microbiol. Ecol. **20:**23-31.

Embley, T. M., and Stackerbrandt, E. 1996. The use of 16S ribosomal RNA sequences in microbial ecology, p. 39-62. *In* R. W. Pickup and J. R. Saunders (ed.), Molecular approaches to environmental microbiology. Ellis Horwood Ltd., New York.

Faust, S. D., and M. A. Osman. 1981. Mercury, arsenic, lead, cadmium, selenium, and chromium in aquatic environments, p. 200-225, Chemistry of natural waters. Ann Arbor Science Publishers, Inc., Ann Arbor, Mich.

Fossing, H., and B. B. Jorgensen. 1989. Measurement of bacterial sulfate reduction in sediments: Evaluation of a single-step chromium reduction method. Biogeochemistry. **8:**205-221.

Fossing, H., and B. B. Jorgensen. 1990. Isotope exchange reactions with radiolabeled sulfur compounds. Biogeochemistry. **9:**223-245.

Frischer, M. E., P. J. Floriani, and S. A. Nierzwicki-Bauer. 1996. Differential sensitivity of 16S rRNA targeted oligonucleotide probes used for fluorescence *in situ* hybridization is a result of ribosomal higher order structure. Can. J. Microbiol. **42:**1061-1071.

Frischer, M. E., J. D. Danforth, M. A. N. Healy, and F. M. Saunders. 2000. Whole-cell versus total RNA extraction for analysis of microbial community structure with 16S rRNA-targeted oligonucleotide probes in salt marsh sediments. Appl. Environ. Microbiol. **66:**3037-3043.

Giblin, A. E., and R. K. Wieder. 1992. Sulphur cycling in marine and freshwater wetlands, p. 85-117. *In* R. W. Howarth, J. W. B. Stewart, and M. V. Ivanov (ed.), Sulphur Cycling on the Continents: Wetlands, Terrestrial Ecosystems, and Associated Water Bodies. John Wiley and Sons, Chichester.

Gibson, G. R. 1990. A review: physiology and ecology of sulfate-reducing bacteria. J. Appl. Bacteriol. **69:**769-797.

Gilmour, C. G., and D. G. Capone. 1987. Relationship between Hg methylation and the sulfur cycle in estuarine sediments. EOS Trans. Amer. Geo. Union. **68:**1718-1725.

Gilmour, C. G., and E. A. Henry. 1991. Mercury methylation in aquatic systems affected by acid deposition. Environ. Pollut. **71:**131-169.

Gilmour, C. C., E. A. Henry, and R. Mitchell. 1992. Sulfate stimulation of mercury methylation in freshwater sediments. Environ. Sci. Technol. **26:**2281-2287.

Gilmour, C. C., and G. S. Riedel. 1995. Measurement of mercury methylation in sediments using high specific-activity ^{203}Hg and ambient incubation. Water Air Soil Pollut. **80:**747-756.

Gilmour, C. C., G. S. Riedel, M. C. Ederington, J. T. Bell, J. M. Benoit, G. A. Gill, and M. C. Stordal. 1998. Methylmercury concentrations and production rates across a trophic gradient in the northern Everglades. Biogeochemistry. **40:**327-345.

Giovannoni, S. J., E. F. DeLong, G. J. Olsen, and N. R. Pace. 1988. Phylogenetic group-specific oligonucleotide probes for identification of single microbial cells. J. Bacteriol. **170:**720-726.

Good, R. E., N. F. Good, and B. R. Frasco. 1982. A review of primary production and decomposition dynamics of the belowground marsh component. *In* V. S. Kennedy (ed.), Estuarine Comparisons. Academic Press, New York.

Haines, E., A. Chalmers, B. Hanson, and B. Sherr. 1977. Nitrogen pools and fluxes in a Georgia salt marsh. *In* M. L. Wiley (ed.), Estuarine Processes. Academic Press, New York.

Hansen, T. A. 1993. Carbon metabolism of sulfate-reducing bacteria perspectives, p. 21-40. *In* J. M. Odom and R. Singleton (ed.), The sulfate-reducing bacteria: contemporary perspectives. Springer-Verlag, New York.

Heller, A. A., and J. H. Weber. 1998. Seasonal study of speciation of mercury (II) and monomethylmercury in *Spartina alterniflora* from the Great Bay Estuary, NH. Sci. Tot. Environ. **221:**181-188.

Hines, M. E., R. S. Evans, B. R. S. Genthner, S. G. Willis, S. Friedman, J. N. Rooney-Varga, and R. Devereux. 1999. Molecular phylogenetic and biogeochemical studies of sulfate-reducing bacteria in the rhizosphere of *Spartina alterniflora*. Appl. Environ. Microbiol. **65**(5)**:**2209-2216.

Holland, H. D. 1978. The Chemistry of the Atmosphere and Oceans. John Wiley and Sons, New York.

Hosokawa, J. 1995. Remediation work for mercury contaminated bay experiences of Minamata Bay Project, Japan. Wat. Sci. Tech. **28:**338-348.

Howarth, R. W., and J. M. Teal. 1979. Sulfate Reduction in a New England salt marsh. Limnol. Oceanogr. **24:**999-1013.

Howarth, R. W., and J. E. Hobbie. 1982. The regulation of decomposition and heterotrophic microbial activity in salt marsh soils, p. 187-207. *In* V. S. Kennedy (ed.), Estuarine Comparisons. Academic Press, New York.

Howarth, R. W., and A. Giblin. 1983. Sulfate reduction in the salt marshes at Sapelo Island, Georgia. Limnol. Oceanogr. **28:**70-82.

Howarth, R. W., and S. Merkel. 1984. Pyrite formation and the measurement of sulfate reduction in salt marsh sediments. Limnol. Oceanogr. **29:**598-608.

Howarth, R. W. 1993. Chapter 10: Microbial processes in salt-marsh sediments, p. 239-259. *In* T. E. Ford (ed.), Aquatic Microbiology: an ecological approach. Blackwell Scientific Publications, Inc., Massachusetts.

Howes, B. L., R. W. Howarth, and J. M. Teal. 1981. Oxidation-reduction potential in a saltmarsh:spatial patterns and interactions with primary production. Limnol. Oceanogr. **34:**578-590.

Howes, B. L., J. W. H. Dacey, and G. M. King. 1984. Carbon flow through oxygen and sulfate reduction pathways in salt marsh sediments. Limnol. Oceanogr. **29:**1037-1051.

Howes, B. L., J. W. H. Dacey, and J. M. Teal. 1985. Annual carbon mineralization and belowground production of *Spartina alterniflora* in a New England salt marsh. Ecology. **66:**595-605.

Ivanov, M. V., A. Y. Lien, M. S. Reeburgh, and G. W. Skyring. 1989. Interaction of sulphur and carbon cycles in marine sediments, p. 125-179. *In* P. Brimblecombe and A. Y. Lien (ed.), Evolution of the Global Biogeochemical Sulphur Cycle. John Wiley and Sons, Chichester.

Jacobson, M. E. 1990. PhD. State University of New York, New York.

Jensen, S., and A. Jernelov. 1969. Biological methylation of mercury in aquatic organisms. Nature (London). **223:**753-755.

Jorgensen, B. B. 1977. The sulfur cycle of a coastal marine sediment. Limnol. Oceanogr. **22:**814-831.

Jorgensen, B. B. 1982. Mineralization of organic matter in the sea bed - the role of sulphate reduction. Nature. **296:**643-645.

Jorgensen, B. B., and F. Bak. 1991. Pathways and microbiology of thiosulfate transformations and sulfate reductions in marine sediments. Appl. Environ. Microbiol. **39:**847-856.

Kaplan, W., I. Valiela, and J. M. Teal. 1979. Denitrification in a salt marsh system. Limnol. Oceanogr. **24:**726-734.

King, G. M., and W. J. Wiebe. 1980. Regulation of sulfate concentrations and methanogenesis in salt marsh soils. Est. Coast. Mar. Sci. **10:**215-223.

King, G. M., M. J. Klug, R. G. Wiegert, and A. G. Chalmers. 1982. Relation of soil water movement and sulfide concentration to *Spartina alterniflora* production in a Georgia salt marsh. Science. **218:**61-63.

King, G. M. 1988. Patterns of sulfate reduction and sulfur cycle in a South Carolina salt marsh. Limnol. Oceanogr. **33:**376-390.

King, J. K., F. M. Saunders, R. M. Lee, and R. A. Jahnke. 1999. Coupling mercury methylation rates to sulfate reduction rates in marine sediments. Environ. Toxicol. Chem. **18:**1362-1369.

King, J. K. 1999. Dissertation. Georgia Institute of Technology, Atlanta.

King, J. K., J. E. Kostka, F. M.E., and F. M. Saunders. 2000. Sulfate-reducing bacteria methylate mercury at variable rates in pure culture and in marine sediments. Appl. Environ. Microbiol. **66**(6)**:**2430-2437.

King, J. K., J. E. Kostka, M. E. Frischer, M. S. Saunders, and R. A. Jahnke. 2001. A quantitative relationship that demonstrates mercury methylation rates in marine sediments are based on the community composition and activity of sulfate-reducing bacteria. Environ. Sci. Technol. **35:**2491-2496.

Kostka, J. E. and G. W. Luther. 1995. Seasonal cycling of Fe in saltmarsh sediments. Biogeochemistry. 29: 159-181.

Krabbenhoft, D. P. 1996. Mercury Studies in the Florida Everglades P5-166-96. U.S. Geological Survey Fact Sheet.

Kraus, D. W., and J. E. Doeller. 1999. Oxidation of sulfide by *Spartina alterniflora* roots. Limnol. Oceanogr. **44:**1155-1159.

Laanbroek, H. J. 1990. Bacterial cycling of minerals that affect plant growth in waterlogged soils: a review. Aquatic Botany. **38:**109-125.

Lasat, M. 2002. Phytoextraction of toxic metals: A review of biological mechanisms. J. Environ. Qual. **31:**109-120.

Lee, R. W., D. W. Kraus, and J. E. Doeller. 1999. Oxidation of sulfide by *Spartina alterniflora* roots. Limnol. Oceanogr. **44:**1155-1159.

Leonard, T. L., G. E. Taylor, Jr., M. S. Gustin, and G. C. J. Fernandez. 1998. Mercury and plants in contaminated soils: 1. Uptake, partitioning, and emission to the atmosphere. Environ. Toxicol. Chem. **17:**2063-2071.

Leonard, T. L., G. E. Taylor, Jr., M. S. Gustin, and G. C. J. Fernandez. 1998. Mercury and plants in contaminated soils. 2. Environmental and physiological factors governing flux to the atmosphere. Environ. Toxicol. Chem. **17:**2072-2079.

Liang, L., M. Horvat, and N. S. Bloom. 1994. An improved speciation method for mercury by GC/CVAFS after aqueous phase ethylation and room temperature precollection. Talanta. **41:**371-379.

Lindberg, S. E., and R. C. Harriss. 1974. Mercury-organic matter associations in estuarine sediments and interstitial water. Environ. Sci. Technol. **8:**459-462.

Lovely, D. L. 1987. Organic mineralization with reduction of ferric iron: a review. Geomicrob. J. **5:**375-399.

Lovely, D. L. and E.J.P. Phillips. 1994. Novel processes for anaerobic sulfate production from elemental sulfur by sulfate-reducing bacteria. Appl. Environ. Microbiol. **60:**2394-2399.

Madigan, M. T., A. M. Martinko, and J. Parker. 2000. Brock's Biology of Microorganisms, 9th ed. Prentice-Hall, Inc., Englewood Cliffs, New Jersey.

Marvin-Dipasquale, M. C., and R. S. Oremland. 1998. Bacterial methylmercury degradation in Florida Everglades peat sediment. Environ. Sci. Technol. **32:**2556-2563.

Matida, Y., H. Kumada, S. Kimura, Y. Saiga, T. Nose, M. Yokote, and H. Kawatsu. 1971. Toxicity of mercury compounds to aquatic organisms and accumulation of the compounds by the organisms. Bull. Freshwater Fish Res. Lab. Jpn. **21:**197-227.

Meagher, R. B., C. L. Rugh, M. K. Kandasamy, G. Gragson, and N. J. Wang. 2000. Engineered phytoremediation of mercury pollution in soils and water using bacterial genes, p. 201-219. *In* N. Terry and G. Banuelos (ed.), Phytoremediation of Contaminated Soil and Water. Lewis Publishers, Boca Raton.

Miskimmin, B. M., J. W. Rudd, and C. A. Kelly. 1992. Influence of dissolved organic carbon, pH, and microbial respiration rates on mercury methylation and demethylation in lake water. Can. J. Fish. Aquatic. Sci. **49:**17-22.

Moore, J. W., and S. Ramamoorthy. 1984. Mercury, p. 125-159, Heavy Metals in Natural Waters: Applied Monitoring and Impact Assessment. Springer-Verlag, New York.

Morris, J. T., and G. J. Whiting. 1985. Gas advection in sediments of a South Carolina salt marsh. Mar. Ecol. Prog. Ser. **27:**187-194.

Munthe, J., and W. J. McElroy. 1992. Some aqueous reactions of potential importance in the atmospheric chemistry of mercury. Atmos. Environ. **26A:**553-557.

Nakamura, S., T. Fujisaki, and H. Tamashiro. 1986. Characteristics of Hg-resistant bacteria isolated from Minamata Bay sediment. Environ. Res. **40:**58-67.

Newell, S. Y. 1982. Content of mercury in leaves of *Spartina alterniflora* Loisel. In Georgia, U.S.A: an update. Estuarine, Coastal, and Shelf Science. **14:**465-469.

Nriagu, J. O. 1979. The Biogeochemistry of Mercury in the Environment. Elsevier, North Holland, Amsterdam.

Ogram, A., W. Sun, F. J. Brockman, and J. K. Fredrickson. 1995. Isolation and characterization of RNA from low-biomass deep-surface sediments. Appl. Environ. Microbiol. **61:**763-768.

Olsen, G. J., D. J. Lane, S. J. Giovannonni, N. R. Pace, and D. A. Stahl. 1986. Microbial ecology and evolution: a ribosomal RNA approach. Annu. Rev. Microbiol. **40:**337-365.

Oremland, R. S., C. W. Culbertson, and M. R. Winfrey. 1991. Methylmercury decomposition in sediments and bacterial cultures: involvement of methanogens and sulfate reducers in oxidative demethylation. Appl. Environ. Microbiol. **57:**130-137.

Oremland, R. S., L. G. Miller, P. Dowdle, T. Connell, and B. T. 1995. Methylmercury oxidative degradation potentials in contaminated and pristine sediments of the Carson River, Nevada. Appl. Environ. Microbiol. **61:**2745 - 2753.

Pace, N. R., D. A. Stahl, D. J. Lane, and G. J. Olsen. 1986. The use of rRNA sequences to characterize natural microbial populations. Adv. Microbial. Ecol. **9:**1-55.

Pak, K.-R., and R. Bartha. 1998. Mercury methylation and demethylation in anoxic lake sediments and by strictly anaerobic bacteria. Appl. Environ. Microbiol. **64**(3)**:**1013-1017.

Pak, K.-R., and R. Bartha. 1998. Mercury methylation by interspecies hydrogen and acetate transfer between sulfidogens and methanogens. Appl. Environ. Microbiol. **64**(6)**:**1987-1990.

Perry, S. J. 2001. Mercury minimization. Wat. Environ. Technol. **13**(92-97).

Pomeroy, L. R., W. M. Darley, E. L. Dunn, J. L. Gallagher, E. B. Haines, and D. M. Whitney. 1981. Primary Production. *In* L. R. Pomeroy and R. G. Wiegert (ed.), Ecology of a Saltmarsh. Springer-Verlag, New York.

Ponnamperuma, F. N. 1972. The chemistry of submerged soils. Advances in Agronomy. **24:**29-96.

Reyes, N. S., M. E. Frischer, and P. A. Sobecky. 1999. Characterization of mercury resistance mechanisms in marine sediment microbial communities. FEMS Microbiol. Ecol. **30**(273-284).

Robinson, J. B., and O. H. Tuovinen. 1984. Mechanisms of microbial resistance and detoxification of mercury and organomercury compounds: physiological, biochemical, and genetic analyses. Microbiological Reviews. **48:**95-124.

Rood, B. E. 1996. Wetland mercury research: A review with case studies. Current Topics in Wetland Biogeochemistry. **2:**73-108.

Rooney-Varga, J. N., R. Devereux, R. S. Evans, and M. E. Hines. 1997. Seasonal changes in the relative abundance of uncultivated sulfate-reducing bacteria in a salt marsh sediment and in the rhizosphere of *Spartina alterniflora*. Appl. Environ. Microbiol. **63:**3895-3901.

Rugh, C. L., H. D. Wilde, N. M. Stack, D. Marin-Thompson, A. O. Summers, and R. B. Meagher. 1996. Mercuric ion reduction and resistance in transgenic *Arabidopsis thaliana* plants expressing a modified bacterial *merA* gene. Proceedings of the National Academy of Sciences USA. **93:**3182-3187.

Sauer, R. 2003. Thesis. Georgia Institute of Technology, Atlanta.

Schroeder, W. H., G. Yarwok, and H. Niki. 1991. Transformation processes involving mercury species in the atmosphere: results from a literature survey. Water, Air, Soil Pollut. **56:**653-661.

Schubauer, J. P., and C. S. Hopkinson. 1984. Above- and belowground emergent macrophyte production and turnover in a coastal marsh ecosystem, Georgia. Limnol. Oceanogr. **29:**1052-1065.

Shariat, M., A. C. Anderson, and J. W. Mason. 1979. Screening of common bacteria capable of demethylation of mercuric chloride. Bull. Environ. Contam. Toxic. **21:**255-261.

Short, F. T., M. W. Davis, R. A. Gibson, and C. F. Zimmermann. 1985. Evidence for phosphorus limitation in carbonate sediments of the seagrass *Syringodium filiforme*. Est. Coast. Shelf Sci. **20:**419-430.

Smith, R. S. 1993. Determination of mercury in environmental samples by isotope dilution/ICP/MS. Anal. Chem. **65:**2485-2488.

Stahl, D. A., B. Flesher, H. R. Mansfield, and L. Montgomery. 1988. Use of phylogenetically based hybridization probes for studies of ruminal microbial ecology. Appl. Environ. Microbiol. **54:**1079-1084.

Stahl, D. A., and R. Amann. 1991. Development and application of nucleic acid probes. *In* E. Staebrandt and M. Goodfellow (ed.), Nucleic acid techniques in bacterial systematics. Wiley and Sons, Ltd., Chichester.

Stein, E. D., Y. Cohen, and A. M. Winer. 1996. Environmental distribution and transformation of mercury compounds. Crit. Rev. Environ. Sci. Technol. **26:**1-43.

Tabatabai, M. A. 1974. A rapid method for determination of sulfate in samples. Environ. Lett. **7:**237-243.

Teal, J. M., and J. Kanwisher. 1961. Gas exchange in Georgia salt marsh. Limnol. Oceanogr. **6:**388-399.

Ting, D., and R. G. Wiegert. 1996. Estimation of the primary productivity of *Spartina alterniflora* using a canopy model. Ecography. **19:**410-423.

USDHHS. 1992. Toxicological Profile for Mercury: Update. United States Department of Health and Human Services.

USEPA. 1997. Mercury Study Report to Congress. EPA-452/R-97-009, Office of Air Quality and Standards and Office of Research and Development. United States Environmental Protection Agency.

Velji, M. I., and L. J. Albright. 1985. Microscopic enumeration of attached marine bacteria of seawater, marine sediments, fecal matter, and kelp blade samples following pyrophosphate and ultrasound treatments. Can. J. Microbiol. **32:**121-126.

Vescio, P. A., and S. A. Nierzwicki-Bauer. 1995. Extraction and purification of CR amplifiable DNA from lacustrine subsurface sediments. J. Microbiol. Methods. **21:**225-233.

Wagner, R. 1994. The regulation of ribosomal RNA synthesis and bacterial cell growth. Appl. Environ. Microbiol. **161:**100-106.

Wakao, N., and C. Furusaka. 1976. Presence of microaggregates containing sulfate-reducing bacteria in a paddy field soil. Soil. Biol. Biochem. **8:**157-159.

Watanabe, I., and C. Furuska. 1980. Microbial ecology of flooded rice soils. Adv. Microbiol. Ecol. **4:**125-168.

Weber, J. H., R. Evans, S. H. Jones, and M. E. Hines. 1998. Conversion of mercury (II) into mercury (0), monomethylmercury cation, and dimethylmercury in saltmarsh sediment slurries. Chemosphere. **36:**1669-1687.

Wheatley, B., and S. Paradis. 1996. Balancing human exposure, risk and reality: questions raised by the Canadian Aboriginal methylmercury program. Neurotoxicology. **17:**241-250.

WHO. 1976. Environmental Health Criteria #1: Mercury. World Health Organization.

WHO. 1990. Environmental Health Criteria #101: Methylmercury. World Health Organization.

Widdel, F. 1988. Microbiology and ecology of sulfate - and sulfur-reducing bacteria. *In* A. J. B. Zehnder (ed.), Ecology of anaerobic microorganisms. John Wiley and Sons, New York.

Widdel, F., and F. Bak. 1992. Gram-negative mesophilic sulfate-reducing bacteria, p. 3352-3378. *In* A. Balows, H.G. Truper, M. Dworkin, W. Harder, and K.-H. Schleifer (ed.), The prokaryotes, 2nd ed. Springer-Verlag, New York.

Williams, S. C., Y. Hong, D. C. A. Danavall, M. H. Howard-Jones, D. Gibson, M. E. Frischer, and P. G. Verity. 1998. Distinguishing between living and nonliving bacteria: evaluation of vital stain propidium iodide and the combined use with molecular probes in aquatic samples. J. Microbiol. Methods. **32:**225-236.

Winfrey, M. R., and J. W. M. Rudd. 1990. Environmental factors affecting the formation of methylmercury in low pH lakes. Environ. Toxicol. Chem. **9:**853-869.

Winger, P. V., P. J. Lasier, and H. Geitner. 1993. Toxicity of sediments and pore water from Brunswick Estuary, Georgia. Arch. Environ. Contam. Toxicol. **25:**371-376.

Zilloux, E. J., D. B. Porcella, and J. M. Benoit. 1965. Mercury cycling and affects in freshwater wetland ecosystems. Environ. Toxicol. and Chem. **12:**2245-2264.